

DIFFERENTIAL USE OF SHALLOW AND DEEP SOIL MOISTURE IN A SEMIARID  
SHRUBLAND: LINKING SAP FLOW AND STABLE ISOTOPE TECHNIQUES TO  
QUANTIFY TEMPORAL VARIABILITY

By

Daphne J. Szutu

---

A Thesis Submitted to the Faculty of the

SCHOOL OF NATURAL RESOURCES AND THE ENVIRONMENT

In Partial Fulfillment of the Requirements

For the Degree of

MASTER OF SCIENCE

WITH A MAJOR IN WATERSHED MANAGEMENT AND ECOHYDROLOGY

In the Graduate College

THE UNIVERSITY OF ARIZONA

2015

## STATEMENT BY AUTHOR

This thesis has been submitted in partial fulfillment of requirements for an advanced degree at the University of Arizona and is deposited in the University Library to be made available to borrowers under rules of the Library.

Brief quotations from this thesis are allowable without special permission, provided that an accurate acknowledgement of the source is made. Requests for permission for extended quotation from or reproduction of this manuscript in whole or in part may be granted by the head of the major department or the Dean of the Graduate College when in his or her judgment the proposed use of the material is in the interests of scholarship. In all other instances, however, permission must be obtained from the author.

SIGNED: Daphne J. Szutu

## APPROVAL BY THESIS DIRECTOR

This thesis has been approved on the date shown below:

---

Shirley Anne Papuga

Date

Professor, Watershed Management and Ecohydrology

## ACKNOWLEDGEMENTS

This research is supported in part by NSF CAREER award EAR-125501 and the NSF National Critical Zone Observatories Program (EAR-0724958).

This work would not be possible without the guidance and dedication of my advisor, Dr. Shirley Papuga. I am also grateful to my committee members for their feedback and suggestions: Dr. Dave Breshears, Dr. Greg Barron-Gafford, and Dr. Ty Ferré. Thank you to Dr. Marek Zreda for use of your split-core soil sampler.

Thank you to the Papuga lab for your camaraderie and feedback at our weekly lab meetings and for innumerable hours of field and lab assistance: Claudia Quilesfogel-Esparza, James Garland, Daniel Wilcox, Lejon Hamman, Alex Schaller, Erika Gallo, Matt Rotunno, Natasha Krell, Rachel Wehr, Adam Killebrew, Vanessa Lentini, Ami Kidder, Zulia Sanchez-Mejia, and Zack Guido. Jen Johnson's thoughtful assistance in developing and troubleshooting isotope analysis methods was indispensable. Working groups in the enthusiastic company of Mallory Barnes and Sera Mirchandani at various cafes around town (mostly Raging Sage) helped make the writing process much more palatable. Finally, thank you to Mike Lum for your unwavering support and the many nights together at Café Adelaide.

My time at the Auwahi dryland forest, Maui, Hawai'i, sparked my graduate studies. To the Leeward Haleakalā Watershed Restoration Partnership and the U.S. Geological Survey Unsaturated Zone Flow Project – mahalo nui loa.

## TABLE OF CONTENTS

LIST OF FIGURES .....	6
ABSTRACT.....	7
1. INTRODUCTION .....	9
1.1 Evapotranspiration Partitioning in Water-Limited Ecosystems .....	9
1.2 Sap Flow Technique for Measuring Transpiration in Water-Limited Ecosystems .....	13
1.3 Stable Water Isotopes for Understanding Sources of Plant Water Use.....	14
1.4 Objectives .....	16
1.5 Our Water-Limited Ecosystem .....	16
1.6 Structure of the Following Chapters.....	18
2. PRESENT STUDY.....	20
2.1 Abstract of Appendix A: Differential use of shallow and deep soil moisture in a semiarid shrubland: Linking sap flow and stable isotope techniques to quantify temporal variability .....	20
2.2 Appendix B: Picarro Analyzer and Induction Module Introduction .....	21
2.3 Appendix C: Protocol for Analyzing Samples on the Picarro L2130-i Analyzer with Induction Module.....	22
2.4 Appendix D: Additional Protocol for Analyzing Stem Samples on the Picarro Induction Module .....	22
2.5 Appendix E: Additional Protocol for Analyzing Soil Samples on the Picarro Induction Module.....	22
2.6 Appendix F: Picarro Analyzer Calibration Test .....	22
2.7 Appendix G: Precipitation Isotope Collection: Testing for Evaporation from Bottle Collectors.....	23
2.8 Summary of Results.....	23
2.9 Future Research Opportunities .....	24
3. REFERENCES .....	27
APPENDIX A: Differential use of shallow and deep soil moisture in a semiarid shrubland: Linking sap flow and stable isotope techniques to quantify temporal variability .....	34
APPENDIX B: Picarro Analyzer and Induction Module Introduction .....	85
APPENDIX C: Protocol for Analyzing Samples on the Picarro L2130-i Analyzer with Induction Module .....	93
APPENDIX D: Additional Protocol for Analyzing Stem Samples on the Picarro Induction Module .....	107

APPENDIX E: Additional Protocol for Analyzing Soil Samples on the Picarro Induction Module	115
APPENDIX F: Picarro Analyzer Calibration Test	119
APPENDIX G: Precipitation Isotope Collection: Testing for Evaporation from Bottle Collectors	121

## LIST OF FIGURES

**Figure 1.** Field site in southern Arizona: a monsoon-dependent creosotebush ecosystem at The Santa Rita Creosote (SRC) AmeriFlux Site.

## **ABSTRACT**

Semiarid shrublands and other dryland ecosystems are highly responsive to precipitation pulses that, depending on their size, differentially influence the distribution of moisture in the soil profile. The spatiotemporal distribution of soil moisture is expected to change in association with changes in the frequency and magnitude of dryland precipitation event. Many ecohydrological studies that examine plant water use strategies have assumed that the soil depths from which plants derive their moisture is a function of the root density profile, i.e., higher root density correlates with greater water uptake. However, recent field studies have shown that in dryland ecosystems, transpiration dynamics and plant productivity are largely a function of deep soil moisture available after large precipitation events regardless of where the majority of plant roots occur. Therefore, changes in precipitation pulses that alter the timing and magnitude of the availability of deep soil moisture are expected to have major consequences for dryland ecosystems. We suggest that adopting a hydrologically defined two-layer conceptual framework of the soil profile is more appropriate for understanding plant water use in dryland ecosystems than a framework that is based on rooting depth. Using the hydrologically defined two-layer framework, the objective of this study is to show how transpiration dynamics vary with the availability of deep soil moisture in dryland ecosystems and how the source of that moisture varies over time. We present eddy covariance, soil moisture, and sap flow measurements taken over 18 months in conjunction with precipitation, shallow soil, deep soil, and stem stable water isotope samples taken biweekly at a creosotebush-dominated shrubland ecosystem at the Santa Rita Experimental Range in southern Arizona. Results from both our sap flow measurements and our stable isotope analysis support that transpiration is associated with the availability of deep soil moisture. While this is especially true in the summer when transpiration rates are highest,

our results suggest that transpiration can also be substantial in wet winters in which the deep soil layer is wetter than average. When transpiration rates are highest, both deep moisture and stem water are more isotopically similar to winter precipitation than summer precipitation, suggesting that winter precipitation can play an important role in supporting these ecosystems. Our study suggests that integrating sap flow and stable isotope techniques with soil moisture measurements offers a better understanding of how plant water use strategies shift with changes in source water and its availability than either technique could offer on its own. We have contributed to understanding where precipitation pulses are distributed in the soil moisture profile and when these pulses are used by plants in dryland ecosystems. Ultimately these findings should help to improve the representation of drylands within regional and global models of land surface atmosphere exchange and their linkages to the hydrologic cycle.

## **1. INTRODUCTION**

### **1.1 Evapotranspiration Partitioning in Water-Limited Ecosystems**

Water-limited ecosystems, also called drylands, consist of subhumid, semiarid, and arid regions. In these ecosystems, annual potential evapotranspiration generally exceeds actual precipitation [Newman *et al.*, 2006]. Water-limited ecosystems experience discrete pulses of rainfall that drive plant productivity [Huxman *et al.*, 2004]. Pulse size and frequency vary from event to event and over the year, and these variations affect biological and physical processes in the drylands [Sala and Lauenroth, 1982; Kurc and Small, 2007; Raz Yaseef *et al.*, 2010]. Research indicates that climate change will affect pulse size and frequency in water-limited ecosystems [Easterling *et al.*, 2000; Seager *et al.*, 2007], including possible decreases in the amount of non-summer precipitation [Goodrich *et al.*, 2008] and less snowfall [e.g., Knowles *et al.*, 2006; Barnett *et al.*, 2008]. These changes in precipitation pattern are likely to exacerbate changes in vegetation dynamics, water resource partitioning, and water supply in water-limited ecosystems [Potts *et al.*, 2006; Knapp *et al.*, 2008], for example vegetation community composition shifts between shrubs and grasses [Bates *et al.*, 2006] and partitioning of precipitation into interception, runoff, and infiltration [Loik *et al.*, 2004]. Water-limited ecosystems currently comprise 40% of terrestrial biomes, and this percentage is projected to grow with current climate trends [Okin *et al.*, 2009]. These drylands are also experiencing rapid population growth [Reynolds *et al.*, 2007], so future water management will need to balance water supply for both urban and ecological demand.

Strategic management of the scarce water resources of water-limited ecosystems requires an understanding of how hydrological processes affect and are affected by biological processes

[Newman *et al.*, 2006]. Ecological and hydrological processes interact with each other in a two-way relationship [Rodriguez-Iturbe, 2000; Newman *et al.*, 2006]. Timing and amount of rainfall affects vegetation cover and distribution at a particular site [Bates *et al.*, 2006; Odorico *et al.*, 2010]. In turn, vegetation cover affects hydrological processes such as infiltration [Ludwig *et al.*, 2005; Perkins *et al.*, 2014], interception [Owens *et al.*, 2006], and groundwater recharge [Scanlon *et al.*, 2005; Newman *et al.*, 2006]. The timing and amount of rainfall also affects soil water storage [Savenije, 2004; Newman *et al.*, 2006; Odorico *et al.*, 2010], which influences ecosystem productivity [Rodriguez-Iturbe, 2000; Scott *et al.*, 2009].

In studying how ecological and hydrological processes interact in water-limited systems, researchers have focused on studying evapotranspiration (*ET*) because it is the dominant component of the water budget in drylands [Wilcox *et al.*, 2003]. *ET* is the total amount of water vapor efflux from the land surface to the atmosphere and accounts for two different processes: evaporation (*E*) from soil water and/or intercepted water on vegetation surfaces and plant transpiration (*T*). In the global water cycle, *T* is a significant process, comprising about 61% of *ET* and returning about 30-50% of precipitation back into the atmosphere [Schlesinger and Jasechko, 2014]. Water lost through *T* is “productive” use of water because it is water used toward biomass accumulation, whereas water lost through *E* is considered “wasted” water because it does not contribute toward plant productivity [Savenije, 2004]. In dryland systems, total *ET* in dryland systems has been successfully estimated using open path eddy covariance systems [e.g., Scott *et al.*, 2006a; Kurc and Small, 2007; Scott, 2010], but the partitioning of *E* and *T* in response to precipitation pulse dynamics remains poorly understood. Historically, models of *ET* were developed in areas with dense canopy and minimal exposed soil, so *E* was

assumed negligible, so  $T$  was assumed to be equal to total  $ET$  [Stannard, 1993]. Therefore,  $ET$  was considered a good estimation of  $T$  and productive water use in environments with limited  $E$  such as humid climates with full canopy cover [Stannard, 1993]. In contrast,  $T$  can be a relatively small component of  $ET$  at sites with sparse canopies and exposed soil like dryland ecosystems [e.g., Huxman *et al.*, 2005; Yopez *et al.*, 2007; Raz Yaseef *et al.*, 2010]. In these water-limited ecosystems with high evaporative demand,  $E$  is an important contributor to  $ET$  [Kurc and Small, 2004], challenging the dense canopy historical perspective that  $ET$  can all be attributed to  $T$ . In addition to separately evaluating the long-term trends in  $E$  and  $T$ , these processes also have significant seasonal variability [Kurc and Small, 2004; Scott *et al.*, 2006b; Cavanaugh *et al.*, 2011]. For example,  $E$  is high immediately following a rainfall event when shallow soil moisture is available [Scott *et al.*, 2006b; Kurc and Small, 2007; Moran *et al.*, 2009], whereas green-up and transpiration may not increase unless there has been sufficient accumulation of soil moisture in the active root zone [Kurc and Benton, 2010; Cavanaugh *et al.*, 2011]. As such, separately evaluating  $T$  and  $E$  enables better assessment of water resource partitioning and ecosystems productivity.

In evaluating water resource partitioning in water-limited systems, the soil moisture balance has emerged as a powerful means to link the interactions and feedbacks between regional water balance, vegetation distribution, and ecosystem productivity [Rodriguez-Iturbe, 2000; Weltzin *et al.*, 2003]. Plants primarily interact with the soil and affect the soil moisture balance through their roots [Denmead and Shaw, 1962], which are the physical structures that partition infiltration between plant water uptake and soil moisture. As climate changes affect the precipitation regimes of the U.S. Southwest [Easterling *et al.*, 2000; Seager *et al.*, 2007], these

changes in rainfall patterns will affect how water is distributed spatially and temporally within the soil profile [Weltzin *et al.*, 2003; Loik *et al.*, 2004]. Understanding the baseline of root water use strategies will help us better understand where these precipitation pulses are distributed in the root profile and when the plants use these pulses for transpiration.

Shallow and deep soil moisture make distinct and separate contributions to the processes of  $E$  and  $T$ .  $E$  is high immediately after a rain event, but decreases very quickly following the rain event: Scott *et al.* [2006b] found that  $E$  peaked and then declined within two days of a rain event in a semiarid shrubland. Kurc and Small [2004] also found at both semiarid shrubland and grassland sites a relationship between shallow soil surface (0-5cm) and  $ET$ , but not between a root zone average soil moisture and  $ET$ , indicating that in these water-limited ecosystems with high evaporative demand,  $E$  is an important contributor to  $ET$ . Cavanaugh *et al.* [2011] used a combination of eddy covariance and sap flow transpiration measurements to determine that after the onset of summer monsoon rains,  $E$  dominated  $ET$ , whereas only a series of large precipitation events increased deep soil moisture and triggered  $T$ . Because the two layers have different drydown dynamics and different controls on  $E$  and  $T$ , land surface-atmosphere models representing soil moisture as a single, root zone average bucket may not represent water cycling dynamics in semiarid systems. Therefore, to address our research questions, we use a two-layer soil moisture framework [Sanchez-Mejia and Papuga, 2014] rather than a single-layer, root zone averaged soil moisture framework to better represent the temporal variations in transpiration and plant water use.

## 1.2 Sap Flow Technique for Measuring Transpiration in Water-Limited Ecosystems

Transpiration can be estimated using a variety of methods including sap flow systems [e.g., *Dugas et al.*, 1993; *Scott et al.*, 2006a; *Raz Yaseef et al.*, 2010] and stable isotope techniques [e.g., *Yepez et al.*, 2005]. Generally speaking, transpiration estimates based on sap flow systems monitor the flux of heat in the stem or trunk of a plant [*Senock and Ham*, 1993; *Kjelgaard et al.*, 1997], and then this flux is scaled up to the ecosystem using allometric relationships [e.g., *Grelle et al.*, 1997; *Kurpius et al.*, 2003; *Kume et al.*, 2010]. In the heat balance method of calculating sap flow, two sets of thermocouples in each sensor measure heat lost by conduction up ( $Q_{up}$ ) and down ( $Q_{down}$ ) the stem and heat lost radially ( $Q_{radial}$ ) away from the stem [*Cavanaugh et al.*, 2011]. Given a user-supplied parameter of heat input,  $Q_{in}$ , the heat balance method uses an energy balance concept to calculate heat transported by convection in sap flow ( $Q_{flow}$ ) (Equation 1) [*Cavanaugh et al.*, 2011]. The sap flow rate ( $F$ ) is a function of the convective heat flux, the specific heat of water ( $c$ ), and the temperature difference between sap flowing in and out of the heated segment of the stem ( $dT$ ) (Equation 2) [*Cavanaugh et al.*, 2011]. The sap flow rate is then scaled with stem cross-section ( $A'$ ) and water density ( $\rho_{water}$ ) to calculate sap flux density ( $SFD$ ) (Equation 3). Finally, stand-level transpiration is calculated by scaling the sap flux density with a site-specific average stem density (Equation 4).

$$\text{Heat balance equation: } Q = Q_{up} + Q_{down} + Q_{radial} + Q_{flow} \quad (1)$$

$$\text{Sap flow rate [g h}^{-1}\text{]: } F = Q_{flow} / c / dT \quad (2)$$

$$\text{Sap flux density [cm h}^{-1}\text{]: } SFD = F / A' / \rho_{water} \quad (3)$$

$$\text{Transpiration [mm h}^{-1}\text{]: } T = SFD * \text{Average stem density} \quad (4)$$

The advantages of sap flow estimates of  $T$  are that they are continuous, can be non-invasive and do not affect the micro-climatic conditions of the plant (relative to chamber measurements of  $T$ ) [Kool *et al.*, 2014]. One main challenge of sap flow estimates of  $T$  is addressing uncertainty in scaling from individual plant-scale sap flow to stand-level  $T$  [Čermák *et al.*, 2004; Kume *et al.*, 2010].

### **1.3 Stable Water Isotopes for Understanding Sources of Plant Water Use**

Stable isotope analysis is well established in hydrology to trace sources of water in groundwater [Clark and Fritz, 1997], and only since the 1990s have stable water isotopes become more commonly used to trace sources of water in plant sap to determine from where plants obtain their moisture [Dawson, 1998; Williams and Ehleringer, 2000; Corbin *et al.*, 2005; Brooks *et al.*, 2010]. Plant water samples, combined with soil water samples at different depths, can be analyzed to determine where in the soil profile plants are obtaining their soil moisture. Isotopic analysis of stable water isotopes ( $^2\text{H}$  and  $^{18}\text{O}$ ) can be used to determine the source of water (e.g., winter or summer precipitation) at different points in the soil profile. Precipitation that forms at different times of the year has different isotopic signatures depending on the temperature at which the precipitation was formed [Clark and Fritz, 1997]: precipitation forming at colder temperatures (i.e., winter precipitation) undergoes more fractionation than precipitation forming at warmer temperatures (i.e., summer precipitation), allowing us to distinguish precipitation formed during winter and summer [e.g., Wright, 2001]. This mixing model theory depends on the assumption that during  $T$ , there is no fractionation of stable water isotopes because there is no mass preference of stable water isotopes during plant uptake of water [Dawson and Ehleringer, 1991; Thorburn *et al.*, 1993]. Two exceptions are that some halophytes [Lin and Sternberg,

1993] and woody xerophytes [Ellsworth and Williams, 2007] discriminate against  $^2\text{H}$  during uptake. Our specific study species, *Larrea tridentata*, does not show evidence of discriminating against  $^2\text{H}$  during uptake [Ellsworth and Williams, 2007].

Our precipitation, stem, and soil samples were analyzed for stable water isotopes on the Picarro L2130-i analyzer with an Induction Module peripheral. The Picarro analyzer uses the isotope-ratio infrared spectroscopy technique to quantify the concentration and isotopic composition of water vapor. This technique leverages the distinct absorption spectra of the three most abundant isotopologues of water vapor ( $^1\text{H}^1\text{H}^{16}\text{O}$ ,  $^1\text{H}^2\text{H}^{16}\text{O}$ ,  $^1\text{H}^1\text{H}^{18}\text{O}$ ). The precipitation, plant, and soil samples are clamped into a metal holder before being inserted into the Induction Module. The Induction Module heats the sample inductively, with the length and intensity of heating prescribed by user-supplied parameters [Berkelhammer *et al.*, 2013]. The available water vapor is then passed by a zero air carrier gas into an infrared absorbance cavity [Berkelhammer *et al.*, 2013]. The oxygen and hydrogen isotope ratios are calculated by using the spectral absorbance at specific wavelengths and the three absorption peaks of the water isotopologues [Martín-Gómez *et al.*, 2015]. An on-line micro-combustion module oxidizes most organic contaminants that may cause spectral interference [Berkelhammer *et al.*, 2013; Martín-Gómez *et al.*, 2015]. All values are reported in standard delta notation in per mil (‰) notation relative to Vienna Mean Ocean Water (VSMOW):

$$\delta = \left( \frac{R_{\text{sample}}}{R_{\text{standard}}} - 1 \right) \times 1000 \quad (5)$$

where R is the isotope ratio of the heavy and light isotope (e.g.,  $^{18}\text{O}/^{16}\text{O}$ ).

## 1.4 Objectives

This thesis reports the research and data collected at the SRC field site from October 2013 through March 2015. This study addresses two objectives within a two-layer conceptual soil moisture framework. The first objective was to examine the temporal dynamics of transpiration and how the relative contribution of transpiration to evapotranspiration ( $T/ET$ ) changes seasonally in a monsoon-dependent semiarid shrubland. The second objective was to examine seasonality of creosotebush water use strategies, i.e., the soil moisture depth at which plants withdraw water.

Appendix A, *Differential use of shallow and deep soil moisture in a semiarid shrubland: Linking sap flow and stable isotope techniques to quantify temporal variability*, presents research addressing the following questions about plant water use strategies, (1) Is transpiration limited to periods when deep soil moisture is available, and how does this dependence vary throughout the year? (2) Are shallow and deep soil moisture isotopically different, and how does this difference vary throughout the year?, and (3) Are stable water isotopes an adequate measure of determining sources of plant water use in a semiarid shrubland?

## 1.5 Our Water-Limited Ecosystem

The work presented here takes place at a water-limited creosotebush shrubland at the Santa Rita Experimental Range (SRER) in southern Arizona (Figure 1). The SRER is located 60 km south of Tucson, Arizona at the foot of the northwestern Santa Rita Mountains. Our research is conducted at The Santa Rita Creosote (SRC) AmeriFlux Site (31.9083 N, 110.8395 W), located in the northern portion of SRER at an elevation of about 950 m. Since at least 1934, creosotebush (*Larrea tridentata*) has been the dominant species near the northern border of

SRER [Humphrey and Mehrhoff, 1958]. The SRC experiences cool winters, warm summers, and a bimodal precipitation pattern, with about 60 % of the precipitation falling during the North American Monsoon (July through September) and about 20% of the precipitation falling during the winter (December through February) [Sanchez-Mejia and Papuga, 2014]. The average annual precipitation is about 345 mm, and the average annual temperature is about 20 °C [Sanchez-Mejia and Papuga, 2014]. Vegetation cover is about 24%, with creosotebush as the dominant vegetation (14% cover) and the remaining 10% accounted for by small grasses, forbs, and cactus [Kurc and Benton, 2010]. The soil type is sandy loam with no caliche layer (to at least 1 m depth) [Kurc and Benton, 2010]. The estimated depth to groundwater near our site is greater than 70 m [Eastoe et al., 2004].

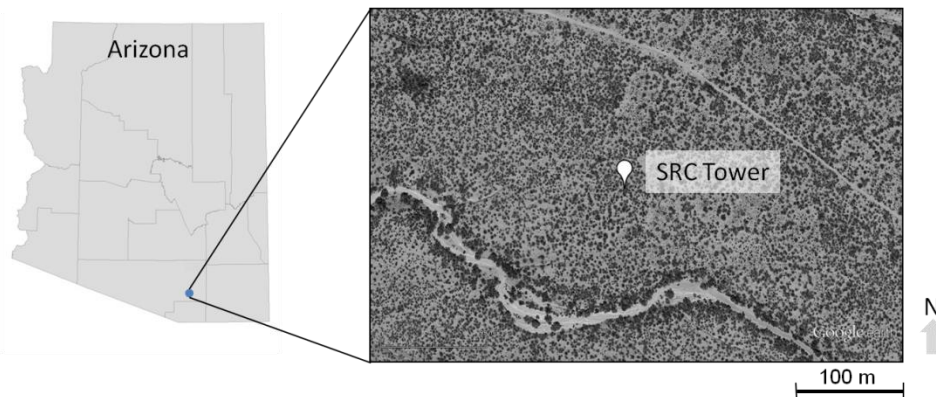


**Figure 1.** Field site in southern Arizona: a monsoon-dependent creosotebush ecosystem at The Santa Rita Creosote (SRC) AmeriFlux Site.

The SRC AmeriFlux Site has been continuously recording micro-meteorological and soil moisture data since 2008. An eddy covariance tower provides half-hourly micro-meteorological measurements [Sanchez-Mejia and Papuga, 2014]. Standard eddy covariance systems uses high-frequency measurements of momentum, temperature, and water vapor to characterize micro-meteorological conditions as well as water, carbon, and energy fluxes [Moncrieff et al., 2000;

*Kool et al.*, 2014]. Water and carbon dioxide fluxes are calculated using 10 Hz measurements from an open path CO<sub>2</sub>/H<sub>2</sub>O infrared gas analyzer (LI-7500, LI-COR Inc., Lincoln, NE, USA) and a 3-D sonic anemometer (CSAT-3, Campbell Scientific Inc., Logan, UT, USA). Incoming and outgoing radiation are calculated from incoming and outgoing shortwave radiation, and incoming and outgoing longwave radiation, measured with a four-component net radiometer (CNR1, Kipp & Zonen, Inc., Delft, Netherlands). Precipitation is measured with a tipping bucket rain gauge (TE525, Texas Electronics Inc., Dallax, TX, USA). Other variables measured include relative humidity and temperature (HMP 45C, Vaisala, Helsinki, Finland).

Volumetric soil moisture content was measured using water content reflectometer (CS 616, Campbell Scientific Inc., Logan, UT, USA) and is derived from the sensitivity of the probes to the dielectric constant of the surrounding soil [*Chandler et al.*, 2004]. These sensors were installed in six profiles, three under the creosotebush canopy and three in the inter-canopy areas, at depths 2.5, 12.5, 22.5, 37.5, 52.5, 67.5, 82.5 cm. Average soil moisture at each depth were calculated by using a weighted average based on percent cover to combine the bare and canopy averages. To calculate average soil moisture in the two soil moisture layers, we use weighted averages based on the relative contribution of each sensor to the shallow (0-20 cm) or deep (20-40 cm) layers of the soil layer.

## **1.6 Structure of the Following Chapter**

The following chapter consists of an abstract of my M.S. research, followed by descriptions of the remaining appendices (technical information about operating the Picarro L2130-i analyzer with Induction Module), summary of results, and future research directions.

My M.S. research is presented as an individual research paper in Appendix A of this document. The manuscript, *Differential use of shallow and deep soil moisture in a semiarid shrubland: Linking sap flow and stable isotope techniques to quantify temporal variability*, is in preparation for submission to the journal *Water Resources Research*. Tables and figures associated with Appendix A appear at the end of Appendix A. Appendices B through G include protocol about running precipitation, stem, and soil samples on the Picarro Induction Module, as well as the results of two tests examining analyzer calibration and precipitation isotope collection methodology.

## **2. PRESENT STUDY**

The methods, results, and conclusions of this research are included in Appendix A. The following abstract summarizes our research investigating the temporal dynamics and plant water use strategies at a semiarid shrubland. The subsequent sections are descriptions of Appendices B through G, technical notes on analyzing stable water isotope samples on the Picarro analyzer with Induction Module.

### **2.1 Abstract of Appendix A: Differential use of shallow and deep soil moisture in a semiarid shrubland: Linking sap flow and stable isotope techniques to quantify temporal variability**

Semiarid shrublands and other dryland ecosystems are highly responsive to precipitation pulses that, depending on their size, differentially influence the distribution of moisture in the soil profile. The spatiotemporal distribution of soil moisture is expected to change in association with changes in the frequency and magnitude of dryland precipitation event. Many ecohydrological studies that examine plant water use strategies have assumed that the soil depths from which plants derive their moisture is a function of the root density profile, i.e., higher root density correlates with greater water uptake. However, recent field studies have shown that in dryland ecosystems, transpiration dynamics and plant productivity are largely a function of deep soil moisture available after large precipitation events regardless of where the majority of plant roots occur. Therefore, changes in precipitation pulses that alter the timing and magnitude of the availability of deep soil moisture are expected to have major consequences for dryland ecosystems. We suggest that adopting a hydrologically defined two-layer conceptual framework of the soil profile is more appropriate for understanding plant water use in dryland ecosystems

than a framework that is based on rooting depth. Using the hydrologically defined two-layer framework, the objective of this study is to show how transpiration dynamics vary with the availability of deep soil moisture in dryland ecosystems and how the source of that moisture varies over time. We present eddy covariance, soil moisture, and sap flow measurements taken over 18 months in conjunction with precipitation, shallow soil, deep soil, and stem stable water isotope samples taken biweekly at a creosotebush-dominated shrubland ecosystem at the Santa Rita Experimental Range in southern Arizona. Results from both our sap flow measurements and our stable isotope analysis support that transpiration is associated with the availability of deep soil moisture. While this is especially true in the summer when transpiration rates are highest, our results suggest that transpiration can also be substantial in wet winters in which the deep soil layer is wetter than average. When transpiration rates are highest, both deep moisture and stem water are more isotopically similar to winter precipitation than summer precipitation, suggesting that winter precipitation can play an important role in supporting these ecosystems. Our study suggests that integrating sap flow and stable isotope techniques with soil moisture measurements offers a better understanding of how plant water use strategies shift with changes in source water and its availability than either technique could offer on its own. We have contributed to understanding where precipitation pulses are distributed in the soil moisture profile and when these pulses are used by plants in dryland ecosystems. Ultimately these findings should help to improve the representation of drylands within regional and global models of land surface atmosphere exchange and their linkages to the hydrologic cycle.

## **2.2 Appendix B: Picarro Analyzer and Induction Module Introduction**

This appendix introduces the theory behind the Picarro analyzer and Induction Module, including internal and external corrections and calibrations.

### **2.3 Appendix C: Protocol for Analyzing Samples on the Picarro L2130-i Analyzer with Induction Module**

This appendix describes the general protocol for analyzing blank, standard, and unknown samples on the Picarro Induction Module, as well as some troubleshooting procedures for common problems.

### **2.4 Appendix D: Additional Protocol for Analyzing Stem Samples on the Picarro Induction Module**

This appendix describes how to analyze plant stem samples for stable water isotopes on the Picarro Induction Module.

### **2.5 Appendix E: Additional Protocol for Analyzing Soil Samples on the Picarro Induction Module**

This appendix describes how to analyze soil samples for stable water isotopes on the Picarro Induction Module.

### **2.6 Appendix F: Picarro Analyzer Calibration Test**

This appendix describes testing the calibration for the Picarro L2130-i analyzer, Serial # HIDS2178.

## **2.7 Appendix G: Precipitation Isotope Collection: Testing for Evaporation from Bottle Collectors**

This appendix describes how to construct bottle and funnel collectors that can be used to collect precipitation samples for stable water isotope analysis and investigates the potential of evaporation from the precipitation collected in these bottle collectors.

## **2.8 Summary of Results**

Results from both continuous sap flow transpiration data and discrete isotopic sampling of precipitation, soil, and stem samples suggest that plants are primarily using deep soil moisture for transpiration. From the isotopic samples, I found that the shallow and deep soils were isotopically distinct, with the shallow soil generally more enriched in  $\delta^{18}\text{O}$  and  $\delta^2\text{H}$  than deep soil. In particular, the  $\delta^2\text{H}$  values of shallow soil samples on each sampling day tended to be more positive than the  $\delta^2\text{H}$  values of deep soil samples, except on days where a large, isotopically depleted storm wetted the whole soil profile. Using sap flow and soil moisture data, I showed that transpiration was generally more strongly correlated with deep moisture, whereas evaporation was more strongly correlated with shallow moisture. This was supported by analysis of our isotopic data, from which I show that stem samples are isotopically similar to deep soil samples, with stem samples clustering around a regression line through deep soil samples. Using a combined approach to understand shrub plant water use in semiarid areas offers us more insights than simply using sap flow or isotopic techniques alone. This is in part because of the complexity of isotopic patterns in the rainfall and the conditions for fractionation. Using our combined approach, we can confidently say that this semiarid shrubland depends on deep moisture for growth and functioning and is therefore vulnerable to shifts in precipitation, such as

a decrease in the number of large storms, which would limit available soil moisture to the shallow surface layer.

## **2.9 Future Research Opportunities**

Based on the results presented here, I identify three directions for future research of plant water use strategies in water-limited ecosystems.

### ***2.9.1 Expanding the framework to a snowmelt-dependent, water-limited ecosystem***

One main research direction is to expand the present study questions to a different water-limited ecosystem with a distinctly different precipitation regime, such as a snowmelt-dependent mixed conifer site within the Santa Catalina Mountains Critical Zone Observatory. Applying the two-layer conceptual soil moisture framework at this site, which experiences soil moisture pulses through both snowmelt and summer rains will help us expand our understanding of plant water use strategies in water-limited ecosystems. One potential site is the Mount Bigelow eddy covariance tower site, at an elevation of 2570 m. This site has had continual eddy covariance, soil moisture, and transpiration measurements over the past few years. I have also collected precipitation, plant, and soil samples down to 45 cm, every two weeks, between June 2014 and April 2015. The climate is semiarid and the site experiences bimodal precipitation: rain and snowfall during the winter (December through March) and rain during the North American Monsoon (July and August) [Brown-Mitic *et al.*, 2007]. The site generally experiences ephemeral snowpack: snow will accumulate, then melt all away within a few days or weeks, a new snowpack will begin to accumulate with fresh snowfall, and finally this new snowpack may again all melt away before the next snowfall event [Nelson *et al.*, 2014]. In these higher-

elevation ecosystems, changes in snow accumulation and melting may have profound implications for ecosystem processes and downstream watersheds [Knowles *et al.*, 2006; Biederman *et al.*, 2014].

### ***2.9.2 Investigating implications of hydraulic redistribution on plant water use strategies in water-limited ecosystems***

A second direction for future work is investigating the potential of hydraulic redistribution in semiarid shrublands and the effect of this redistribution on plant water use strategies. These questions could be addressed in a greenhouse experiment where creosoteshrub are planted in specially designed two-layer planters that prevent water flow between a shallow soil layer and a deep soil layer. Then, the creosotebush could be differentially irrigated under several different treatments, including deuterated water ( $^2\text{H}_2\text{O}$ ) in the shallow layer only and deuterated water in the deep layer only. Collection and analysis of irrigation, soil, and plant water from the different irrigation treatments for stable water isotopes could be used to test for evidence of hydraulic redistribution between the shallow and deep soil layers. The phenomena of hydraulic redistribution has been discovered only in the past decade [Burgess *et al.*, 1998; Nadezhdina *et al.*, 2010], so it will be exciting to see how this biological process adds further detail in understanding plant water use strategies in water-limited ecosystems.

### ***2.9.3 Quantifying uncertainties of stable water isotope analysis in ecohydrologic studies***

Finally, more work is needed in developing universally reliable and consistent methods for analyzing stable water isotopes in soil and plant samples on the Picarro L2130-i analyzer with Induction Module (Induction Module - Cavity Ring Down Spectroscopy). Although the

Induction Module in conjunction with the isotope ratio infrared spectroscopy method can be faster, more mobile, and less expensive than the classic vacuum distillation - isotope ratio mass spectroscopy method, the potential for and correction of spectroscopic interference from organic contaminants in biological samples is not well understood [*West et al.*, 2010; *Schultz et al.*, 2011; *Schmidt et al.*, 2012; *Martín-Gómez et al.*, 2015].

### 3. REFERENCES

- Barnett, T. P. et al. (2008), Human-Induced Changes in the Hydrology of the Western United States, *Science*, 319(5866), 1080–1083, doi:10.1126/science.1152538.
- Bates, J. D., T. Svejcar, R. F. Miller, and R. A. Angell (2006), The effects of precipitation timing on sagebrush steppe vegetation, *J. Arid Environ.*, 64(4), 670–697, doi:10.1016/j.jaridenv.2005.06.026.
- Berkelhammer, M., J. Hu, A. Bailey, D. C. Noone, C. J. Still, H. Barnard, D. Gochis, G. S. Hsiao, T. Rahn, and A. Turnipseed (2013), The nocturnal water cycle in an open-canopy forest, *J. Geophys. Res. Atmospheres*, 118(17), 10,225–10,242, doi:10.1002/jgrd.50701.
- Biederman, J. A., P. D. Brooks, A. A. Harpold, D. J. Gochis, E. Gutmann, D. E. Reed, E. Pendall, and B. E. Ewers (2014), Multiscale observations of snow accumulation and peak snowpack following widespread, insect-induced lodgepole pine mortality, *Ecohydrology*, 7(1), 150–162, doi:10.1002/eco.1342.
- Brooks, J. R., Holly R. Barnard, Rob Coulombe, and Jeffrey J. McDonnell (2010), Ecohydrologic separation of water between trees and streams in a Mediterranean climate, *Nat. Geosci.*, 3(2), 100–104, doi:10.1038/ngeo722.
- Brown-Mitic, C., W. J. Shuttleworth, R. Chawn Harlow, J. Petti, E. Burke, and R. Bales (2007), Seasonal water dynamics of a sky island subalpine forest in semi-arid southwestern United States, *J. Arid Environ.*, 69(2), 237–258, doi:10.1016/j.jaridenv.2006.09.005.
- Burgess, S. S. O., M. A. Adams, N. C. Turner, and C. K. Ong (1998), The redistribution of soil water by tree root systems, *Oecologia*, 115(3), 306–311, doi:10.1007/s004420050521.
- Cavanaugh, M. L., S. A. Kurc, and R. L. Scott (2011), Evapotranspiration partitioning in semiarid shrubland ecosystems: a two-site evaluation of soil moisture control on transpiration, *Ecohydrology*, 4(5), 671–681, doi:10.1002/eco.157.
- Čermák, J., J. Kučera, and N. Nadezhdina (2004), Sap flow measurements with some thermodynamic methods, flow integration within trees and scaling up from sample trees to entire forest stands, *Trees*, 18(5), 529–546, doi:10.1007/s00468-004-0339-6.
- Chandler, D. G., M. Seyfried, M. Murdock, and J. P. McNamara (2004), Field calibration of water content reflectometers, *Soil Sci. Soc. Am. J.*, 68(5), 1501–1507.
- Clark, I. D., and P. Fritz (1997), *Environmental Isotopes in Hydrogeology*, CRC Press.

- Corbin, J. D., M. A. Thomsen, T. E. Dawson, and C. M. D'Antonio (2005), Summer water use by California coastal prairie grasses: fog, drought, and community composition, *Oecologia*, 145(4), 511–521, doi:10.1007/s00442-005-0152-y.
- Dawson, T. E. (1998), Fog in the California redwood forest: ecosystem inputs and use by plants, *Oecologia*, 117(4), 476–485, doi:10.1007/s004420050683.
- Dawson, T. E., and J. R. Ehleringer (1991), Streamside trees that do not use stream water, *Nature*, 350(6316), 335–337, doi:10.1038/350335a0.
- Denmead, O. T., and R. H. Shaw (1962), Availability of Soil Water to Plants as Affected by Soil Moisture Content and Meteorological Conditions<sup>1</sup>, *Agron. J.*, 54(5), 385, doi:10.2134/agronj1962.00021962005400050005x.
- D'Odorico, P., F. Laio, A. Porporato, L. Ridolfi, A. Rinaldo, and I. Rodriguez-Iturbe (2010), Ecohydrology of Terrestrial Ecosystems, *BioScience*, 60(11), 898–907, doi:10.1525/bio.2010.60.11.6.
- Dugas, W. A., J. S. Wallace, S. J. Allen, and J. M. Roberts (1993), Heat balance, porometer, and deuterium estimates of transpiration from potted trees, *Agric. For. Meteorol.*, 64(1–2), 47–62, doi:10.1016/0168-1923(93)90093-W.
- Easterling, D. R., G. A. Meehl, C. Parmesan, S. A. Changnon, T. R. Karl, and L. O. Mearns (2000), Climate Extremes: Observations, Modeling, and Impacts, *Science*, 289(5487), 2068–2074, doi:10.1126/science.289.5487.2068.
- Eastoe, C. J., A. Gu, and A. Long (2004), The origins, ages and flow paths of groundwater in Tucson basin: Results of a study of multiple isotope systems, in *Groundwater Recharge in a Desert Environment: The Southwestern United States*, *Water Sci. Appl. Ser.*, vol. 9, edited by J. F. Hogan, F. M. Philips, and B. R. Scanlon, pp. 217–234, AGU, Washington, D. C.
- Ellsworth, P. Z., and D. G. Williams (2007), Hydrogen isotope fractionation during water uptake by woody xerophytes, *Plant Soil*, 291(1-2), 93–107, doi:10.1007/s11104-006-9177-1.
- Goodrich, D. C., C. L. Unkrich, T. O. Keefer, M. H. Nichols, J. J. Stone, L. R. Levick, and R. L. Scott (2008), Event to multidecadal persistence in rainfall and runoff in southeast Arizona, *Water Resour. Res.*, 44(5), W05S14, doi:10.1029/2007WR006222.
- Grelle, A., A. Lundberg, A. Lindroth, A.-S. Morén, and E. Cienciala (1997), Evaporation components of a boreal forest: variations during the growing season, *J. Hydrol.*, 197(1–4), 70–87, doi:10.1016/S0022-1694(96)03267-2.
- Humphrey, R. R., and L. A. Mehrhoff (1958), Vegetation Changes on a Southern Arizona Grassland Range, *Ecology*, 39(4), 720–726, doi:10.2307/1931612.

- Huxman, T. E., K. A. Snyder, D. Tissue, A. J. Leffler, K. Ogle, W. T. Pockman, D. R. Sandquist, D. L. Potts, and S. Schwinning (2004), Precipitation pulses and carbon fluxes in semiarid and arid ecosystems, *Oecologia*, 141(2), 254–268, doi:10.1007/s00442-004-1682-4.
- Huxman, T. E., B. P. Wilcox, D. D. Breshears, R. L. Scott, K. A. Snyder, E. E. Small, K. Hultine, W. T. Pockman, and R. B. Jackson (2005), Ecohydrological implications of woody plant encroachment, *Ecology*, 86(2), 308–319, doi:10.1890/03-0583.
- Kjelgaard, J. F., C. O. Stockle, R. A. Black, and G. S. Campbell (1997), Measuring sap flow with the heat balance approach using constant and variable heat inputs, *Agric. For. Meteorol.*, 85(3–4), 239–250, doi:10.1016/S0168-1923(96)02397-0.
- Knapp, A. K. et al. (2008), Consequences of More Extreme Precipitation Regimes for Terrestrial Ecosystems, *BioScience*, 58(9), 811–821, doi:10.1641/B580908.
- Knowles, N., M. D. Dettinger, and D. R. Cayan (2006), Trends in Snowfall versus Rainfall in the Western United States, *J. Clim.*, 19(18), 4545–4559, doi:10.1175/JCLI3850.1.
- Kool, D., N. Agam, N. Lazarovitch, J. L. Heitman, T. J. Sauer, and A. Ben-Gal (2014), A review of approaches for evapotranspiration partitioning, *Agric. For. Meteorol.*, 184, 56–70, doi:10.1016/j.agrformet.2013.09.003.
- Kume, T., K. Tsuruta, H. Komatsu, T. Kumagai, N. Higashi, Y. Shinohara, and K. Otsuki (2010), Effects of sample size on sap flux-based stand-scale transpiration estimates, *Tree Physiol.*, 30(1), 129–138, doi:10.1093/treephys/tpp074.
- Kurc, S. A., and L. M. Benton (2010), Digital image-derived greenness links deep soil moisture to carbon uptake in a creosotebush-dominated shrubland, *J. Arid Environ.*, 74(5), 585–594, doi:10.1016/j.jaridenv.2009.10.003.
- Kurc, S. A., and E. E. Small (2004), Dynamics of evapotranspiration in semiarid grassland and shrubland ecosystems during the summer monsoon season, central New Mexico, *Water Resour. Res.*, 40(9), W09305, doi:10.1029/2004WR003068.
- Kurc, S. A., and E. E. Small (2007), Soil moisture variations and ecosystem-scale fluxes of water and carbon in semiarid grassland and shrubland, *Water Resour. Res.*, 43(6), W06416, doi:10.1029/2006WR005011.
- Kurpius, M. R., J. A. Panek, N. T. Nikolov, M. McKay, and A. H. Goldstein (2003), Partitioning of water flux in a Sierra Nevada ponderosa pine plantation, *Agric. For. Meteorol.*, 117(3–4), 173–192, doi:10.1016/S0168-1923(03)00062-5.
- Lin, G. H., and L. da S. L. Sternberg (1993), Hydrogen isotopic fractionation by plant roots during water uptake in coastal wetland plants., pp. 497–510, Academic Press Inc.

- Loik, M. E., D. D. Breshears, W. K. Lauenroth, and J. Belnap (2004), A multi-scale perspective of water pulses in dryland ecosystems: climatology and ecohydrology of the western USA, *Oecologia*, 141(2), 269–281, doi:10.1007/s00442-004-1570-y.
- Ludwig, J. A., B. P. Wilcox, D. D. Breshears, D. J. Tongway, and A. C. Imeson (2005), Vegetation patches and runoff-erosion as interacting ecohydrological processes in semiarid landscapes, *Ecology*, 86(2), 288–297, doi:10.1890/03-0569.
- Martín-Gómez, P., A. Barbeta, J. Voltas, J. Peñuelas, K. Dennis, S. Palacio, T. E. Dawson, and J. P. Ferrio (2015), Isotope-ratio infrared spectroscopy: a reliable tool for the investigation of plant-water sources?, *New Phytol.*, n/a–n/a, doi:10.1111/nph.13376.
- Moncrieff, J. B., P. G. Jarvis, and R. Valentini (2000), Canopy Fluxes, in *Methods in Ecosystem Science*, edited by O. E. Sala, R. B. Jackson, H. A. Mooney, and R. W. Howarth, pp. 161–180, Springer New York.
- Moran, M. S., R. L. Scott, T. O. Keefer, W. E. Emmerich, M. Hernandez, G. S. Nearing, G. B. Paige, M. H. Cosh, and P. E. O’Neill (2009), Partitioning evapotranspiration in semiarid grassland and shrubland ecosystems using time series of soil surface temperature., *Agric. For. Meteorol.*, 149(1), 59–72, doi:10.1016/j.agrformet.2008.07.004.
- Nadezhkina, N. et al. (2010), Trees never rest: the multiple facets of hydraulic redistribution, *Ecohydrology*, 3(4), 431–444, doi:10.1002/eco.148.
- Nelson, K., S. A. Kurc, G. John, R. Minor, and G. A. Barron-Gafford (2014), Influence of snow cover duration on soil evaporation and respiration efflux in mixed-conifer ecosystems, *Ecohydrology*, 7(2), 869–880, doi:10.1002/eco.1425.
- Newman, B. D., B. P. Wilcox, S. R. Archer, D. D. Breshears, C. N. Dahm, C. J. Duffy, N. G. McDowell, F. M. Phillips, B. R. Scanlon, and E. R. Vivoni (2006), Ecohydrology of water-limited environments: A scientific vision, *Water Resour. Res.*, 42(6), W06302, doi:10.1029/2005WR004141.
- Okin, G. S., A. J. Parsons, J. Wainwright, J. E. Herrick, B. T. Bestelmeyer, D. C. Peters, and E. L. Fredrickson (2009), Do Changes in Connectivity Explain Desertification?, *BioScience*, 59(3), 237–244, doi:10.1525/bio.2009.59.3.8.
- Owens, M. K., R. K. Lyons, and C. L. Alejandro (2006), Rainfall partitioning within semiarid juniper communities: effects of event size and canopy cover, *Hydrol. Process.*, 20(15), 3179–3189, doi:10.1002/hyp.6326.
- Perkins, K. S., J. R. Nimmo, A. C. Medeiros, D. J. Szutu, and E. von Allmen (2014), Assessing effects of native forest restoration on soil moisture dynamics and potential aquifer recharge, *Auwahi, Maui, Ecohydrology*, n/a–n/a, doi:10.1002/eco.1469.

- Potts, D. L., T. E. Huxman, J. M. Cable, N. B. English, D. D. Ignace, J. A. Eilts, M. J. Mason, J. F. Weltzin, and D. G. Williams (2006), Antecedent moisture and seasonal precipitation influence the response of canopy-scale carbon and water exchange to rainfall pulses in a semi-arid grassland, *New Phytol.*, 170(4), 849–860, doi:10.1111/j.1469-8137.2006.01732.x.
- Raz Yaseef, N., D. Yakir, E. Rotenberg, G. Schiller, and S. Cohen (2010), Ecohydrology of a semi-arid forest: partitioning among water balance components and its implications for predicted precipitation changes, *Ecohydrology*, 3(2), 143–154, doi:10.1002/eco.65.
- Reynolds, J. F. et al. (2007), Global Desertification: Building a Science for Dryland Development, *Science*, 316(5826), 847–851, doi:10.1126/science.1131634.
- Rodriguez-Iturbe, I. (2000), Ecohydrology: A hydrologic perspective of climate-soil-vegetation dynamics, *Water Resour. Res.*, 36(1), 3–9, doi:10.1029/1999WR900210.
- Sala, O. E., and W. K. Lauenroth (1982), Small rainfall events: An ecological role in semiarid regions, *Oecologia*, 53(3), 301–304, doi:10.1007/BF00389004.
- Sanchez-Mejia, Z. M., and S. A. Papuga (2014), Observations of a two-layer soil moisture influence on surface energy dynamics and planetary boundary layer characteristics in a semiarid shrubland, *Water Resour. Res.*, 50(1), 306–317, doi:10.1002/2013WR014135.
- Savenije, H. H. G. (2004), The importance of interception and why we should delete the term evapotranspiration from our vocabulary, *Hydrol. Process.*, 18(8), 1507–1511, doi:10.1002/hyp.5563.
- Scanlon, B. R., R. C. Reedy, D. A. Stonestrom, D. E. Prudic, and K. F. Dennehy (2005), Impact of land use and land cover change on groundwater recharge and quality in the southwestern US, *Glob. Change Biol.*, 11(10), 1577–1593, doi:10.1111/j.1365-2486.2005.01026.x.
- Schlesinger, W. H., and S. Jasechko (2014), Transpiration in the global water cycle, *Agric. For. Meteorol.*, 189–190, 115–117, doi:10.1016/j.agrformet.2014.01.011.
- Schmidt, M., K. Maseyk, C. Lett, P. Biron, P. Richard, T. Bariac, and U. Seibt (2012), Reducing and correcting for contamination of ecosystem water stable isotopes measured by isotope ratio infrared spectroscopy, *Rapid Commun. Mass Spectrom.*, 26(2), 141–153.
- Schultz, N. M., T. J. Griffis, X. Lee, and J. M. Baker (2011), Identification and correction of spectral contamination in 2H/1H and 18O/16O measured in leaf, stem, and soil water, *Rapid Commun. Mass Spectrom.*, 25(21), 3360–3368.

- Scott, R. L. (2010), Using watershed water balance to evaluate the accuracy of eddy covariance evaporation measurements for three semiarid ecosystems, *Agric. For. Meteorol.*, 150(2), 219–225, doi:10.1016/j.agrformet.2009.11.002.
- Scott, R. L., T. E. Huxman, D. G. Williams, and D. C. Goodrich (2006a), Ecohydrological impacts of woody-plant encroachment: seasonal patterns of water and carbon dioxide exchange within a semiarid riparian environment, *Glob. Change Biol.*, 12(2), 311–324, doi:10.1111/j.1365-2486.2005.01093.x.
- Scott, R. L., T. E. Huxman, W. L. Cable, and W. E. Emmerich (2006b), Partitioning of evapotranspiration and its relation to carbon dioxide exchange in a Chihuahuan Desert shrubland, *Hydrol. Process.*, 20(15), 3227–3243, doi:10.1002/hyp.6329.
- Scott, R. L., G. D. Jenerette, D. L. Potts, and T. E. Huxman (2009), Effects of seasonal drought on net carbon dioxide exchange from a woody-plant-encroached semiarid grassland, *J. Geophys. Res. Biogeosciences*, 114(G4), G04004, doi:10.1029/2008JG000900.
- Seager, R. et al. (2007), Model Projections of an Imminent Transition to a More Arid Climate in Southwestern North America, *Science*, 316(5828), 1181–1184, doi:10.1126/science.1139601.
- Senock, R. S., and J. M. Ham (1993), Heat balance sap flow gauge for small diameter stems, *Plant Cell Environ.*, 16(5), 593–601, doi:10.1111/j.1365-3040.1993.tb00908.x.
- Stannard, D. I. (1993), Comparison of Penman-Monteith, Shuttleworth-Wallace, and Modified Priestley-Taylor Evapotranspiration Models for wildland vegetation in semiarid rangeland, *Water Resour. Res.*, 29(5), 1379–1392, doi:10.1029/93WR00333.
- Thorburn, P. J., G. R. Walker, and J.-P. Brunel (1993), Extraction of water from Eucalyptus trees for analysis of deuterium and oxygen-18 : laboratory and field techniques, *Plant Cell Environ.*, 16(3), 269–277.
- Weltzin, J. F. et al. (2003), Assessing the Response of Terrestrial Ecosystems to Potential Changes in Precipitation, *BioScience*, 53(10), 941–952, doi:10.1641/0006-3568(2003)053[0941:ATROTE]2.0.CO;2.
- West, A. G., G. R. Goldsmith, P. D. Brooks, and T. E. Dawson (2010), Discrepancies between isotope ratio infrared spectroscopy and isotope ratio mass spectrometry for the stable isotope analysis of plant and soil waters, *Rapid Commun. Mass Spectrom.*, 24(14), 1948–1954, doi:10.1002/rcm.4597.
- Wilcox, B. P., D. D. Breshears, and M. S. Seyfried (2003), Rangelands, water balance on, *Environ. Water Sci.*, 791–794.

- Williams, D. G., and J. R. Ehleringer (2000), Intra- and interspecific variation for summer precipitation use in pinyon–juniper woodlands, *Ecol. Monogr.*, 70(4), 517–537, doi:10.1890/0012-9615(2000)070[0517:IAIVFS]2.0.CO;2.
- Wright, W. E. (2001), Delta-deuterium and delta-oxygen-18 in mixed conifer systems in the United States southwest: The potential of delta-oxygen-18 in *Pinus ponderosa* tree rings as a natural environmental recorder,
- Yepez, E. A., T. E. Huxman, D. D. Ignace, N. B. English, J. F. Weltzin, A. E. Castellanos, and D. G. Williams (2005), Dynamics of transpiration and evaporation following a moisture pulse in semiarid grassland: A chamber-based isotope method for partitioning flux components, *Agric. For. Meteorol.*, 132(3–4), 359–376, doi:10.1016/j.agrformet.2005.09.006.
- Yepez, E. A., R. L. Scott, W. L. Cable, and D. G. Williams (2007), Intraseasonal Variation in Water and Carbon Dioxide Flux Components in a Semiarid Riparian Woodland, *Ecosystems*, 10(7), 1100–1115, doi:10.1007/s10021-007-9079-y.

APPENDIX A: DIFFERENTIAL USE OF SHALLOW AND DEEP SOIL MOISTURE IN A  
SEMIARID SHRUBLAND: LINKING SAP FLOW AND STABLE ISOTOPE TECHNIQUES  
TO QUANTIFY TEMPORAL VARIABILITY

Daphne J. Szutu<sup>1,2</sup>, Shirley A. Papuga<sup>1</sup>

Targeted for publication in *Water Resources Research*

<sup>1</sup>School of Natural Resources and the Environment, University of Arizona, Tucson, AZ 85721

USA

<sup>2</sup>[daphne@email.arizona.edu](mailto:daphne@email.arizona.edu)

## **Abstract**

Semiarid shrublands and other dryland ecosystems are highly responsive to precipitation pulses that, depending on their size, differentially influence the distribution of moisture in the soil profile. The spatiotemporal distribution of soil moisture is expected to change in association with changes in the frequency and magnitude of dryland precipitation event. Many ecohydrological studies that examine plant water use strategies have assumed that the soil depths from which plants derive their moisture is a function of the root density profile, i.e., higher root density correlates with greater water uptake. However, recent field studies have shown that in dryland ecosystems, transpiration dynamics and plant productivity are largely a function of deep soil moisture available after large precipitation events regardless of where the majority of plant roots occur. Therefore, changes in precipitation pulses that alter the timing and magnitude of the availability of deep soil moisture are expected to have major consequences for dryland ecosystems. We suggest that adopting a hydrologically defined two-layer conceptual framework of the soil profile is more appropriate for understanding plant water use in dryland ecosystems than a framework that is based on rooting depth. Using the hydrologically defined two-layer framework, the objective of this study is to show how transpiration dynamics vary with the availability of deep soil moisture in dryland ecosystems and how the source of that moisture varies over time. We present eddy covariance, soil moisture, and sap flow measurements taken over 18 months in conjunction with precipitation, shallow soil, deep soil, and stem stable water isotope samples taken biweekly at a creosotebush-dominated shrubland ecosystem at the Santa Rita Experimental Range in southern Arizona. Results from both our sap flow measurements and our stable isotope analysis support that transpiration is associated with the availability of deep soil moisture. While this is especially true in the summer when transpiration rates are highest,

our results suggest that transpiration can also be substantial in wet winters in which the deep soil layer is wetter than average. When transpiration rates are highest, both deep moisture and stem water are more isotopically similar to winter precipitation than summer precipitation, suggesting that winter precipitation can play an important role in supporting these ecosystems. Our study suggests that integrating sap flow and stable isotope techniques with soil moisture measurements offers a better understanding of how plant water use strategies shift with changes in source water and its availability than either technique could offer on its own. We have contributed to understanding where precipitation pulses are distributed in the soil moisture profile and when these pulses are used by plants in dryland ecosystems. Ultimately these findings should help to improve the representation of drylands within regional and global models of land surface atmosphere exchange and their linkages to the hydrologic cycle.

**Key words:** plant water use, transpiration, sap flow, deep soil moisture, stable water isotopes

## 1. Introduction

Water-limited ecosystems currently account for about 40 % of terrestrial biomes, and this area is projected to expand with current climate trends [Okin *et al.*, 2009]. These drylands also experience high population growth [Reynolds *et al.*, 2007], and future water management will need to balance water supply for both urban and ecological demand. Unlike their energy-limited counterparts that are driven by temperature cues, water-limited ecosystems experience pulses of moisture that drive plant productivity [Huxman *et al.*, 2004; Loik *et al.*, 2004]. Pulse size and frequency vary from event to event and over the year, and these variations affect biological and physical processes in the drylands [Sala and Lauenroth, 1982; Kurc and Small, 2007; Raz Yaseef *et al.*, 2010]. Further, plant response to pulse rainfall is not linear [Ogle and Reynolds, 2004] and exhibits memory effects, where grassland systems may be more responsive to current-year drought and rainy periods, and woody systems may have a lagged response to current-year precipitation patterns [Jenerette *et al.*, 2012; Ogle *et al.*, 2015]. Climate models project long-term changes in the frequency and magnitude of precipitation events in water-limited ecosystems [Easterling *et al.*, 2000; Seager *et al.*, 2007]; specifically in the Western U.S., this could include decreases in the amount of non-summer precipitation [Goodrich *et al.*, 2008] and less snowfall [Knowles *et al.*, 2006; Barnett *et al.*, 2008]. These changes are likely to exacerbate changes in vegetation dynamics and partitioning of water resources [e.g., Potts *et al.*, 2006], affect the water supply in water-limited ecosystems [e.g., Knapp *et al.*, 2008], and affect strategies for ecological restoration in dryland systems [e.g., Merino-Martín *et al.*, 2012].

Recently, the soil moisture balance has emerged as a powerful means of linking the interactions and feedbacks between ecosystem productivity, vegetation distribution, and regional water

balance [Rodriguez-Iturbe, 2000; Weltzin *et al.*, 2003; Scott *et al.*, 2014]. In dryland ecosystems, long-term changes in the frequency and magnitude of precipitation events [Easterling *et al.*, 2000; Seager *et al.*, 2007] are expected to have an effect on moisture distribution in the soil profile [Weltzin *et al.*, 2003; Loik *et al.*, 2004]. For example, an increase in the number of larger rainfall events could offer more occurrences in which the deep soil moisture layer is recharged, i.e. water that is out of reach of atmospheric evaporative demand and is readily available for plant water use [Scott *et al.*, 2006b; Kurc and Small, 2007].

While plants primarily interact with the soil and affect the soil moisture balance through their roots, quantifying from where in the soil profile roots extract moisture has been challenging due to limitations in monitoring technologies [e.g., Zarebanadkouki *et al.*, 2013] and confounding physical processes such as hydraulic redistribution [Burgess *et al.*, 1998; Nadezhdina *et al.*, 2010]. Despite these complexities, particularly in desert ecosystems, Walter's Two-Layer Hypothesis of niche partitioning [Walter, 1939], in which deeper-rooted plants such as trees generally make use of deeper soil moisture and shallower-rooted plants such as grasses generally make use of shallow soil moisture, has dominated ecohydrological thinking [e.g., Ogle and Reynolds, 2004; Holdo, 2013; Germino and Reinhardt, 2014]. In fact, in a highly referenced study, Ehleringer *et al.* [1991] make use of Walter's Hypothesis to support that deep-rooted desert plants make use of deep soil moisture and shallow-rooted desert plants make use of shallow soil moisture. Their analysis assumed that because deep-rooted desert plants look isotopically similar to winter rains, therefore deep-rooted desert plants are using winter moisture available from the deep soil layers; conversely, because shallow-rooted desert plants look isotopically similar to summer rains, therefore shallow-rooted desert plants are using summer

moisture available from the shallow soil layers. However, their study did not measure the isotopic composition of the moisture in the shallow and deep soil layers and only assumed the use of water at specific depths based on root profiles.

Additional recent research has demonstrated that the density profile of plant roots does not necessarily correspond to the depth of water that the plants are actively using for photosynthesis and transpiration. For example, regardless of their rooting profile, in shallow-rooted desert grassland and deeper-rooted desert shrublands, plant response was always most strongly associated with moisture deep in the soil profile (i.e., > 37.5 cm) [Kurc and Small, 2007; Kurc and Benton, 2010; Cavanaugh et al., 2011]. Furthermore, stable water isotope research has illustrated that roots can be hydraulically isolated from the soil, i.e., root water was isotopically different from that of the surrounding soil [Thorburn and Ehleringer, 1995]. Clearly the presence of roots alone does not indicate where plants are extracting water from in the soil profile, so understanding plant water use strategies must go beyond understanding the physical distribution of plant roots.

Based on previous ecohydrological research in water-limited ecosystems, Sanchez-Mejia and Papuga [2014] proposed working within a hydrologically defined two-layer framework in which shallow soil moisture (0-20 cm) is primarily lost to  $E$  [Kurc and Small, 2004; Gowing et al., 2006], while deep soil moisture (20-60 cm) is primarily used for transpiration [Kurc and Small, 2007; Cavanaugh et al. 2011]. In this conceptual framework, four soil moisture cases are possible [Sanchez-Mejia and Papuga, 2014]: Case 1 with a dry shallow layer and a dry deep layer; Case 2 with a wet shallow layer and a dry deep layer; Case 3 with a wet shallow layer and

a wet deep layer; and Case 4 with a dry shallow layer and a wet deep layer (Figure 1a). This framework shifts the focus of the two layers from the physical location of the plant roots such as in Walter's Hypothesis to the location of soil moisture availability and the physical processes dominating the movement of soil moisture.

To make use of this hydrologically defined two layer conceptual framework, we make the assumption that there are measureable isotopic differences between the shallow and deep soil layers based on isotopic differences between small storms and large storms as a result of the "amount effect" [Dansgaard, 1964; Rozanski *et al.*, 1993] and as a result of isotopic fractionation that occurs during water efflux processes (Figure 1b). Precipitation falling during a small storm is enriched (more positive  $\delta^{18}\text{O}$  and  $\delta^2\text{H}$  values) relative to a large storm because of the amount effect [Dansgaard, 1964; Rozanski *et al.*, 1993] caused by both evaporation [e.g., Dansgaard, 1964; Lee and Fung, 2008] and exchange processes [e.g., Friedman *et al.*, 1962; Field *et al.*, 2010]. Therefore, we expect small storms to have moisture with relatively higher  $\delta^{18}\text{O}$  and  $\delta^2\text{H}$  values compared to large storms, and that these small storms will wet only the shallow soil layer [Sala and Lauenroth, 1982; Kurc and Small, 2007]. On the other hand, a large storm will wet both the shallow and deep soil layers [Sanchez-Mejia and Papuga, 2014] with a moisture that has relatively low  $\delta^{18}\text{O}$  and  $\delta^2\text{H}$  values. Evaporation will deplete shallow soil moisture and preferentially evaporate isotopically lighter water molecules, thus leaving water with relatively higher  $\delta^{18}\text{O}$  and  $\delta^2\text{H}$  values in the shallow soil layer [e.g., Kulmatiski *et al.*, 2006; Newman *et al.*, 2010]. We expect the combination of these processes through time will lead to a soil profile that has isotopically distinct shallow and deep soil moisture layers, with the shallow soil moisture tending to be more enriched in  $^{18}\text{O}$  and  $^2\text{H}$  than the deep soil moisture. Within this

framework, assuming shallow soil moisture and deep soil moisture differ in their water isotopic signatures, the soil layer from which desert plants are drawing their moisture can be identified and potentially linked to summer or winter precipitation [*Ehleringer et al.*, 1991; *Ingraham et al.*, 1991; *Williams and Ehleringer*, 2000].

In this study, we use the hydrologically defined two-layer conceptual framework with a combination of sap flow and stable water isotopes techniques over an 18-month period in a semiarid shrubland of southeastern Arizona to answer three main questions:

1. Is transpiration limited to periods when deep soil moisture is available, and how does this dependence vary throughout the year?
2. Are shallow and deep soil moisture isotopically different, and how does this difference vary throughout the year?
3. Are stable water isotopes an adequate measure of determining sources of plant water use in a semiarid shrubland?

Here, we combine discrete isotopic sampling with continuous measurements of transpiration and soil moisture through the rooting zone. Combining these measurements yields a more detailed image of plant water use, both spatially and temporally, than either sap flow or isotopic analyses could provide alone. Understanding the differential water use of plants in desert ecosystems is becoming increasingly important as we anticipate how they will be able to respond to changes in the precipitation regime that will undoubtedly create changes in the depths at which soil moisture is available and the timing of the soil moisture availability associated with those depths.

## **2. Methods**

## 2.1 Study Site: Santa Rita Experimental Range

The Santa Rita Experimental Range (SRER) is located 60 km south of Tucson, Arizona at the foot of the northwestern Santa Rita Mountains. Our research was conducted at The Santa Rita Creosote (SRC) AmeriFlux Site (31.9083 N, 110.8395 W), located in the northern portion of SRER at an elevation of about 950 m. An eddy covariance tower provided half-hourly micro-meteorological measurements [Sanchez-Mejia and Papuga, 2014]. Since at least 1934, creosotebush (*Larrea tridentata*) has been the dominant species near the northern border of SRER [Humphrey and Mehrhoff, 1958]. The SRC experiences cool winters, warm summers, and a bimodal precipitation pattern, with about 60% of the precipitation falling during the North American Monsoon (July through September) and about 20% of the precipitation falling during the winter rainy season (December through February) [Sanchez-Mejia and Papuga, 2014]. The average annual precipitation is about 345 mm, and the average annual temperature is about 20 °C [Sanchez-Mejia and Papuga, 2014]. Vegetation cover is about 24%, with creosotebush as the dominant vegetation (14% cover) and the remaining 10% accounted for by small grasses, forbs, and cactus [Kurc and Benton, 2010]. The soil type is sandy loam with no caliche layer (to at least 1 m depth) [Kurc and Benton, 2010]. The estimated depth to groundwater near our site is greater than 70 m [Eastoe et al., 2004].

## 2.2 Soil Moisture

At SRC, six soil moisture profiles are located within the eddy covariance tower footprint and provided half hourly soil moisture data. Three profiles are located under creosotebush canopy and three are located in the inter-canopy “bare” soil. Soil moisture was measured with water content reflectometers (CS616, Campbell Scientific, Inc., Logan, UT, USA), with each sensor

assumed to be measuring a source area with radius 7.5 cm [*Sanchez-Mejia and Papuga, 2014*].

At SRC, seven depths were measured for soil moisture in each profile: 2.5, 12.5, 22.5, 37.5, 52.5, 67.5, 82.5 cm.

Soil moisture profiles were averaged together and weighted based on fractional cover of canopy and inter-canopy spaces. Then, the profiles were divided into shallow (0 -20 cm) and deep (20-60 cm) soil moisture layers per the two-layer soil moisture conceptual framework [*Sanchez-Mejia and Papuga, 2014*]. To calculate soil moisture in the two different soil moisture layers, we used weighted averages based on the relative contribution of each sensor in the shallow or deep layers of the soil layer. At SRC, average soil water content was calculated with the following equations [*Sanchez-Mejia and Papuga, 2014*] :

$$\theta_{shallow} = 0.33\theta_{2.5} + 0.5\theta_{12.5} + 0.17\theta_{22.5} \quad (1)$$

$$\theta_{deep} = 0.25\theta_{22.5} + 0.375\theta_{37.5} + 0.375\theta_{52.5} \quad (2)$$

$\theta_{2.5}$  is the soil water content at 2.5 cm,  $\theta_{12.5}$  is the soil water content at 12.5 cm, etc.

Soil moisture Cases for the conceptual framework are defined by soil moisture thresholds set in *Sanchez-Mejia and Papuga* [2014] (0.1229 % for  $\theta_{shallow}$  and 0.1013 % for  $\theta_{deep}$ ), resulting in n = 306 days for Case 1, n = 10 days for Case 2, n = 164 days for Case 3, and n = 68 days for Case 4 over our 18-month study period. Further, we divide each year into soil moisture seasons.

Following *Sanchez-Mejia and Papuga* [2014], we defined two distinct seasons: Winter (December – February), and Summer (July - September). All four soil moisture Cases were found in both Winter and Summer seasons. A total of 158 days were classified as Winter: 51 days fell into Case 1 (32%), 4 days fell into Case 2 (4%), 97 days fell into Case 3 (61%), and 6

days fell into Case 4 (4%). A total of 79 days were classified as Summer: 26 days fell into Case 1 (33%), 2 days fell into Case 2 (2%), 25 days fell into Case 3 (32%), and 26 days fell into Case 4 (33%).

### **2.3 Transpiration and Evaporation**

Heat balance sap flow sensors (DynaGauge, Dynamax Inc., Houston, TX, USA) were used to measure half hourly sap flow rate and to continuously monitor transpiration. These sensors use an energy budget to interpret heat fluxes from a constant heat source [*Senock and Ham, 1993*]. Eight sap flow sensors were installed on four creosotebush shrub, with two sensors on each shrub. The sizes of the sensors were 5 mm, 9 mm, and 16 mm (designed to be installed on stems with the respective diameters). Two shrubs had two 16 mm sensors each, and the other two shrubs each had one 5 mm and one 9 mm sensor. To reduce the effect of irradiation heat on the sensors, the sensors were covered with reflective bubble wrap, and the length of trunk below the sensor were wrapped with several layers of heavy-duty aluminum foil [*J. Ji, pers. comm.; Langensiepen et al., 2012*]. Stand-level transpiration was calculated by scaling the sap flow rate with a site-specific average stem density and percent cover [*Cavanaugh et al., 2011*]. Evaporation was estimated by subtracting transpiration (measured from the sap flow system) from evapotranspiration (measured by the eddy covariance tower).

### **2.4 Isotopic Field Campaigns**

From July 2014 through March 2015, plant tissue, soil samples, and precipitation samples were collected approximately every two weeks at three collection sites within the footprint of the eddy covariance tower. These three collection sites were co-located with three installed time-lapse

phenological cameras [Kurc and Benton, 2010], and all isotopic samples were collected within 10 m of the phenological camera at each collection site. Nine plants total, three at each collection site, of an intermediate size class (height between 1.5 and 2 m) were sampled on each collection date; different plants were chosen at each collection date. On each plant, a mature, suberized stem was collected with clippers to minimize effects of stem-water evaporation [Dawson and Ehleringer, 1993]. Soil samples were collected destructively every 5 cm down to 45 cm depth using a 5 cm diameter split-core soil sampler (AMS, Inc., American Falls, ID, USA) [e.g., Williams and Ehleringer, 2000]. Two soil cores were sampled on each collection date, one under the canopy and one in the inter-canopy space. The stem and soil samples were immediately sealed in a 20 ml glass vial with a polycone cap, and the vial was wrapped with parafilm. Four precipitation samples were also collected within the tower footprint, two samples located under the creosotebush canopy and two samples located in the inter-canopy space. The collection bottles (250 ml HDPE bottles with a funnel inserted into the cap) were prepped with a 5 mm layer of mineral oil to minimize isotopic enrichment through evaporation [e.g., Williams and Ehleringer, 2000; West et al., 2007]. All samples collected were placed immediately in a cooler with ice until transported back to the lab where they were stored in a refrigerator until analysis [e.g., Hopkins et al., 2014]. In the lab, approximately 20 ml of precipitation from each HDPE collection bottle was filtered through a cellulose filter into a 20 ml glass vial with polycone cap. The vial was wrapped with parafilm and stored in the lab refrigerator.

Samples were analyzed using an isotopic water analyzer (Picarro L2130-i) that uses an Induction Module-Cavity Ring-Down Spectroscopy (IM-CRDS) system [e.g., Crosson, 2008; Leffler and

Welker, 2013] and calibrated against the primary isotopic standards of Vienna Standard Mean Ocean Water 2 and Standard Light Antarctic Precipitation 2.

### **3. Results**

#### **3.1 Time Series**

Summer precipitation for our study period totaled 237 mm. Our observation period included two Winter seasons (Dec 2013 - Feb 2014; Dec 2014 - Feb 2015). These two Winter seasons had quite different precipitation patterns. In Winter 2013-2014, the total precipitation was about 25 mm, distributed across 3 day of precipitation, but in Winter 2014-2015, the total precipitation was about 115 mm, distributed across 18 days of precipitation (Figure 2a). Winter 2014-2015 had more frequent rain events with an average smaller magnitude (Figure 2a). Vapor pressure deficit (VPD) was low during and immediately following rainfall and was generally higher in the summer than in the winter (Figure 2a), which is expected because higher temperatures in the summer raises the saturation vapor pressure.

Shallow soil moisture ranged from 0.06 to 0.21 m<sup>3</sup> m<sup>-3</sup>, and deep soil moisture ranged from 0.08 to 0.16 m<sup>3</sup> m<sup>-3</sup>. Shallow soil moisture increased after both small and large rain events (Figure 2b, see November and December 2013), but deep soil moisture increased only after large rain events only (Figure 2b, see March 2014) or after a series of small rain events (Figure 2b, see January 2015). Overall, there were no substantial differences between average shallow (~ 0.13 m<sup>3</sup> m<sup>-3</sup>) or deep (~ 0.11 m<sup>3</sup> m<sup>-3</sup>) soil moisture in the Summer and Winter seasons for our study period. However, differences in precipitation resulted in very different ranges of soil moisture between the two Winter seasons themselves: Winter 2013-2014 had a maximum shallow and deep soil

moisture of 0.16 and 0.11 m<sup>3</sup> m<sup>-3</sup>, respectively, whereas Winter 2014-2015 had a maximum shallow and deep soil moisture of 0.21 and 0.16 m<sup>3</sup> m<sup>-3</sup> (Figure 2b).

*ET* averaged 0.5 mm day<sup>-1</sup> over the observation period, with a maximum of 3.3 mm day<sup>-1</sup>. *T* averaged 0.4 mm day<sup>-1</sup>, with a maximum of 0.8 mm day<sup>-1</sup> (Figure 2c). While *ET* always increased immediately following rain events, the contribution of *T* to *ET*, i.e., the ratio *T/ET*, was low immediately following a rain event, only increasing a few days after the rain event (Figure 2c). As expected, Summer averages of *T* (0.5 mm day<sup>-1</sup>) and *ET* (1.2 mm day<sup>-1</sup>) were higher than Winter averages of *T* (0.3 mm day<sup>-1</sup>) and *ET* (0.5 mm day<sup>-1</sup>). Interestingly, the different precipitation patterns of our two Winter seasons resulted in different average *ET* but similar average *T*. The "drier" Winter in 2013-2014 had an average *ET* about 0.2 mm lower than the "wetter" Winter in 2014-2015, while the average *T* was only about 0.02 mm lower.

The δ<sup>2</sup>H values of precipitation and stem samples had an increasing trend from July through the middle of September (Figure 2d). Later in September and in October, precipitation values of δ<sup>18</sup>O and δ<sup>2</sup>H dropped (Figure 2d, δ<sup>18</sup>O values not shown), reflecting the influence of isotopically light tropical storms at that time [Gedzelman and Lawrence, 1990; Eastoe et al., 2015]. The δ<sup>2</sup>H values of stem samples tended to decrease in conjunction with the precipitation before increasing again, a pattern which appears to continue throughout the winter (Figure 2d). The δ<sup>2</sup>H values of shallow soil samples were generally higher and temporally dynamic than for deep soil samples (Figure 2e). The δ<sup>2</sup>H values of shallow soil samples were only lower than for deep soil samples when associated with post-monsoon isotopically lighter precipitation events (e.g., Figures 3d and 3e; late Sept, early Dec, early Feb), suggesting those events mainly recharge the shallow soil.

Deuterium excess (*d-excess*) is defined as  $d - excess = \delta^2H - 8 * \delta^{18}O$  [Dansgaard, 1964]. Points that fall on the Global Meteoric Water line (GMWL) have a *d-excess* of 10 ‰, and variations away from this indicate variation away from the GMWL [Dawson and Simonin, 2011; Zhao et al., 2014]. The *d-excess* of stem samples (Figure 2f) appear to converge toward the *d-excess* of precipitation samples after large precipitation events and then deviate away from the precipitation *d-excess* in between these large precipitation events. *D-excess* of the shallow soil samples was more positive and closer to *d-excess* of precipitation samples than the *d-excess* of the deep soil samples from mid-December through early February (Figure 2g), possibly suggesting that shallow soil moisture is most similar to precipitation and least influenced by evaporation or other external factors during this period [Gat and Airey, 2006].

### 3.2 Relationships between Soil Moisture and Transpiration

In both Winter and Summer seasons, more of the variation in  $T$  is explained by  $\theta_{deep}$  ( $R^2=0.20$  in Winter and  $R^2=0.36$  in Summer) than  $\theta_{shallow}$  ( $R^2=0.02$  in Winter and  $R^2=0.08$  in Summer) (Figures 3a and 3b; Table 1). In addition, more of the variation in  $E$  is explained by  $\theta_{shallow}$  ( $R^2=0.37$  in Winter and  $R^2=0.45$  in Summer) than  $\theta_{deep}$  ( $R^2=0.30$  in Winter and  $R^2=0.17$  in Summer) (Figures 3c and 3d; Table 1). However, the relationship between  $ET$  and  $\theta_{shallow}$  and  $ET$  and  $\theta_{deep}$  differ between Winter and Summer. In Winter, more of the variation in  $ET$  is explained by  $\theta_{deep}$  ( $R^2=0.44$ ) than  $\theta_{shallow}$  ( $R^2=0.25$ ); in Summer, more of the variation in  $ET$  is explained by  $\theta_{shallow}$  ( $R^2=0.48$ ) than  $\theta_{deep}$  ( $R^2=0.29$ ) (Figures 4e and 4f; Table 1). These results suggest that different processes are dominant at different times of the year: in Winter,  $T$  is the dominant process in  $ET$ , but in Summer,  $E$  is the dominant process in  $ET$ .

Very few days were classified as Case 2 (wet shallow layer, dry deep layer;  $n_{\text{winter}} = 4$ ;  $n_{\text{summer}} = 2$ ) or Case 4 in the winter (dry shallow layer, dry deep layer;  $n_{\text{winter}} = 6$ ). Although the number of days classified as Case 1 (dry shallow layer, dry deep layer;  $n_{\text{winter}} = 51$ ;  $n_{\text{summer}} = 26$ ) would not necessarily exclude it from data analysis, we do not expect to make meaningful interpretations because there is not much water available for either  $T$  or  $E$ . Therefore, we focus on Case 3 (wet shallow layer and wet deep layer;  $n_{\text{winter}} = 97$ ;  $n_{\text{summer}} = 25$ ) (Figure 5; Table 1), but also include analyses for Case 4 (Table 1).

For Winter Case 3, the linear regression relationships between the two independent variables ( $\theta_{\text{shallow}}$  and  $\theta_{\text{deep}}$ ) and the three response variables ( $ET$ ,  $T$ ,  $E$ ) were similar to the linear regression relationships for the whole Winter season (Figures 3 and 4; Table 1). Variation in  $\theta_{\text{deep}}$  explained more of the variation in  $ET$  and  $T$  ( $R^2=0.32$  and  $0.35$ , respectively) relative to variation in  $\theta_{\text{shallow}}$  ( $R^2=0.04$  and  $0.13$ , respectively); variation in  $\theta_{\text{shallow}}$  ( $R^2 = 0.16$ ) explained slightly more of the variation in  $E$  than  $\theta_{\text{deep}}$  ( $R^2 = 0.14$ ). Additionally, for Winter Case 3, all of the six linear relationships analyzed had significant regression line slopes at  $\alpha = 0.05$  (Table 1). In comparison, for Summer Case 3, most of the linear regression relationships were much weaker: only two of the linear relationships analyzed ( $T$  and  $\theta_{\text{shallow}}$ ,  $E$  and  $\theta_{\text{shallow}}$  were significant at  $\alpha = 0.05$  and one linear regression ( $T$  and  $\theta_{\text{deep}}$ ) was significant at  $\alpha = 0.10$ . These statistically weaker relationships could be because we had more data to analyze in Winter ( $n = 97$ ) than in Summer ( $n = 25$ ) (Table 1). Interestingly, in Summer Case 3,  $\theta_{\text{shallow}}$  ( $R^2 = 0.28$ ) explained more of the variation in  $T$  than  $\theta_{\text{deep}}$  ( $R^2 = 0.11$ ), and the linear regression relationship between  $\theta_{\text{shallow}}$  and  $T$  had a significant, negative slope ( $m = -3.61$ ,  $p\text{-value} = 0.01$ ). This is in contrast to the analysis of all of

Summer, where  $\theta_{\text{deep}}$  explained about 32% more of the variation in  $T$  than  $\theta_{\text{shallow}}$ , and the linear regression relationship between  $\theta_{\text{shallow}}$  and  $T$  had a significant, positive slope ( $m = 1.47$ ,  $p\text{-value} = 0.01$ ). This seems to indicate that during Summer Case 3 days,  $T$  is not necessarily limited by the amount of soil moisture available, but by meteorological conditions (i.e., temperature and VPD) as shallow soil moisture evaporates, decreases VPD above the soil, and decreases atmospheric demand of water at the plant stomata. In Summer Case 4, there are significant relationships between  $ET$  and  $\theta_{\text{shallow}}$ ,  $T$  and  $\theta_{\text{deep}}$ , and  $E$  and  $\theta_{\text{shallow}}$  at  $\alpha = 0.05$ .

Notably, for Case 3 there is a significant, negative relationship between  $\theta_{\text{shallow}}$  and  $T$  for both Winter ( $m = -3.61$ ,  $p\text{-value} = 0.01$ ) and Summer ( $m = -2.25$ ,  $p\text{-value} < 0.01$ ) seasons. This relationship can be explained by examining the relationship between  $\theta_{\text{shallow}}$ , VPD, and  $T$  (Figure 5). Immediately following a rain event, the shallow soil moisture will be recharged (e.g., Figure 2b). However, in the following few days as most of the shallow soil moisture is evaporated, relative humidity increases and VPD decreases: the linear regression between shallow soil moisture and VPD has a significantly negative slope of  $-10.68$  ( $p\text{-value} < 0.01$ ; Figure 5a). As VPD increases, the rate of  $T$  increases because there is greater atmospheric demand of water from the stomata: the linear regression between VPD and  $T$  has a significantly positive slope of  $0.07$  ( $p\text{-value} < 0.01$ ; Figure 5b). This relationship between  $\theta_{\text{shallow}}$ , VPD, and  $T$  offers an explanation for the negative relationship between  $\theta_{\text{shallow}}$  and  $T$ .

### 3.3 Analysis of Stable Water Isotopes

The overall average of precipitation samples had a  $\delta^{18}\text{O}$  value of  $-5.4\text{‰}$  and a  $\delta^2\text{H}$  value of  $-46\text{‰}$ . The average of Summer precipitation samples had a  $\delta^{18}\text{O}$  value of  $-4.6\text{‰}$  and a  $\delta^2\text{H}$  value

of -45 ‰, whereas the average of Winter precipitation samples had a  $\delta^{18}\text{O}$  value of -7.6 ‰ and a  $\delta^2\text{H}$  value of -57 ‰ (Figure 6; note: volume-weighted averages of Summer and Winter precipitation samples, respectively, had a  $\delta^{18}\text{O}$  value of -4.6 ‰ and -7.2 ‰ and a  $\delta^2\text{H}$  value of -49 ‰ and -53 ‰). Average Summer precipitation was more enriched in  $^{18}\text{O}$  and  $^2\text{H}$ . These averages are consistent with other published values of long-term Tucson precipitation: Summer  $\delta^{18}\text{O}$  averages -6.0 ‰ and  $\delta^2\text{H}$  averages -43 ‰, and Winter  $\delta^{18}\text{O}$  averages -8.9 ‰ and  $\delta^2\text{H}$  averages -56 ‰ [Wright, 2001].

The overall average of shallow soil samples had a  $\delta^{18}\text{O}$  value of -5.0 ‰ and a  $\delta^2\text{H}$  value of -53 ‰. The averages of Summer and Winter shallow soil samples, respectively, had a  $\delta^{18}\text{O}$  value of -2.5 ‰ and -7.5 ‰ and a  $\delta^2\text{H}$  value of -48 ‰ and -63 ‰ (Figure 6). Average Summer shallow soil samples were more enriched in  $^2\text{H}$  than average Winter shallow soil samples. This also holds true when only considering Case 3, i.e., the average of Case 3 shallow soil samples has a higher  $\delta^2\text{H}$  value in the Summer than in the Winter (Figure 7). Because Summer precipitation is more enriched in  $^2\text{H}$  than Winter precipitation, Summer shallow soil moisture is likely recharged by Summer precipitation, whereas the Winter shallow soil moisture is likely recharged by Winter precipitation.

The overall average of deep soil samples had a  $\delta^{18}\text{O}$  value of -2.6 ‰ and a  $\delta^2\text{H}$  value of -51 ‰. The averages of Summer and Winter deep soil samples, respectively, were a  $\delta^{18}\text{O}$  value of -2.9 ‰ and -2.4 ‰ and a  $\delta^2\text{H}$  value of -59 ‰ and -47 ‰. Unlike the average shallow soil samples, the Summer deep soil samples were more depleted in  $^2\text{H}$  than the Winter deep soil samples. Again, this also holds true when only considering Case 3, i.e., the average of Case 3 deep soil

samples has a lower  $\delta^2\text{H}$  value in the Summer than in the Winter (Figure 7). Because Summer precipitation is more enriched in  $^2\text{H}$  than Winter precipitation, Summer deep soil moisture is likely recharged in part by Winter precipitation and Winter deep soil moisture is likely recharged in part by Summer precipitation.

The overall average of plant stem samples had  $\delta^{18}\text{O}$  value of 2.3 ‰ and a  $\delta^2\text{H}$  value of -39 ‰. The averages of Summer and Winter stem samples, respectively, had  $\delta^{18}\text{O}$  values of 3.0 ‰ and 1.5 ‰ and  $\delta^2\text{H}$  values of -39 ‰ and -41 ‰. In Winter, the stem samples had slightly lower  $\delta^2\text{H}$  values relative to Summer stem samples. However, when only Case 3 data were considered, the average of Summer stem sample had slightly lower  $\delta^2\text{H}$  values than the average of Winter stem samples (Figure 7). This unexpected difference could be caused by a potential plant sample “outlier” in Case 1 that had a  $\delta^2\text{H}$  value of -7 ‰. With all Cases considered, this “outlier” point pulls the Summer stem average more positive, therefore the Summer stem average has a higher  $\delta^2\text{H}$  value than the Winter stem average. The average stem values of  $\delta^{18}\text{O}$  and  $\delta^2\text{H}$  did not fall between shallow and deep soil moisture as expected; average stem  $\delta^{18}\text{O}$  and  $\delta^2\text{H}$  values were higher than average shallow and deep soil  $\delta^{18}\text{O}$  and  $\delta^2\text{H}$  values. The range of stem sample  $\delta^2\text{H}$  values were -63 to -7 ‰, but if we exclude the stem sample with the highest  $\delta^2\text{H}$  value, then the range of stem sample  $\delta^2\text{H}$  values were -63 to -25 ‰. In that case, the  $\delta^2\text{H}$  range of both deep soil samples (-73 to -37 ‰) and plant samples (-63 to -25 ‰) had a similar  $\delta^2\text{H}$  range of about 37 ‰. The  $\delta^2\text{H}$  range of both precipitation samples (-101 to -16 ‰) and shallow soil samples (-110 to -26 ‰) had a similar  $\delta^2\text{H}$  range of about 85 ‰.

Using an unpaired t-test assuming unequal variance, the only statistically significantly different averages were between deep soil samples and stem samples for overall (p-value <0.01) and in Summer (p-value <0.01). However, again, the range of  $\delta^2\text{H}$  values of deep soil samples and stem samples overlapped much more than the  $\delta^2\text{H}$  values of stem samples compared to shallow soil samples or precipitation samples. Most of the variables tested under different time sub-periods (Winter season, all of Case 2 and Case 4, and most of Case 1 and Case 3 data) did not meet normality assumptions or had less than the minimum number of observations required for the Anderson-Darling normality test [e.g., *Hedberg et al.*, 2012; *Reyes Gómez et al.*, 2015].

Precipitation samples fell close to the LMWL, with the summer samples tending more to the right of the LMWL (Figure 8a), which we expect because precipitation arriving during the warmer summer months is more enriched in the heavy isotopes  $^{18}\text{O}$  and  $^2\text{H}$  relative to precipitation during the cooler winter months [*Dansgaard*, 1964]. An overall precipitation regression line is  $\delta^2\text{H} = 7.8 * \delta^{18}\text{O} - 3.8$  (Table 2). The shallow soil samples were similar to the precipitation isotope samples in that they fell along the LMWL, with the summer shallow soil samples tending more to the right of the winter shallow soil samples (Figure 8b). Again, this is what we expect because the shallow soil undergoes more evaporative enrichment during the warmer summer months than during the cooler winter months [*Gat*, 1996]. The overall shallow soil regression line is  $\delta^2\text{H} = 5.1 * \delta^{18}\text{O} - 28$  (Table 2). The daily deep soil isotope samples all fell to the right of the LMWL (Figure 8c), which seems to indicate that shallow and deep soil moisture are isotopically different and that deep soil moisture may be influenced by processes such as plant discrimination against heavier isotopes ( $^{18}\text{O}$  and  $^2\text{H}$ ) during water uptake [e.g., *Lin and Sternberg*, 1993; *Ellsworth and Williams*, 2007]. In addition, the overall deep soil regression

line is  $\delta^2\text{H} = 2.9 * \delta^{18}\text{O} - 43$  (Table 2), and a regression slope of about 3 can indicate water exposed to a low humidity, evaporative environment, such as soil water in water-limited environments [Gat, 1996; West *et al.*, 2007]. The stem samples fell along the deep soil regression line, and similar to the deep soil samples, and do not display a consistent seasonal bias like the precipitation and shallow soil samples (Figure 8d).

### **3.4 Relationship between Transpiration and Stable Water Isotopes**

To integrate transpiration and stable water isotopes, we examined the linear regressions between  $\delta^2\text{H}$  values of precipitation, shallow soil, deep soil, and plant samples and three-day sums of  $T$  (the two days prior to and including the isotope sampling date). The  $\delta^2\text{H}$  range of precipitation and shallow soil were similar (Figures 9a and 9b), while the  $\delta^2\text{H}$  range of deep soil and plant samples are similar, especially if the plant sample with an unusually high  $\delta^2\text{H}$  value ( $\delta^2\text{H} = -7$  ‰) is excluded (Figure 9c and 9d). Precipitation  $\delta^2\text{H}$  values have a positive trend with increasing  $T$  (Figure 9a); this is expected because of the higher  $T$  during Summer when  $\delta^2\text{H}$  values of precipitation are generally more positive relative to Winter precipitation. The shallow soil  $\delta^2\text{H}$  values do not seem to have any linear trend with  $T$  (Figure 9b). The only statistically significant linear regression is between  $\delta^2\text{H}$  values of deep soil and  $T$  ( $p$ -value  $< 0.01$ ; Figure 9c, Table 3). The negative slope of the regression line indicates that higher  $T$  (which occurs in the Summer) is correlated with a more negative  $\delta^2\text{H}$  whereas lower  $T$  is correlated with a more positive  $\delta^2\text{H}$ . Because Winter precipitation tends to have a more negative  $\delta^2\text{H}$  value than Summer precipitation, higher  $T$  is associated with deep soil  $\delta^2\text{H}$  values that are more similar to Winter precipitation than to Summer precipitation (Figure 6 and 9c). This result seems to indicate that high Summer  $T$  is associated with deep soil moisture that has been recharged by Winter

precipitation. The slightly negative slope of stem  $\delta^2\text{H}$  values with  $T$  (Figure 9d), indicate that higher  $T$  is correlated with more negative  $\delta^2\text{H}$  values in the stem water. Taking the deep soil and stem regressions together, the plant appears to be using deep soil water during period of high  $T$  (Summer), and that this deep soil water available in the summer was recharged by Winter precipitation.

## **4. Discussion**

### **4.1 Deep Soil Moisture Influence on Transpiration Dynamics**

Overall, periods of high deep soil moisture were associated with periods of high  $T$  and periods of high shallow soil moisture were associated with periods of high  $E$  (Figures 2, 3 and 4). This is consistent with other studies in dryland ecosystems [*Kurc and Small, 2004, 2007; Scott et al., 2006b; Cavanaugh et al., 2011*]. Additionally, the  $\delta^2\text{H}$  values of the stem samples all fell along the regression line for the  $\delta^2\text{H}$  values of the deep soil samples, further suggesting that plants are largely dependent on deep soil moisture [*West et al., 2007*]. In combining our transpiration data and our stable isotope data (Figure 9), we are able to further refine our understanding of plant source water use. During periods associated with high  $T$  (Summer from Figure 2), shrubs appear to be dependent on moisture from the deep soil layer (Figures 3b, 4b, 8d), and this deep Summer soil moisture is likely recharged by Winter precipitation based on the similarity in isotopic composition of Winter precipitation (i.e.,  $\delta^2\text{H}$  of  $-57\text{‰}$ ) with those of deep soil water and stem water samples at high  $T$  (Figures 9c and 9d). Because the shrubs are dependent on deep soil moisture for transpiration and biomass productivity [*Kurc and Small 2007; Kurc and Benton 2010; Cavanaugh et al. 2011*], a hypothetical decrease in large precipitation events would decrease deep soil moisture, which could reduce water available for transpiration and biomass

accumulation, with major consequences for the health and functioning of these dryland ecosystems.

Previous studies have tended to emphasize summer transpiration dynamics [e.g., *Yepez et al.*, 2003, 2005; *Scott et al.*, 2006b; *Cavanaugh et al.*, 2011]. However, our study suggests that under certain conditions, Winter transpiration may be an important component of the water budget in desert shrubland ecosystems. Our results showed that  $ET$  in the “drier” Winter was dominated by  $E$ , but in the “wetter” Winter was dominated by  $T$ . The “drier” Winter 2013-2014 had an average shallow and deep soil moisture of 0.11 and 0.10  $m^3 m^{-3}$ , respectively, whereas the “wetter” Winter 2014-2015 had an average shallow and deep soil moisture of 0.14 and 0.12  $m^3 m^{-3}$  which were both higher than the Summer or Winter averages (Figure 3b). This suggests that transpiration can indeed occur in the Winter and may be largely limited by soil moisture. Because we found that in the “drier” Winter increasing deep soil moisture was correlated with decreasing  $T$  but the in the “wetter” Winter, increasing deep soil moisture was correlated with increasing  $T$ , we suspect this has more to do with availability of deep soil moisture than with shallow soil moisture.

#### **4.2 Implications of Complexities in Stable Water Isotopes for Understanding Shrub Plant Water Use**

In hydrological research using stable isotopes, end-member mixing models have been used to determine the source waters for reservoirs such as groundwater [e.g., *Gat and Dansgaard*, 1972; *Connolly et al.*, 1990], lake water [e.g., *Dincer et al.*, 1974; *Krabbenhof et al.*, 1990], or stream water [e.g., *Hooper et al.*, 1990; *Kendall and Coplen*, 2001]. An important implication resulting from this type of mixing model analysis is in understanding how changes in the climate regime

that impact the source waters will further impact the reservoir [e.g., *Palmer and Räisänen*, 2002; *Kundzewicz et al.*, 2008]. Increasingly in ecohydrological research, stable water isotopes have also been used for understanding the source waters for plants [e.g., *Dawson and Ehleringer*, 1991; *Ehleringer et al.*, 1991; *Flanagan and Ehleringer*, 1991; *Dawson et al.*, 1993; *Snyder and Williams*, 2000; *Williams and Ehleringer*, 2000; *Schwinning et al.*, 2002; *Brooks et al.*, 2010]. Isotopically distinct source water end-members such as groundwater or shallow soil moisture can be combined in a linear function to determine the contribution of each end-member to the isotopic composition of the mixed plant component [*Dawson*, 1998; *Phillips and Gregg*, 2001; *Dawson et al.*, 2002; *Corbin et al.*, 2005].

In our study, we hypothesized that shallow soil moisture and deep soil moisture would be isotopically distinct from each other because they would be recharged by isotopically distinct precipitation events, i.e., Winter precipitation would be isotopically distinct from Summer precipitation [*Clark and Fritz*, 1997; *Dutton et al.*, 2005], and that these isotopically distinct events would recharge different layers [*Ehleringer et al.*, 1991; *Williams and Ehleringer*, 2000], or because small events would be isotopically distinct from large events [*Miller et al.*, 2006], and that these differently sized events would recharge different layers [*Sala and Lauenroth*, 1982; *Kurc and Small*, 2004, 2007; *Huxman et al.*, 2005]. In addition, evaporation of shallow soil moisture would fractionate the shallow soil moisture and lead to higher  $\delta^{18}\text{O}$  and  $\delta^2\text{H}$  values in the shallow soil moisture than in the deep soil moisture [e.g., *Kulmatiski et al.*, 2006; *Newman et al.*, 2010]. As such, shallow soil moisture and deep soil moisture could serve as the two end-members for the mixed plant component of our desert shrubland ecosystem where groundwater is assumed to be out of the reach of the shrubs. By working within this context, we can develop

an understanding about the implications of changes in precipitation regime on the plant water use of this ecosystem.

During this particular study period, southern Arizona experienced four tropical storms during August, September, and October 2014 (Figure 3), whereas tropical storms in this region usually average one every three years (*C. Eastoe*, pers. comm.). Because tropical storm precipitation is generally depleted relative to the average summer precipitation [*Miller et al.*, 2006], their  $\delta^{18}\text{O}$  and  $\delta^2\text{H}$  values tend to be more similar to winter precipitation than summer precipitation (which tends to be more enriched), which was the case for the tropical storms that fell during our study period (Figure 2). Because these isotopically light tropical storms fell during the Summer season, averages in Winter and Summer precipitation were not isotopically distinct during our study period (Figure 6). We expect that this in part led to the lack of isotopic distinction between averages in shallow and deep soil moisture (Figure 6). In addition, even though the daily shallow soil moisture isotope values fell close to the LMWL (Figure 8b), the daily deep soil moisture  $\delta^{18}\text{O}$  and  $\delta^2\text{H}$  values unexpectedly fell to the right of the LMWL (Figure 8c). One explanation of this deep soil moisture isotopic characteristic is that the deep soil moisture, rather than reflecting only the isotopic signature of large precipitation events, is instead a mix of precipitation with tightly bound soil water that could be relatively enriched in  $^{18}\text{O}$  and  $^2\text{H}$  [e.g., *Robertson and Gazis*, 2006; *Brooks et al.*, 2010]. Another possibility is that this deep soil moisture reflects subsurface mixing of infiltrating precipitation with antecedent soil moisture [*Barnes and Turner*, 1998; *Gazis and Feng*, 2004], e.g., precipitation from isotopically light and large storms mixes, during infiltration to the deep soil layer, with shallow soil moisture that had been enriched in  $^{18}\text{O}$  and in  $^2\text{H}$  because of evaporative fractionation.

Stable water isotope values associated with plants are complex to interpret [Dawson *et al.*, 2002; Meißner *et al.*, 2013; Gessler *et al.*, 2014]. Notably, stem samples were on average more enriched in both  $^{18}\text{O}$  and  $^2\text{H}$  relative to the shallow and deep soil samples, i.e., the stem samples did not fall between the expected end-members of conceptual linear mixing model framework. Plant samples of stable water isotopes may be affected through both mixing processes and fractionation processes [Gessler *et al.*, 2014]. Therefore that the stem sample average does not fall between the expected end-members could indicate that we did not consider all possible end-members [e.g., Brooks *et al.*, 2010] or did not recognize the effect of fractionation processes between the soil water and the sampled plant water [e.g., Gessler *et al.*, 2014]. Our sampling technique could also lead uncertainty associated with certain artifacts. For instance, we know that soil moisture is exceptionally spatially heterogeneous in dryland ecosystems [e.g., Weltzin *et al.*, 2003; D'Odorico *et al.*, 2007], in part because of soil differences related to pore distribution and soil microtopography [e.g., Brunel *et al.*, 1995]. Our sampling design assumed that a vertical soil core under the canopy and a vertical soil core in the inter-canopy space were representative of overall soil moisture conditions of the ecosystem. We also assumed that the uncertainty associated with time of sampling soil or stem water was negligible because the diurnal variation would be smaller than the seasonal variation [Zhao *et al.*, 2014].

Despite these complications, we were able to identify some isotopic distinction between the shallow soil and deep soil samples: the slope of the deep soil regression line ( $m=2.91$ ; Figure 8c and Table 2) is much less positive than the shallow soil regression line slope ( $m=5.05$ ; Figure 8b and Table 2), possibly indicating a greater effect of evaporative enrichment or different mixing

process in the two soil layers [Tang and Feng, 2001]. Using different regression lines for shallow soil and deep soil samples, we did see that the stem samples fell along the deep soil regression line (Figure 8d), indicating that the plants are primarily drawing from deep soil moisture rather than shallow soil moisture. Furthermore, similar to the deep soil samples, the stem samples do not display a consistent seasonal bias like the precipitation and shallow soil samples.

## 5. Conclusions

Results from both continuous sap flow transpiration data and discrete isotopic sampling of precipitation, soil, and stem samples suggest that plants are primarily using deep soil moisture for transpiration. From the isotopic samples, we found that the shallow and deep soils were isotopically distinct, with the shallow soil generally more enriched in  $^{18}\text{O}$  and  $^2\text{H}$  than deep soil. In particular, the  $\delta^2\text{H}$  values of shallow soil samples on each sampling day tended to be more positive than the  $\delta^2\text{H}$  values of deep soil samples, except on days where a large, isotopically depleted storm wetted the whole soil profile. Using sap flow and soil moisture data, we showed that transpiration was generally more strongly correlated with deep moisture, whereas evaporation was more strongly correlated with shallow moisture. This was supported by analysis of our isotopic data, from which we show that stem samples are isotopically similar to deep soil samples, with stem samples clustering around a regression line through deep soil samples. Using a combined approach to understand shrub plant water use in semiarid areas offers us more insights than simply using sap flow or isotopic techniques alone. This is in part because of the complexity of isotopic patterns in the rainfall and the conditions for fractionation. Using our combined approach, we can confidently say that this semiarid shrubland depends on deep moisture for growth and functioning and is therefore vulnerable to shifts in precipitation, such as

a decrease in the number of large storms, which would limit available soil moisture to the shallow surface layer.

## References

- Barnes, C. J., and J. V. Turner (1998), Chapter 5 - Isotopic Exchange in Soil Water, in *Isotope Tracers in Catchment Hydrology*, edited by C. K. J. McDONNELL, pp. 137–163, Elsevier, Amsterdam.
- Barnett, T. P. et al. (2008), Human-Induced Changes in the Hydrology of the Western United States, *Science*, 319(5866), 1080–1083, doi:10.1126/science.1152538.
- Brooks, J. R., Holly R. Barnard, Rob Coulombe, and Jeffrey J. McDonnell (2010), Ecohydrologic separation of water between trees and streams in a Mediterranean climate, *Nat. Geosci.*, 3(2), 100–104, doi:10.1038/ngeo722.
- Brunel, J.-P., G. R. Walker, and A. K. Kennett-Smith (1995), Field validation of isotopic procedures for determining sources of water used by plants in a semi-arid environment, *J. Hydrol.*, 167(1–4), 351–368, doi:10.1016/0022-1694(94)02575-V.
- Burgess, S. S. O., M. A. Adams, N. C. Turner, and C. K. Ong (1998), The redistribution of soil water by tree root systems, *Oecologia*, 115(3), 306–311, doi:10.1007/s004420050521.
- Cavanaugh, M. L., S. A. Kurc, and R. L. Scott (2011), Evapotranspiration partitioning in semiarid shrubland ecosystems: a two-site evaluation of soil moisture control on transpiration, *Ecohydrology*, 4(5), 671–681, doi:10.1002/eco.157.
- Clark, I. D., and P. Fritz (1997), *Environmental Isotopes in Hydrogeology*, CRC Press.
- Connolly, C. A., L. M. Walter, H. Baadsgaard, and F. J. Longstaffe (1990), Origin and evolution of formation waters, Alberta Basin, Western Canada Sedimentary Basin. II. Isotope systematics and water mixing, *Appl. Geochem.*, 5(4), 397–413, doi:10.1016/0883-2927(90)90017-Y.
- Corbin, J. D., M. A. Thomsen, T. E. Dawson, and C. M. D’Antonio (2005), Summer water use by California coastal prairie grasses: fog, drought, and community composition, *Oecologia*, 145(4), 511–521, doi:10.1007/s00442-005-0152-y.
- Crosson, E. R. (2008), A cavity ring-down analyzer for measuring atmospheric levels of methane, carbon dioxide, and water vapor, *Appl. Phys. B*, 92(3), 403–408, doi:10.1007/s00340-008-3135-y.

- Dansgaard, W. (1964), Stable isotopes in precipitation, *Tellus A*, 16(4).
- Dawson, T. E. (1998), Fog in the California redwood forest: ecosystem inputs and use by plants, *Oecologia*, 117(4), 476–485, doi:10.1007/s004420050683.
- Dawson, T. E., and J. R. Ehleringer (1991), Streamside trees that do not use stream water, *Nature*, 350(6316), 335–337, doi:10.1038/350335a0.
- Dawson, T. E., and J. R. Ehleringer (1993), Isotopic enrichment of water in the “woody” tissues of plants: Implications for plant water source, water uptake, and other studies which use the stable isotopic composition of cellulose, *Geochim. Cosmochim. Acta*, 57(14), 3487–3492, doi:10.1016/0016-7037(93)90554-A.
- Dawson, T. E., and K. A. Simonin (2011), The roles of stable isotopes in forest hydrology and biogeochemistry, in *Forest Hydrology and Biogeochemistry*, pp. 137–161, Springer.
- Dawson, T. E., J. R. Ehleringer, A. E. Hall, and G. D. Farquhar (1993), Water sources of plants as determined from xylem-water isotopic composition: perspectives on plant competition, distribution, and water relations., in *Stable isotopes and plant carbon-water relations.*, pp. 465–496, Academic Press Inc.
- Dawson, T. E., S. Mambelli, A. H. Plamboeck, P. H. Templer, and K. P. Tu (2002), Stable Isotopes in Plant Ecology, *Annu. Rev. Ecol. Syst.*, 33, 507–559.
- D'Odorico, P., K. Caylor, G. S. Okin, and T. M. Scanlon (2007), On soil moisture–vegetation feedbacks and their possible effects on the dynamics of dryland ecosystems, *J. Geophys. Res. Biogeosciences*, 112(G4), n/a–n/a, doi:10.1029/2006JG000379.
- Dutton, A., B. H. Wilkinson, J. M. Welker, G. J. Bowen, and K. C. Lohmann (2005), Spatial distribution and seasonal variation in  $^{18}\text{O}/^{16}\text{O}$  of modern precipitation and river water across the conterminous USA, *Hydrol. Process.*, 19(20), 4121–4146, doi:10.1002/hyp.5876.
- Easterling, D. R., G. A. Meehl, C. Parmesan, S. A. Changnon, T. R. Karl, and L. O. Mearns (2000), Climate Extremes: Observations, Modeling, and Impacts, *Science*, 289(5487), 2068–2074, doi:10.1126/science.289.5487.2068.
- Eastoe, C. J., A. Gu, and A. Long (2004), The origins, ages and flow paths of groundwater in Tucson Basin: results of a study of multiple isotope systems, *Hogan JF Philips FM Scanlon BR Eds Groundw. Recharge Desert Environ. Southwest. U. S. Water Sci. Appl. Ser. Vol 9 AGU Wash. DC Pp 217–234*.
- Eastoe, C. J., G. Hess, and S. Mahieux (2015), Identifying Recharge from Tropical Cyclonic Storms, Baja California Sur, Mexico, *Groundwater*, 53(S1), 133–138, doi:10.1111/gwat.12183.

- Ehleringer, J. R., S. L. Phillips, W. S. F. Schuster, and D. R. Sandquist (1991), Differential utilization of summer rains by desert plants, *Oecologia*, 88(3), 430–434, doi:10.1007/BF00317589.
- Ellsworth, P. Z., and D. G. Williams (2007), Hydrogen isotope fractionation during water uptake by woody xerophytes, *Plant Soil*, 291(1-2), 93–107, doi:10.1007/s11104-006-9177-1.
- Field, R. D., D. Jones, and D. P. Brown (2010), Effects of postcondensation exchange on the isotopic composition of water in the atmosphere, *J. Geophys. Res. Atmospheres 1984–2012*, 115(D24).
- Flanagan, L. B., and J. R. Ehleringer (1991), Stable isotope composition of stem and leaf water: applications to the study of plant water use, *Funct. Ecol.*, 270–277.
- Friedman, I., L. Machta, and R. Soller (1962), Water-vapor exchange between a water droplet and its environment, *J. Geophys. Res.*, 67(7), 2761–2766.
- Gat, J. R. (1996), Oxygen and Hydrogen Isotopes in the Hydrologic Cycle, *Annu. Rev. Earth Planet. Sci.*, 24(1), 225–262, doi:10.1146/annurev.earth.24.1.225.
- Gat, J. R., and P. L. Airey (2006), Stable water isotopes in the atmosphere/biosphere/lithosphere interface: Scaling-up from the local to continental scale, under humid and dry conditions, *Glob. Planet. Change*, 51(1–2), 25–33, doi:10.1016/j.gloplacha.2005.12.004.
- Gat, J. R., and W. Dansgaard (1972), Stable isotope survey of the fresh water occurrences in Israel and the Northern Jordan Rift Valley, *J. Hydrol.*, 16(3), 177–211, doi:10.1016/0022-1694(72)90052-2.
- Gazis, C., and X. Feng (2004), A stable isotope study of soil water: evidence for mixing and preferential flow paths, *Geoderma*, 119(1), 97–111.
- Gedzelman, S. D., and J. R. Lawrence (1990), The isotopic composition of precipitation from two extratropical cyclones, *Mon. Weather Rev.*, 118(2), 495–509.
- Germino, M. J., and K. Reinhardt (2014), Desert shrub responses to experimental modification of precipitation seasonality and soil depth: relationship to the two-layer hypothesis and ecohydrological niche, *J. Ecol.*, 102(4), 989–997.
- Gessler, A., J. P. Ferrio, R. Hommel, K. Treydte, R. A. Werner, and R. K. Monson (2014), Stable isotopes in tree rings: towards a mechanistic understanding of isotope fractionation and mixing processes from the leaves to the wood, *Tree Physiol.*, tpu040, doi:10.1093/treephys/tpu040.

- Goodrich, D. C., C. L. Unkrich, T. O. Keefer, M. H. Nichols, J. J. Stone, L. R. Levick, and R. L. Scott (2008), Event to multidecadal persistence in rainfall and runoff in southeast Arizona, *Water Resour. Res.*, *44*(5), W05S14, doi:10.1029/2007WR006222.
- Gowing, J. W., F. Konukcu, and D. A. Rose (2006), Evaporative flux from a shallow watertable: The influence of a vapour–liquid phase transition, *J. Hydrol.*, *321*(1–4), 77–89, doi:10.1016/j.jhydrol.2005.07.035.
- Hedberg, P., W. Kotowski, P. Saetre, K. Mälson, H. Rydin, and S. Sundberg (2012), Vegetation recovery after multiple-site experimental fen restorations, *Biol. Conserv.*, *147*(1), 60–67, doi:10.1016/j.biocon.2012.01.039.
- Holdo, R. M. (2013), Revisiting the two-layer hypothesis: coexistence of alternative functional rooting strategies in savannas,
- Hooper, R. P., N. Christophersen, and N. E. Peters (1990), Modelling streamwater chemistry as a mixture of soilwater end-members — An application to the Panola Mountain catchment, Georgia, U.S.A., *J. Hydrol.*, *116*(1–4), 321–343, doi:10.1016/0022-1694(90)90131-G.
- Hopkins, C. B., J. C. McIntosh, C. Eastoe, J. E. Dickinson, and T. Meixner (2014), Evaluation of the importance of clay confining units on groundwater flow in alluvial basins using solute and isotope tracers: the case of Middle San Pedro Basin in southeastern Arizona (USA), *Hydrogeol. J.*, *22*(4), 829–849, doi:10.1007/s10040-013-1090-0.
- Humphrey, R. R., and L. A. Mehrhoff (1958), Vegetation Changes on a Southern Arizona Grassland Range, *Ecology*, *39*(4), 720–726, doi:10.2307/1931612.
- Huxman, T. E., K. A. Snyder, D. Tissue, A. J. Leffler, K. Ogle, W. T. Pockman, D. R. Sandquist, D. L. Potts, and S. Schwinning (2004), Precipitation pulses and carbon fluxes in semiarid and arid ecosystems, *Oecologia*, *141*(2), 254–268, doi:10.1007/s00442-004-1682-4.
- Huxman, T. E., B. P. Wilcox, D. D. Breshears, R. L. Scott, K. A. Snyder, E. E. Small, K. Hultine, W. T. Pockman, and R. B. Jackson (2005), Ecohydrological implications of woody plant encroachment, *Ecology*, *86*(2), 308–319, doi:10.1890/03-0583.
- Ingraham, N. L., B. F. Lyles, R. L. Jacobson, and J. W. Hess (1991), Stable isotopic study of precipitation and spring discharge in southern Nevada, *J. Hydrol.*, *125*(3–4), 243–258, doi:10.1016/0022-1694(91)90031-C.
- Jenerette, G. D., G. A. Barron-Gafford, A. J. Guswa, J. J. McDonnell, and J. C. Villegas (2012), Organization of complexity in water limited ecohydrology, *Ecohydrology*, *5*(2), 184–199, doi:10.1002/eco.217.
- Kendall, C., and T. B. Coplen (2001), Distribution of oxygen-18 and deuterium in river waters across the United States, *Hydrol. Process.*, *15*(7), 1363–1393, doi:10.1002/hyp.217.

- Knapp, A. K. et al. (2008), Consequences of More Extreme Precipitation Regimes for Terrestrial Ecosystems, *BioScience*, 58(9), 811–821, doi:10.1641/B580908.
- Knowles, N., M. D. Dettinger, and D. R. Cayan (2006), Trends in Snowfall versus Rainfall in the Western United States, *J. Clim.*, 19(18), 4545–4559, doi:10.1175/JCLI3850.1.
- Krabbenhoft, D. P., C. J. Bowser, M. P. Anderson, and J. W. Valley (1990), Estimating groundwater exchange with lakes: 1. The stable isotope mass balance method, *Water Resour. Res.*, 26(10), 2445–2453, doi:10.1029/WR026i010p02445.
- Kulmatiski, A., K. H. Beard, and J. M. Stark (2006), Exotic plant communities shift water-use timing in a shrub-steppe ecosystem, *Plant Soil*, 288(1-2), 271–284.
- Kundzewicz, Z. W., L. J. Mata, N. W. Arnell, P. Döll, B. Jimenez, K. Miller, T. Oki, Z. Şen, and I. Shiklomanov (2008), The implications of projected climate change for freshwater resources and their management,
- Kurc, S. A., and L. M. Benton (2010), Digital image-derived greenness links deep soil moisture to carbon uptake in a creosotebush-dominated shrubland, *J. Arid Environ.*, 74(5), 585–594, doi:10.1016/j.jaridenv.2009.10.003.
- Kurc, S. A., and E. E. Small (2004), Dynamics of evapotranspiration in semiarid grassland and shrubland ecosystems during the summer monsoon season, central New Mexico, *Water Resour. Res.*, 40(9), W09305, doi:10.1029/2004WR003068.
- Kurc, S. A., and E. E. Small (2007), Soil moisture variations and ecosystem-scale fluxes of water and carbon in semiarid grassland and shrubland, *Water Resour. Res.*, 43(6), W06416, doi:10.1029/2006WR005011.
- Langensiepen, M., M. Kupisch, M. T. van Wijk, and F. Ewert (2012), Analyzing transient closed chamber effects on canopy gas exchange for optimizing flux calculation timing, *Agric. For. Meteorol.*, 164, 61–70, doi:10.1016/j.agrformet.2012.05.006.
- Lee, J.-E., and I. Fung (2008), “Amount effect” of water isotopes and quantitative analysis of post-condensation processes, *Hydrol. Process.*, 22(1), 1–8.
- Leffler, A. J., and J. M. Welker (2013), Long-term increases in snow pack elevate leaf N and photosynthesis in *Salix arctica*: responses to a snow fence experiment in the High Arctic of NW Greenland, *Environ. Res. Lett.*, 8(2), 025023, doi:10.1088/1748-9326/8/2/025023.
- Lin, G. H., and L. da S. L. Sternberg (1993), Hydrogen isotopic fractionation by plant roots during water uptake in coastal wetland plants., pp. 497–510, Academic Press Inc.

- Loik, M. E., D. D. Breshears, W. K. Lauenroth, and J. Belnap (2004), A multi-scale perspective of water pulses in dryland ecosystems: climatology and ecohydrology of the western USA, *Oecologia*, 141(2), 269–281, doi:10.1007/s00442-004-1570-y.
- Meißner, M., M. Köhler, L. Schwendenmann, D. Hölscher, and J. Dyckmans (2013), Soil water uptake by trees using water stable isotopes ( $\delta^2\text{H}$  and  $\delta^{18}\text{O}$ )—a method test regarding soil moisture, texture and carbonate, *Plant Soil*, 376(1-2), 327–335, doi:10.1007/s11104-013-1970-z.
- Merino-Martín, L., D. D. Breshears, M. Moreno-de las Heras, J. C. Villegas, S. Pérez-Domingo, T. Espigares, and J. M. Nicolau (2012), Ecohydrological Source-Sink Interrelationships between Vegetation Patches and Soil Hydrological Properties along a Disturbance Gradient Reveal a Restoration Threshold, *Restor. Ecol.*, 20(3), 360–368, doi:10.1111/j.1526-100X.2011.00776.x.
- Miller, D. L., C. I. Mora, H. D. Grissino-Mayer, C. J. Mock, M. E. Uhle, and Z. Sharp (2006), Tree-ring isotope records of tropical cyclone activity, *Proc. Natl. Acad. Sci.*, 103(39), 14294–14297, doi:10.1073/pnas.0606549103.
- Nadezhdina, N. et al. (2010), Trees never rest: the multiple facets of hydraulic redistribution, *Ecohydrology*, 3(4), 431–444, doi:10.1002/eco.148.
- Newman, B. D., D. D. Breshears, and M. O. Gard (2010), Evapotranspiration Partitioning in a Semiarid Woodland: Ecohydrologic Heterogeneity and Connectivity of Vegetation Patches, *Vadose Zone J.*, 9(3), 561, doi:10.2136/vzj2009.0035.
- Ogle, K., and J. F. Reynolds (2004), Plant responses to precipitation in desert ecosystems: integrating functional types, pulses, thresholds, and delays, *Oecologia*, 141(2), 282–294, doi:10.1007/s00442-004-1507-5.
- Ogle, K., J. J. Barber, G. A. Barron-Gafford, L. P. Bentley, J. M. Young, T. E. Huxman, M. E. Loik, and D. T. Tissue (2015), Quantifying ecological memory in plant and ecosystem processes, *Ecol. Lett.*, 18(3), 221–235, doi:10.1111/ele.12399.
- Okin, G. S., A. J. Parsons, J. Wainwright, J. E. Herrick, B. T. Bestelmeyer, D. C. Peters, and E. L. Fredrickson (2009), Do Changes in Connectivity Explain Desertification?, *BioScience*, 59(3), 237–244, doi:10.1525/bio.2009.59.3.8.
- Palmer, T. N., and J. Räisänen (2002), Quantifying the risk of extreme seasonal precipitation events in a changing climate, *Nature*, 415(6871), 512–514, doi:10.1038/415512a.
- Phillips, D. L., and J. W. Gregg (2001), Uncertainty in source partitioning using stable isotopes, *Oecologia*, 127(2), 171–179, doi:10.1007/s004420000578.

- Potts, D. L., T. E. Huxman, J. M. Cable, N. B. English, D. D. Ignace, J. A. Eilts, M. J. Mason, J. F. Weltzin, and D. G. Williams (2006), Antecedent moisture and seasonal precipitation influence the response of canopy-scale carbon and water exchange to rainfall pulses in a semi-arid grassland, *New Phytol.*, 170(4), 849–860, doi:10.1111/j.1469-8137.2006.01732.x.
- Raz Yaseef, N., D. Yakir, E. Rotenberg, G. Schiller, and S. Cohen (2010), Ecohydrology of a semi-arid forest: partitioning among water balance components and its implications for predicted precipitation changes, *Ecohydrology*, 3(2), 143–154, doi:10.1002/eco.65.
- Reyes Gómez, V. M., O. Viramontes Olivas, J. T. Arredondo Moreno, E. Huber Sannwald, and A. R. Rodríguez (2015), Functional ecohydrological differences among native and exotic grassland covers in sub-urban landscapes of Chihuahua city, Mexico, *Landsc. Urban Plan.*, 139, 54–62, doi:10.1016/j.landurbplan.2015.03.005.
- Reynolds, J. F. et al. (2007), Global Desertification: Building a Science for Dryland Development, *Science*, 316(5826), 847–851, doi:10.1126/science.1131634.
- Robertson, J. A., and C. A. Gazis (2006), An oxygen isotope study of seasonal trends in soil water fluxes at two sites along a climate gradient in Washington state (USA), *J. Hydrol.*, 328(1), 375–387.
- Rodriguez-Iturbe, I. (2000), Ecohydrology: A hydrologic perspective of climate-soil-vegetation dynamics, *Water Resour. Res.*, 36(1), 3–9, doi:10.1029/1999WR900210.
- Rozanski, K., L. Araguás-Araguás, and R. Gonfiantini (1993), Isotopic patterns in modern global precipitation, *Clim. Change Cont. Isot. Rec.*, 1–36.
- Sala, O. E., and W. K. Lauenroth (1982), Small rainfall events: An ecological role in semiarid regions, *Oecologia*, 53(3), 301–304, doi:10.1007/BF00389004.
- Sanchez-Mejia, Z. M., and S. A. Papuga (2014), Observations of a two-layer soil moisture influence on surface energy dynamics and planetary boundary layer characteristics in a semiarid shrubland, *Water Resour. Res.*, 50(1), 306–317, doi:10.1002/2013WR014135.
- Schwinning, S., K. Davis, L. Richardson, and J. R. Ehleringer (2002), Deuterium enriched irrigation indicates different forms of rain use in shrub/grass species of the Colorado Plateau, *Oecologia*, 130(3), 345–355, doi:10.1007/s00442-001-0817-0.
- Scott, R. L., T. E. Huxman, W. L. Cable, and W. E. Emmerich (2006), Partitioning of evapotranspiration and its relation to carbon dioxide exchange in a Chihuahuan Desert shrubland, *Hydrol. Process.*, 20(15), 3227–3243, doi:10.1002/hyp.6329.
- Scott, R. L., T. E. Huxman, G. A. Barron-Gafford, G. Darrel Jenerette, J. M. Young, and E. P. Hamerlynck (2014), When vegetation change alters ecosystem water availability, *Glob. Change Biol.*, 20(7), 2198–2210, doi:10.1111/gcb.12511.

- Seager, R. et al. (2007), Model Projections of an Imminent Transition to a More Arid Climate in Southwestern North America, *Science*, 316(5828), 1181–1184, doi:10.1126/science.1139601.
- Senock, R. S., and J. M. Ham (1993), Heat balance sap flow gauge for small diameter stems, *Plant Cell Environ.*, 16(5), 593–601, doi:10.1111/j.1365-3040.1993.tb00908.x.
- Snyder, K. A., and D. G. Williams (2000), Water sources used by riparian trees varies among stream types on the San Pedro River, Arizona, *Agric. For. Meteorol.*, 105(1–3), 227–240, doi:10.1016/S0168-1923(00)00193-3.
- Tang, K., and X. Feng (2001), The effect of soil hydrology on the oxygen and hydrogen isotopic compositions of plants' source water, *Earth Planet. Sci. Lett.*, 185(3–4), 355–367, doi:10.1016/S0012-821X(00)00385-X.
- Thorburn, P. J., and J. R. Ehleringer (1995), Root water uptake of field-growing plants indicated by measurements of natural-abundance deuterium, *Plant Soil*, 177(2), 225–233, doi:10.1007/BF00010129.
- Walter, H. (1939), Grasland, Savanne und Busch der arideren Teile Afrikas in ihrer ökologischen Bedingtheit., *Jahrb. Für Wiss. Bot.*, 87, 750–860.
- Weltzin, J. F. et al. (2003), Assessing the Response of Terrestrial Ecosystems to Potential Changes in Precipitation, *BioScience*, 53(10), 941–952, doi:10.1641/0006-3568(2003)053[0941:ATROTE]2.0.CO;2.
- West, A. G., K. R. Hultine, K. G. Burtch, and J. R. Ehleringer (2007), Seasonal variations in moisture use in a piñon–juniper woodland, *Oecologia*, 153(4), 787–798, doi:10.1007/s00442-007-0777-0.
- Williams, D. G., and J. R. Ehleringer (2000), Intra- and interspecific variation for summer precipitation use in pinyon–juniper woodlands, *Ecol. Monogr.*, 70(4), 517–537, doi:10.1890/0012-9615(2000)070[0517:IAIVFS]2.0.CO;2.
- Wright, W. E. (2001), Delta-deuterium and delta-oxygen-18 in mixed conifer systems in the United States southwest: The potential of delta-oxygen-18 in *Pinus ponderosa* tree rings as a natural environmental recorder,
- Yepez, E. A., D. G. Williams, R. L. Scott, and G. Lin (2003), Partitioning overstory and understory evapotranspiration in a semiarid savanna woodland from the isotopic composition of water vapor, *Agric. For. Meteorol.*, 119(1–2), 53–68, doi:10.1016/S0168-1923(03)00116-3.
- Yepez, E. A., T. E. Huxman, D. D. Ignace, N. B. English, J. F. Weltzin, A. E. Castellanos, and D. G. Williams (2005), Dynamics of transpiration and evaporation following a moisture pulse in semiarid grassland: A chamber-based isotope method for partitioning flux

components, *Agric. For. Meteorol.*, 132(3–4), 359–376,  
doi:10.1016/j.agrformet.2005.09.006.

Zarebanadkouki, M., Y. X. Kim, and A. Carminati (2013), Where do roots take up water? Neutron radiography of water flow into the roots of transpiring plants growing in soil, *New Phytol.*, 199(4), 1034–1044, doi:10.1111/nph.12330.

Zhao, L., L. Wang, X. Liu, H. Xiao, Y. Ruan, and M. Zhou (2014), The patterns and implications of diurnal variations in the d-excess of plant water, shallow soil water and air moisture, *Hydrol Earth Syst Sci*, 18(10), 4129–4151, doi:10.5194/hess-18-4129-2014.

## Tables

**Table 1.** Linear regression statistics ( $R^2$ , slope, and slope p-value) for regression analysis. Case 1 (dry shallow layer and dry deep layer) was excluded from the analysis because there was limited water available for  $ET$ . Case 2 was excluded from the analysis because few days fell into Case 2 (4 days in Winter and 2 days in Summer). Note: \* denotes a p-value<0.05, \*\* denotes a p-value<0.01.

	All Cases				Case 3				Case 4			
	Winter (n = 158)		Summer (n = 79)		Winter (n = 97)		Summer (n = 25)		Winter (n = 6)		Summer (n = 26)	
	$R^2$	Slope	$R^2$	Slope	$R^2$	Slope	$R^2$	Slope	$R^2$	Slope	$R^2$	Slope
$ET$ and $\theta_{\text{shallow}}$	0.25	4.3**	0.48	14.2**	0.04	2.9	0.10	7.0	0.52	8.3	0.35	35.4**
$ET$ and $\theta_{\text{deep}}$	0.44	7.9**	0.29	37.2**	0.32	8.1**	0.05	13.1	0.21	27.1	0	0.1
$T$ and $\theta_{\text{shallow}}$	0.02	-0.41	0.08	1.5*	0.13	-2.3**	0.28	-3.6*	0.32	4.7	0.01	1.1
$T$ and $\theta_{\text{deep}}$	0.21	2.0**	0.36	10.6**	0.35	3.6**	0.11	6.0	0.39	16.7	0.26	12.2*
$E$ and $\theta_{\text{shallow}}$	0.37	4.7**	0.45	12.7**	0.16	5.1**	0.21	10.6*	0.10	3.6	0.34	34.3**
$E$ and $\theta_{\text{deep}}$	0.30	5.9**	0.17	26.6**	0.14	4.5**	0.01	7.1	0	0.4	0.01	-12.1

**Table 2.** Linear regression statistics ( $R^2$ , slope, and slope p-value) for regression analysis between  $\delta^{18}\text{O}$  and  $\delta^2\text{H}$  values for precipitation, shallow soil, deep soil, and stem samples. Note:

\*denotes a p-value  $<0.05$ , \*\* denotes a p-value  $<0.01$

<b>Overall</b>				
	<b>n</b>	<b>R<sup>2</sup></b>	<b>Slope</b>	<b>Y-intercept</b>
Precipitation	16	0.88	7.8**	-3.8
Shallow Soil	12	0.76	5.1**	-28
Deep Soil	12	0.45	2.9*	-4
Stem	30	0.69	3.9**	-48
<b>Summer</b>				
	<b>n</b>	<b>R<sup>2</sup></b>	<b>Slope</b>	<b>Y-intercept</b>
Precipitation	9	0.97	8.1**	-7.3
Shallow Soil	6	0.76	4.2*	-35
Deep Soil	6	0.07	0.7	-55
Stem	11	0.81	5.0**	-53
<b>Winter</b>				
	<b>n</b>	<b>R<sup>2</sup></b>	<b>Slope</b>	<b>Y-intercept</b>
Precipitation	4	0.93	9.6*	18
Shallow Soil	6	0.85	6.8*	-10
Deep Soil	6	0.87	4.0**	-36
Stem	10	0.59	4.3*	-10

**Table 3.** Linear regression statistics for regression analysis between three-day  $T$  and  $\delta^2\text{H}$  values for precipitation, shallow soil, deep soil, and stem samples. Note: \* denotes a p-value<0.05

	<b>n</b>	<b>R<sup>2</sup></b>	<b>Slope</b>
Precipitation	16	0.10	0.0065
Shallow Soil	12	0.0079	0.0019
Deep Soil	12	0.47	-0.036*
Stem	30	0.021	-0.0061

## Figure Captions

**Figure 1.** (a) Two-layer hydrologically defined soil conceptual framework: Case 1 (dry/dry) with dry shallow soil layer and dry deep soil layer; Case 2 (wet/dry) with wet shallow soil layer and dry deep soil layer; Case 3 (wet/wet) with wet shallow and deep soil layers; Case 4 (dry/wet) with wet deep soil layer and dry shallow soil layer. (b) Conceptual figure of how the hydrologically defined shallow and deep soil layers become isotopically distinct through precipitation and evaporation: small storms have a relatively higher  $\delta_{\text{water}}$  ( $\delta^{18}\text{O}$  and  $\delta^2\text{H}$ ) values and wet only the shallow soil layer; large storms have a relatively lower  $\delta_{\text{water}}$  values and wet both the shallow and deep soil layers; and evaporation causes enrichment of  $\delta_{\text{water}}$  values in the shallow layer. These three types of events lead to an isotopic distinction between the shallow and deep soil layers.

**Figure 2.** Time series of (a) daily precipitation [mm], vapor pressure deficit (VPD) [kPa]; (b) shallow and deep volumetric soil moisture ( $\theta$ , [ $\text{m}^3 \text{m}^{-3}$ ]); (c) transpiration ( $T$ ) [ $\text{mm day}^{-1}$ ], the relative contribution of  $T$  to  $ET$  ( $T/ET$ ); (d)  $\delta^2\text{H}$  values [‰] of precipitation and stem samples; (e)  $\delta^2\text{H}$  values [‰] of shallow and deep soil samples; (f)  $d$ -excess values [‰] of precipitation and stem samples; (g)  $d$ -excess values [‰] of shallow and deep soil samples.

**Figure 3.** Linear regressions between (a)  $\theta_{\text{shallow}}$  and  $ET$ ; (b)  $\theta_{\text{deep}}$  and  $ET$ ; (c)  $\theta_{\text{shallow}}$  and  $T$ ; (d)  $\theta_{\text{deep}}$  and  $T$ ; (e)  $\theta_{\text{shallow}}$  and  $ET$ ; and (f)  $\theta_{\text{deep}}$  and  $E$ . Solid lines represent Summer regression and dotted lines represent Winter regression.

**Figure 4.** Linear regressions for Case 3 days between (a)  $\theta_{\text{shallow}}$  and  $ET$ ; (b)  $\theta_{\text{deep}}$  and  $ET$ ; (c)  $\theta_{\text{shallow}}$  and  $T$ ; (d)  $\theta_{\text{deep}}$  and  $T$ ; (e)  $\theta_{\text{shallow}}$  and  $ET$ ; and (f)  $\theta_{\text{deep}}$  and  $E$ . Solid lines represent Summer regression and dotted lines represent Winter regression.

**Figure 5.** Linear regressions between (a)  $\theta_{\text{shallow}}$  and VPD and (b) VPD and  $T$ .

**Figure 6.**  $\delta^2\text{H}$  values of precipitation, shallow soil, deep soil, and stem samples. Daily samples are indicated by a circle and the averages are indicated by an asterisk (\*).

**Figure 7.**  $\delta^2\text{H}$  values of precipitation, shallow soil, deep soil, and stem samples for each Case considered separately. Daily samples are indicated by a circle and the averages are indicated by an asterisk (\*). Note: No isotope samples collected on a Case 2 day or on a Case 4 Winter day.

**Figure 8.** Daily precipitation, shallow soil, deep soil, and stem samples plotted with the global meteoric water line (gray dotted line), and the local meteoric water line (gray dashed line,  $\delta^2\text{H} = 6.67 * \delta^{18}\text{O} - 3.7 \text{‰}$  [Gallo *et al.*, 2012]).

**Figure 9.** Linear regressions of 3-day transpiration [ $\text{mm 3-day}^{-1}$ ] versus daily  $\delta^2\text{H}$  values of (a) precipitation, (b) shallow soil, (c) deep soil, and (d) stem samples.

Figures

Figure 1.

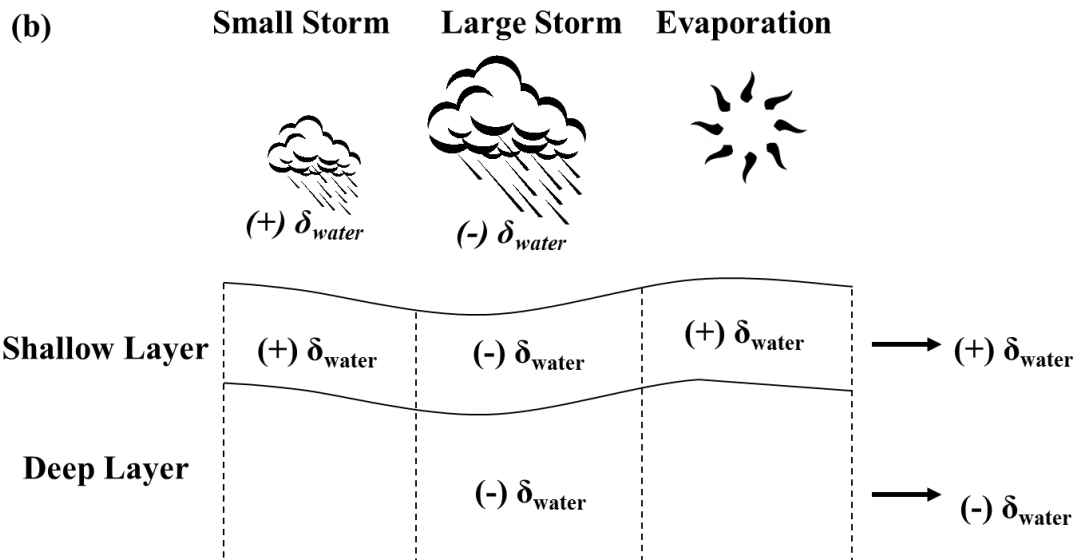
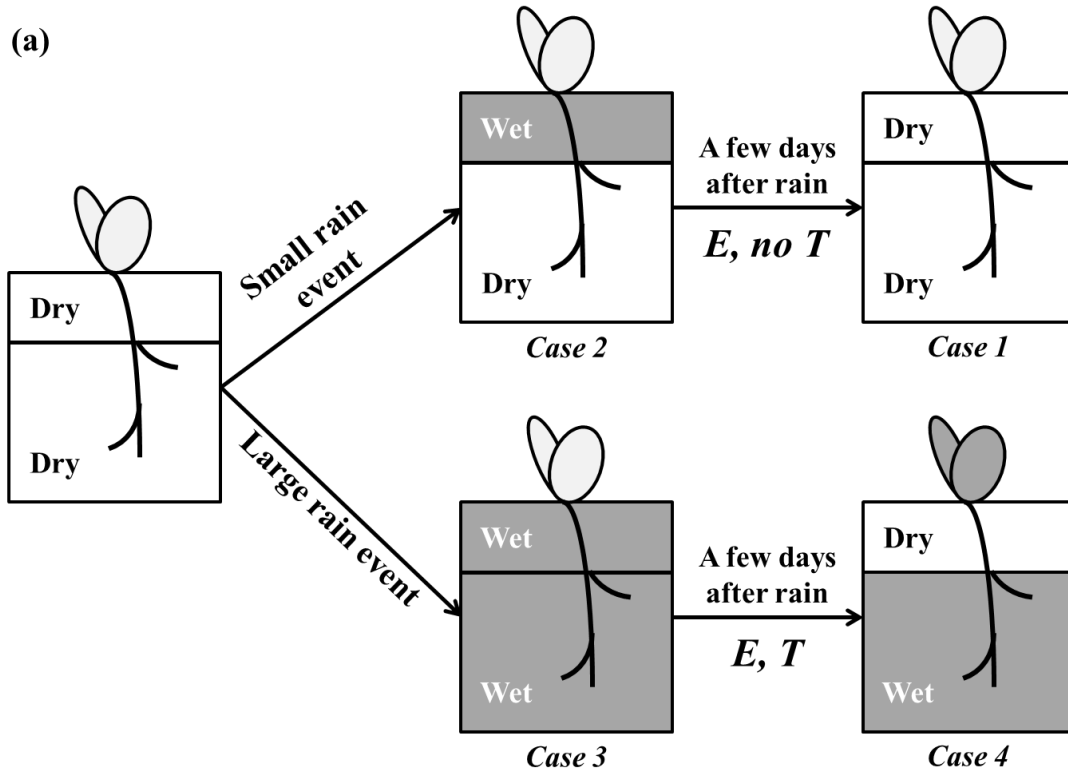


Figure 2.

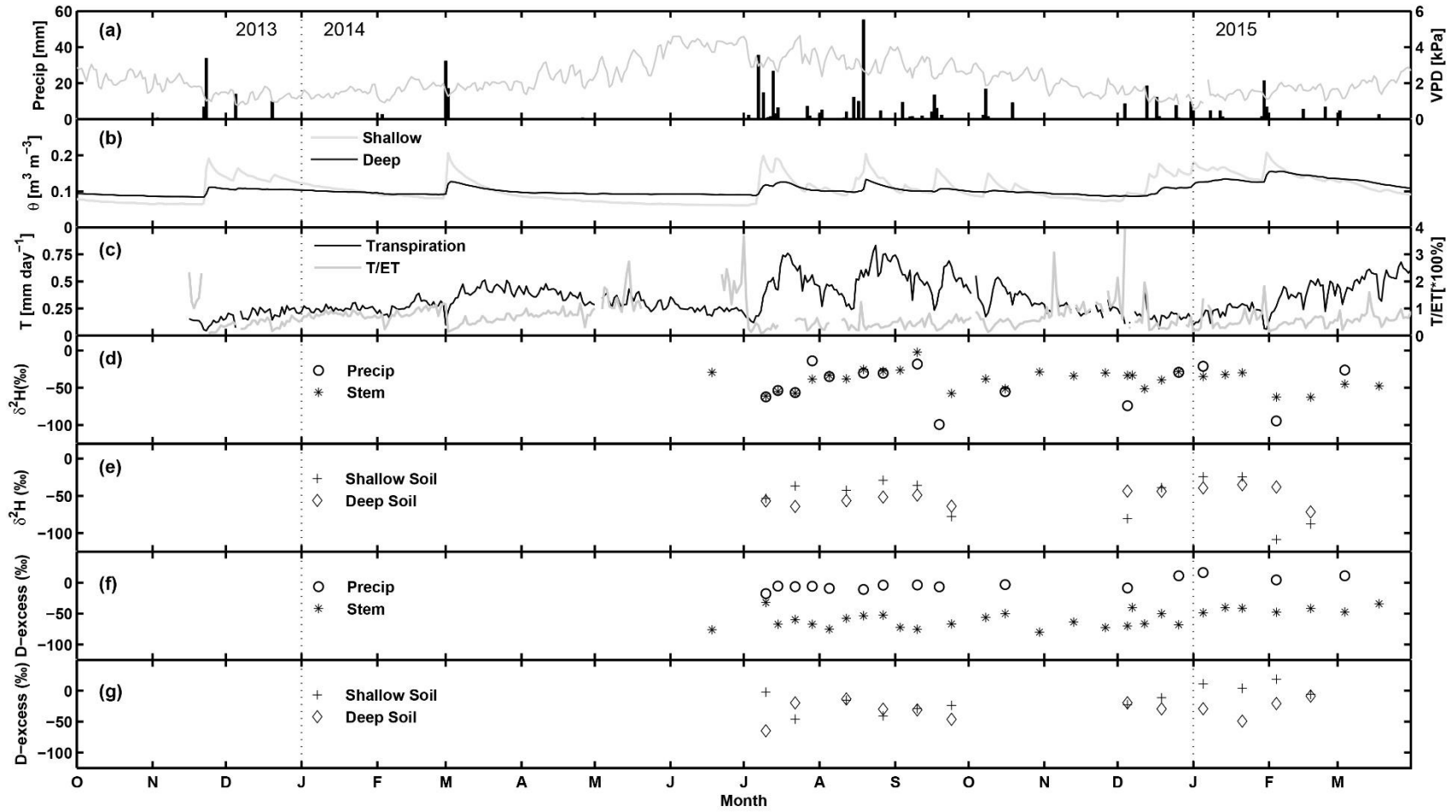


Figure 3.

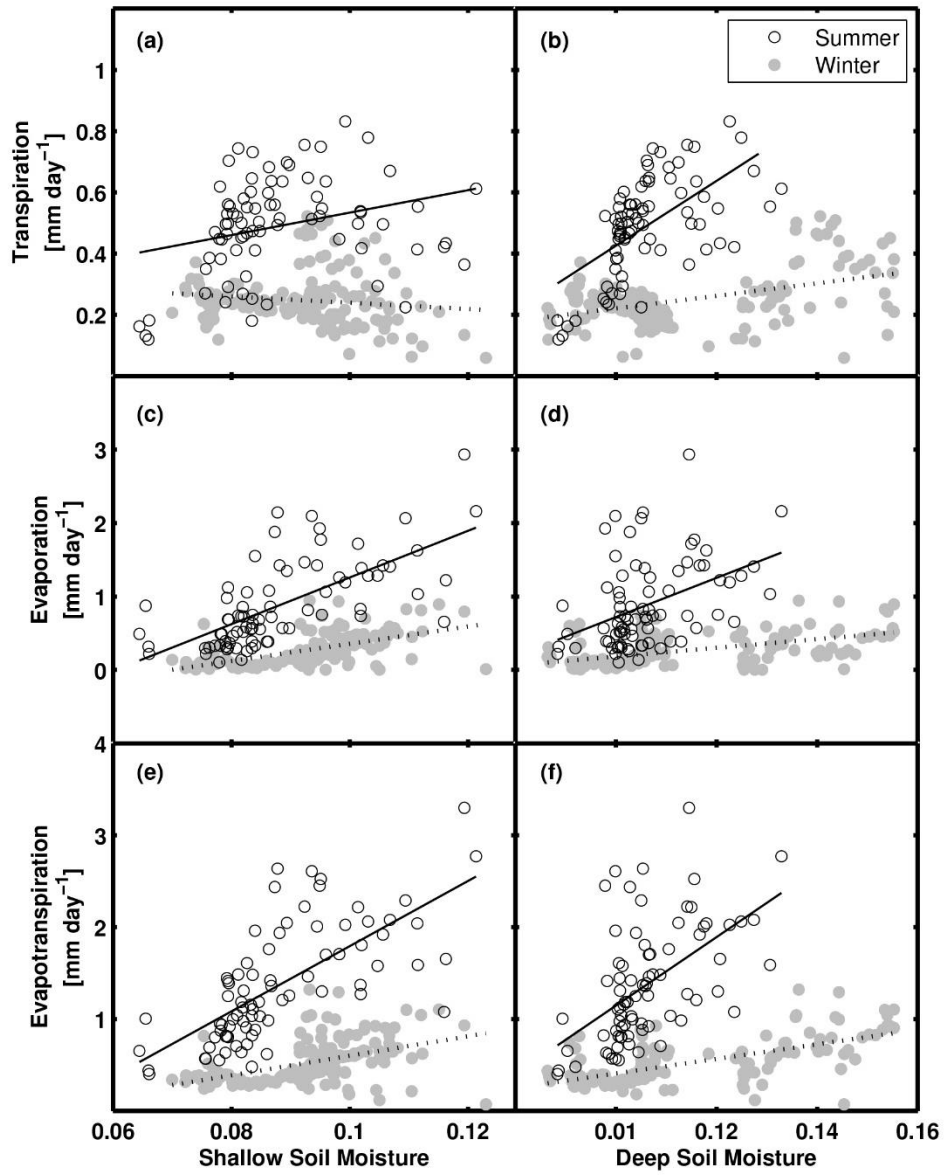


Figure 4.

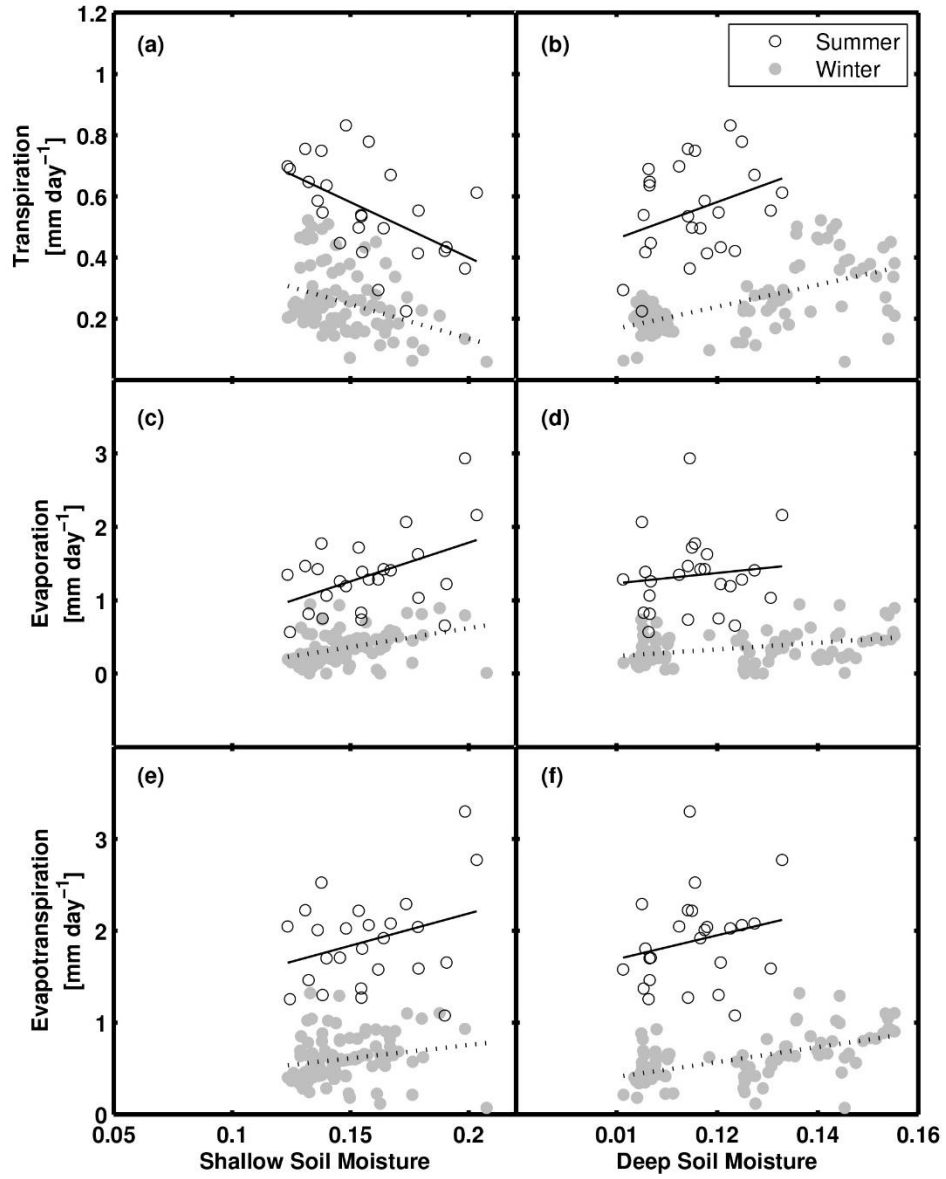


Figure 5.

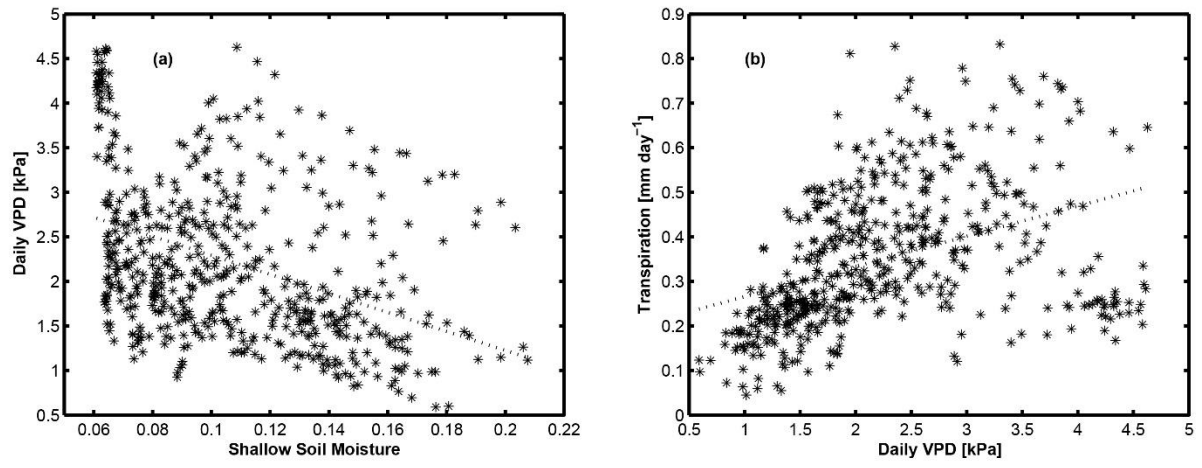


Figure 6.

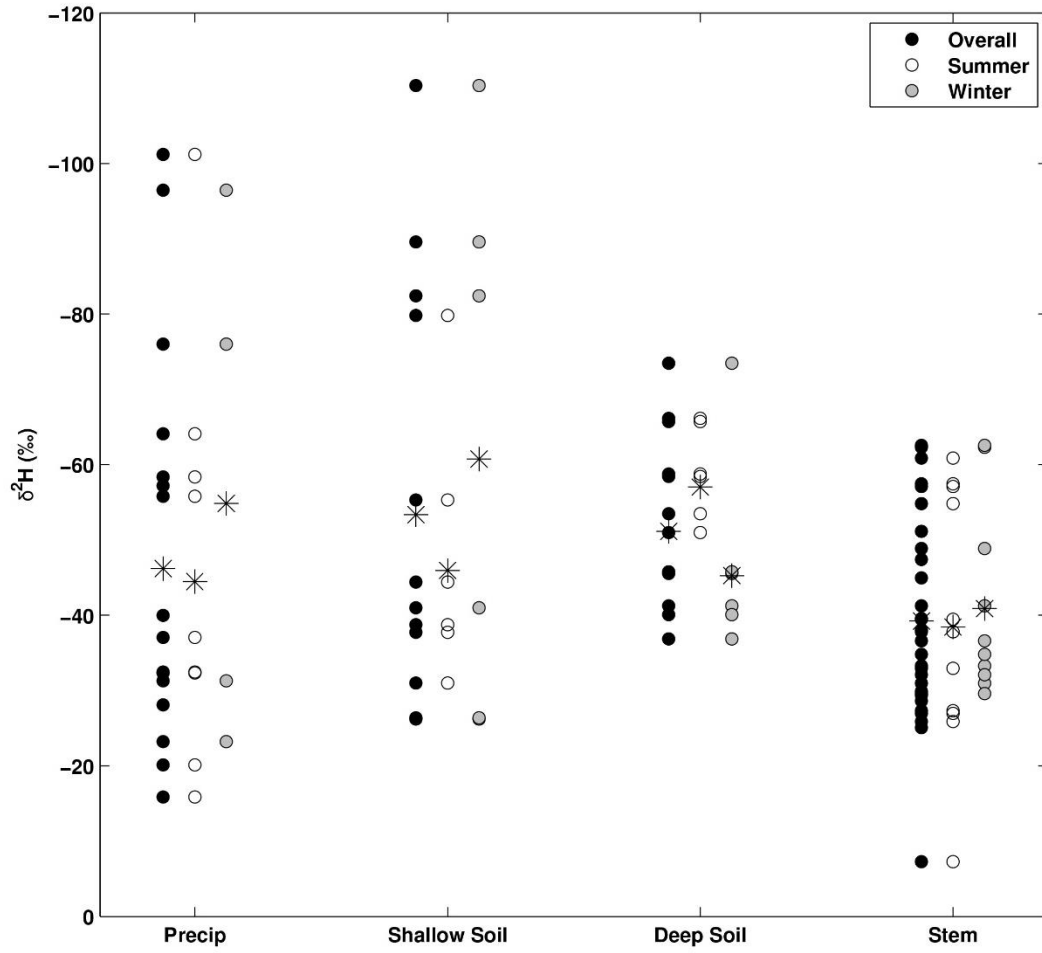


Figure 7.

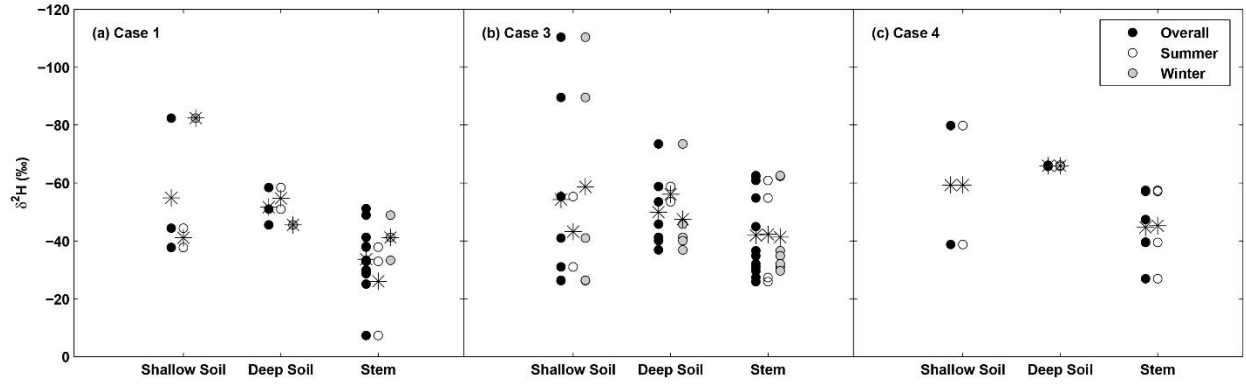


Figure 8.

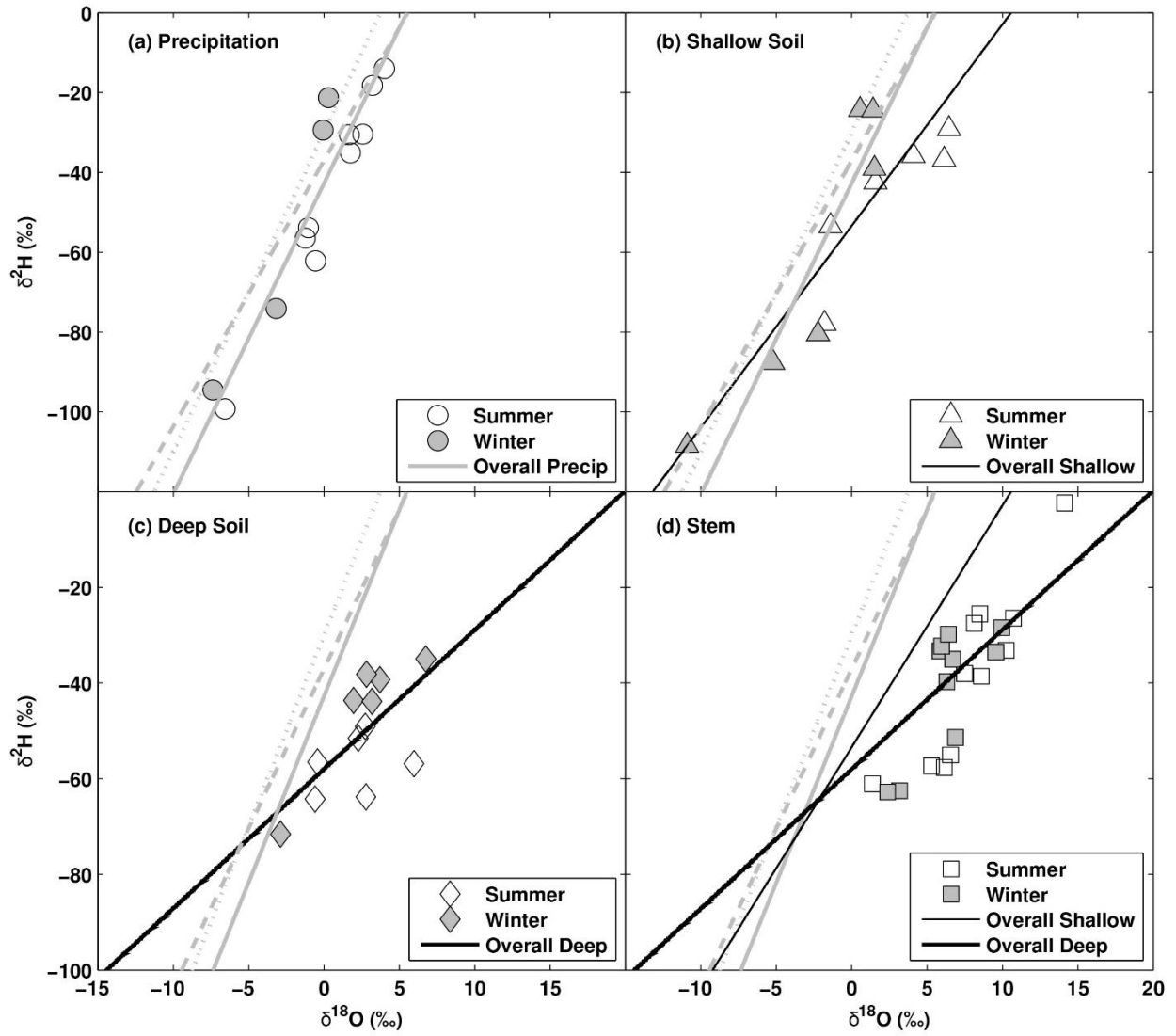
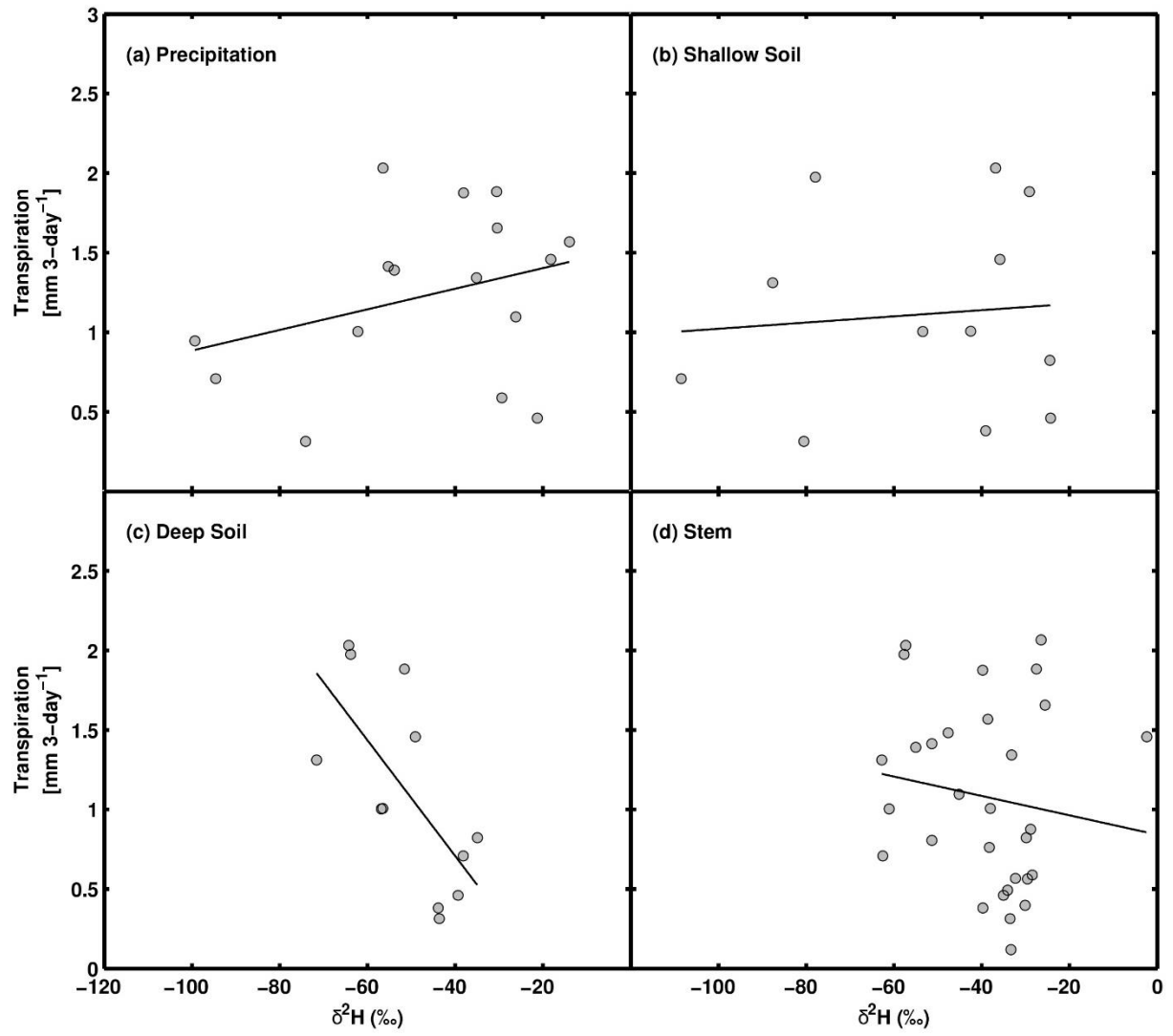


Figure 9.



## APPENDIX B: PICARRO ANALYZER AND INDUCTION MODULE INTRODUCTION

Daphne J. Szutu<sup>1,2</sup>

<sup>1</sup>School of Natural Resources and the Environment, University of Arizona, Tucson, AZ 85721

USA

<sup>2</sup>[daphne@email.arizona.edu](mailto:daphne@email.arizona.edu)

## 1. Theory

Stable water isotope analysis is well established in hydrology to trace sources of groundwater [Clark and Fritz, 1997], but it has recently emerged as a powerful tool in ecohydrologic studies to trace movement of water in the soil-plant-atmosphere continuum [Dawson *et al.*, 2002; Herczeg and Leaney, 2011; Werner *et al.*, 2012]. For example, isotopic analysis of stable water isotopes can be used to trace where in the soil the plants are getting their water [e.g., Dawson and Ehleringer, 1991; Brooks *et al.*, 2010], the sources of that water [e.g., Williams and Ehleringer, 2000; West *et al.*, 2007], as well as the relative effect of evaporation and transpiration on the remaining soil moisture [e.g., Yopez *et al.*, 2003; Williams *et al.*, 2004]. The Picarro L2130-i analyzer uses isotope ratio infrared spectroscopy (IRIS) technique to quantify the concentration and isotopic composition of water vapor. The three most common isotopologues of water vapor ( $^1\text{H}^1\text{H}^{16}\text{O}$ ,  $^1\text{H}^2\text{H}^{16}\text{O}$ ,  $^1\text{H}^1\text{H}^{18}\text{O}$ ) have distinct absorption spectra [Martín-Gómez *et al.*, 2015]. The Picarro analyzer calculates  $\delta^{18}\text{O}$  and  $\delta^2\text{H}$  values by measuring spectral absorbance at specific wavelengths using cavity ring-down spectroscopy. All isotope values are reported in standard delta notation in per mil (‰) notation relative to Vienna Standard Mean Ocean Water (VSMOW):

$$\delta = \left( \frac{R_{\text{sample}}}{R_{\text{standard}}} - 1 \right) \times 1000 \quad (1)$$

where R is the isotope ratio of the heavy and light isotope (e.g.,  $^{18}\text{O}/^{16}\text{O}$ ).

The Picarro Induction Module peripheral can extract water vapor bound in a matrix, such as small (the size of a hole punch) samples of plant tissue, soil, or precipitation samples dispensed onto a piece of dry glass filter paper. The precipitation, plant, and soil samples are clamped into a metal holder before being inserted into the Induction Module, where the sample is heated

inductively, with the length and intensity of heating prescribed by user-supplied parameters [Berkelhammer *et al.*, 2013]. The available water vapor is then passed by a zero air carrier gas into the analyzer's infrared absorbance cavity [Berkelhammer *et al.*, 2013].

Analytical precision in measuring  $\delta^{18}\text{O}$  and  $\delta^2\text{H}$  values are comparable in IRIS and the classical isotope ratio mass spectroscopy, especially when comparing pure water samples [Lis *et al.*, 2008; Brand *et al.*, 2009; Gupta *et al.*, 2009]. One concern with IRIS analysis is the potential for spectral interference from organic contaminants, including some compounds commonly found in environmental samples such as plant and soil samples [West *et al.*, 2010; Schultz *et al.*, 2011; Schmidt *et al.*, 2012; Martín-Gómez *et al.*, 2015]. Picarro has developed an on-line micro-combustion module that oxidizes some organic contaminants that may cause spectral interference [Berkelhammer *et al.*, 2013; Martín-Gómez *et al.*, 2015].

## **2. Corrections**

### **2.1 Memory**

Most gas analyzers experience memory effects, where residual water vapor remains in the instrument after analysis because water molecules adsorb to internal instrument surfaces; as a result, each analyzed samples contains a small percentage of the previous sample [Schmidt *et al.*, 2012; van Geldern and Barth, 2012]. Multiple memory correction methods are available [van Geldern and Barth, 2012], and the one I primarily used was to run each sample multiple times until the isotope values stabilized, then ignoring the first injection(s) and calculating the final value from the stabilized isotope values. The number of runs depended on difference in isotope values between adjacent samples [van Geldern and Barth, 2012], where adjacent samples that

were further apart in isotope values required more runs to stabilize than adjacent samples that were similar in isotope values.

## **2.2 Vial Headspace**

After the sample vial is heated, all available water vapor is carried to the analyzer, and this water vapor includes both water vapor extracted from the sample and background water vapor present in the sample vial. This background water vapor causes headspace error, and the magnitude of headspace error depends on your sample concentration and on the isotopic difference between atmospheric air and your sample [Picarro, Inc., 2013]. There are two parts to reducing headspace error. The first part is to flush the sample vials with zero air before inserting the sample; this standardizes the background air in the sample vial during analysis. The second part is to run blanks before running standard or unknown samples, which involves running capped, empty vials at the beginning of the day. These blank runs capture the water content and isotopic values of the background air in the sample vials, and the Induction Module Coordinator software manages on-line calculation of the blank runs and automatically adjusts the concentration and isotopic concentration of water vapor in the subsequent sample runs.

## **3. Analyzer Calibration**

### **3.1 Primary Standards**

In order to compare isotope values across studies, individual laboratories calibrate their isotopic values relative to international reference standards [Gonfiantini, 1978; Coplen, 1995]. The international water standard scale is the Vienna Standard Mean Ocean Water – Standard Light Antarctic Precipitation (VSMOW-SLAP). The two international water standards are VSMOW2,

defined as  $\delta^{18}\text{O} = 0 \pm 0.02 \text{ ‰}$ ,  $\delta^2\text{H} = 0 \pm 0.3 \text{ ‰}$  and SLAP2, defined as  $\delta^{18}\text{O} = -55.5 \pm 0.02 \text{ ‰}$ ,  $\delta^2\text{H} = -427.5 \pm 0.3 \text{ ‰}$  [IAEA, 2009]. Since the primary standards VSMOW2 and SLAP2 waters are in limited supply, most laboratories use secondary (i.e., internal) standards for daily calibration after they calibrate the secondary standards against VSMOW2 and SLAP2. The two secondary standards we used are Shantz DI water ( $\delta^{18}\text{O} = -9.0 \pm 0.8 \text{ ‰}$ ,  $\delta^2\text{H} = -70 \pm 3 \text{ ‰}$ ) and Destiny Deep Sea Water ( $\delta^{18}\text{O} = 0 \pm 0.8 \text{ ‰}$ ,  $\delta^2\text{H} = -1 \pm 3 \text{ ‰}$ ). We analyzed the two primary standards and the two secondary standards on the same day to create a regression line for true versus apparent isotopic values. For example, our apparent  $\delta^{18}\text{O}$  value for VSMOW2 was 0.74 ‰, our apparent  $\delta^{18}\text{O}$  value for SLAP2 was -58.0 ‰, and our regression line is  $\delta^{18}\text{O}_{\text{true}} = 0.95 * \delta^{18}\text{O}_{\text{apparent}} - 0.70$ . We then used this regression line to calculate  $\delta^{18}\text{O}_{\text{true}}$  for the two secondary standards, and followed the same method for calculating  $\delta^2\text{H}_{\text{true}}$  for the two secondary standards.

### 3.2 Secondary Standards

After the secondary standards were calibrated against the primary standards, we used daily runs of the secondary standards to correct the isotopic values of the unknown sample relative to the VSMOW-SLAP scale. One option was to run two secondary standards daily and to create a regression line between the two standards to correct the unknown samples (similar method as calibrating the primary standards). This first option accounts for shifts in both the slope and the intercept of the calibration regression line, but increases the daily time needed to run samples. The second option was to run one secondary standard daily and to do an offset correction. For example, if my apparent  $\delta^{18}\text{O}_{\text{Shantz}}$  was -8.9 ‰ and my true  $\delta^{18}\text{O}_{\text{Shantz}}$  was -9.0 ‰, then my offset of  $\delta^{18}\text{O}$  values for samples run that day would be 0.1 ‰. A similar method would be used to

calculate the offset of  $\delta^2\text{H}$  values for samples run that day. I chose this second option because it decreased the daily time needed to run samples by about one hour a day. The tradeoff was that this second option depended on the day-to-day stability of the analyzer because it assumed the slope of the calibration regression line remained constant and only accounted for changes in the intercept of the calibration regression line. This second option was limited to samples where  $\delta^{18}\text{O}$  values are within 15 ‰ and  $\delta^2\text{H}$  values are within 50 ‰ of the secondary standards [N. Saad, pers. Comm.].

#### 4. References

- Berkelhammer, M., J. Hu, A. Bailey, D. C. Noone, C. J. Still, H. Barnard, D. Gochis, G. S. Hsiao, T. Rahn, and A. Turnipseed (2013), The nocturnal water cycle in an open-canopy forest, *J. Geophys. Res. Atmospheres*, 118(17), 10,225–10,242, doi:10.1002/jgrd.50701.
- Brand, W. A., H. Geilmann, E. R. Crosson, and C. W. Rella (2009), Cavity ring-down spectroscopy versus high-temperature conversion isotope ratio mass spectrometry; a case study on  $\delta^2\text{H}$  and  $\delta^{18}\text{O}$  of pure water samples and alcohol/water mixtures, *Rapid Commun. Mass Spectrom.*, 23(12), 1879–1884.
- Brooks, J. R., Holly R. Barnard, Rob Coulombe, and Jeffrey J. McDonnell (2010), Ecohydrologic separation of water between trees and streams in a Mediterranean climate, *Nat. Geosci.*, 3(2), 100–104, doi:10.1038/ngeo722.
- Clark, I. D., and P. Fritz (1997), *Environmental Isotopes in Hydrogeology*, CRC Press.
- Coplen, T. B. (1995), Reporting of stable hydrogen, carbon, and oxygen isotopic abundances, *Geothermics*, 24(5), 707–712.
- Dawson, T. E., and J. R. Ehleringer (1991), Streamside trees that do not use stream water, *Nature*, 350(6316), 335–337, doi:10.1038/350335a0.
- Dawson, T. E., S. Mambelli, A. H. Plamboeck, P. H. Templer, and K. P. Tu (2002), Stable Isotopes in Plant Ecology, *Annu. Rev. Ecol. Syst.*, 33, 507–559.
- van Geldern, R., and J. A. C. Barth (2012), Optimization of instrument setup and post-run corrections for oxygen and hydrogen stable isotope measurements of water by isotope

- ratio infrared spectroscopy (IRIS), *Limnol. Oceanogr. Methods*, 10(12), 1024–1036, doi:10.4319/lom.2012.10.1024.
- Gonfiantini, R. (1978), Standards for stable isotope measurements in natural compounds, *Nature*, 271(5645), 534–536, doi:10.1038/271534a0.
- Gupta, P., D. Noone, J. Galewsky, C. Sweeney, and B. H. Vaughn (2009), Demonstration of high-precision continuous measurements of water vapor isotopologues in laboratory and remote field deployments using wavelength-scanned cavity ring-down spectroscopy (WS-CRDS) technology, *Rapid Commun. Mass Spectrom.*, 23(16), 2534–2542.
- Herczeg, A. L., and F. W. Leaney (2011), Review: environmental tracers in arid-zone hydrology, *Hydrogeol. J.*, 19(1), 17–29.
- IAEA (2009), Reference Sheet for VSMOW2 and SLAP2 international measurement standards.,
- Lis, G., L. I. Wassenaar, and M. J. Hendry (2008), High-precision laser spectroscopy D/H and  $^{18}\text{O}/^{16}\text{O}$  measurements of microliter natural water samples, *Anal. Chem.*, 80(1), 287–293.
- Martín-Gómez, P., A. Barbeta, J. Voltas, J. Peñuelas, K. Dennis, S. Palacio, T. E. Dawson, and J. P. Ferrio (2015), Isotope-ratio infrared spectroscopy: a reliable tool for the investigation of plant-water sources?, *New Phytol.*, n/a–n/a, doi:10.1111/nph.13376.
- Picarro, Inc. (2013), *Induction Module - CRDS Setup: User's Manual*, 40039 Rev. A.
- Schmidt, M., K. Maseyk, C. Lett, P. Biron, P. Richard, T. Bariac, and U. Seibt (2012), Reducing and correcting for contamination of ecosystem water stable isotopes measured by isotope ratio infrared spectroscopy, *Rapid Commun. Mass Spectrom.*, 26(2), 141–153.
- Schultz, N. M., T. J. Griffis, X. Lee, and J. M. Baker (2011), Identification and correction of spectral contamination in  $2\text{H}/^{1}\text{H}$  and  $^{18}\text{O}/^{16}\text{O}$  measured in leaf, stem, and soil water, *Rapid Commun. Mass Spectrom.*, 25(21), 3360–3368.
- Werner, C., H. Schnyder, M. Cuntz, C. Keitel, M. J. Zeeman, T. E. Dawson, F.-W. Badeck, E. Brugnoli, J. Ghashghaie, and T. E. E. Grams (2012), Progress and challenges in using stable isotopes to trace plant carbon and water relations across scales,
- West, A. G., K. R. Hultine, K. G. Burtch, and J. R. Ehleringer (2007), Seasonal variations in moisture use in a piñon–juniper woodland, *Oecologia*, 153(4), 787–798, doi:10.1007/s00442-007-0777-0.
- West, A. G., G. R. Goldsmith, P. D. Brooks, and T. E. Dawson (2010), Discrepancies between isotope ratio infrared spectroscopy and isotope ratio mass spectrometry for the stable

- isotope analysis of plant and soil waters, *Rapid Commun. Mass Spectrom.*, 24(14), 1948–1954, doi:10.1002/rcm.4597.
- Williams, D. G., and J. R. Ehleringer (2000), Intra- and interspecific variation for summer precipitation use in pinyon–juniper woodlands, *Ecol. Monogr.*, 70(4), 517–537, doi:10.1890/0012-9615(2000)070[0517:IAIVFS]2.0.CO;2.
- Williams, D. G. et al. (2004), Evapotranspiration components determined by stable isotope, sap flow and eddy covariance techniques, *Agric. For. Meteorol.*, 125(3–4), 241–258, doi:10.1016/j.agrformet.2004.04.008.
- Yepez, E. A., D. G. Williams, R. L. Scott, and G. Lin (2003), Partitioning overstory and understory evapotranspiration in a semiarid savanna woodland from the isotopic composition of water vapor, *Agric. For. Meteorol.*, 119(1–2), 53–68, doi:10.1016/S0168-1923(03)00116-3.

APPENDIX C: PROTOCOL FOR ANALYZING SAMPLES ON THE PICARRO L2130-i  
ANALYZER WITH INDUCTION MODULE

Daphne J. Szutu<sup>1,2</sup>

<sup>1</sup>School of Natural Resources and the Environment, University of Arizona, Tucson, AZ 85721

USA

<sup>2</sup>[daphne@email.arizona.edu](mailto:daphne@email.arizona.edu)

## **1. Preparing to Analyze Samples**

### **1.1 Turning on the Induction Module**

1. If the pump and analyzer are off, turn on the vacuum pump first, then the analyzer. Let the analyzer run on ambient air until it is stabilized, then turn on the dry gas. The analyzer is stabilized once the Instrument Status windows are green and the Status log window says “Measuring...”. Important: When the analyzer is on, the vacuum pump **MUST** remain on and connected, otherwise there could be analyzer damage.
2. Turn on the Induction Module (IM) using the physical switch at the back of the IM. The green power light at the front of the IM will turn on.
3. Start the IM Coordinator by selecting the “Coordinator Launcher” icon on the Desktop and choosing “IM CRDS” from the drop-down menu. The Coordinator is the Picarro analyzer software that lets you view status and data of sample analysis as well as upload sample descriptions.
4. Insert an empty, capped vial into the IM to help with analyzer drydown.
5. If gas is not already flowing, turn on zero air gas to 2.5 psi. Note how much gas remains in the gas tank.
6. On the analyzer Graphical User Interface (GUI), the top time series is H<sub>2</sub>O (ppm) measured inside the analyzer. After you start the IM Coordinator and turn on the gas, H<sub>2</sub>O (ppm) will start decreasing. When H<sub>2</sub>O (ppm) decreases to <250 ppm, you will be ready to run samples. This drydown takes about 15-20 minutes.
7. In the meantime, take 2 empty, uncapped 4 ml IM glass vials and place them upside down on the vial flush apparatus to prepare them for sample analysis.

## 1.2 Run Sequence

The objective is to run the blanks, standards, and unknown samples with the same recipe and with consistent sample loading technique. Blank runs account for headspace in the 4 ml IM vial and are included in the internal corrections run by the Coordinator. Therefore, the blanks must be run each time a new Coordinator window is started. Standards are used for external (i.e., user-directed) calibration of the sample isotopic values, so that values can be reported relative to the international VSMOW-SLAP standard. We run one standard sample for every five unknown samples. Assuming that the isotope values stabilize in six runs per sample, a typical daily run sequence is:

- Runs 1-3: Blank
- Runs 4-9: Standard sample (Shantz DI water or Destiny Deep Seawater)
- Runs 10-15: Unknown 1
- Runs 16-21: Unknown 2
- Runs 22-27: Unknown 3
- Runs 28-33: Unknown 4
- Runs 34-39: Unknown 5

The Coordinator software distinguishes between “Blank” runs and “Sample” runs, so be sure to choose the correct option depending on if you are running a blank (choose “Blank” option) or a standard or unknown sample (choose “Sample” option). After the analyzer finishes a “Blank” run, the Coordinator window will ask you if you want to “Include” or “Exclude” the blank in its internal calculations. We “Exclude” the first run of the day and “Include” the second and third blank run if the peak shape appears normal. To run a blank,

flush a 4 ml vial with zero air for at least 6 minutes (the length of one sample run) and insert this flushed, empty, capped vial into the IM. To run a water standard or sample, dispense 3  $\mu$ l of sample onto the sample holder, insert the sample holder into the 4 ml IM vial, and insert the vial into the IM (see section 2.3).

### **1.3 Avoiding Contamination**

Contamination of the sample (i.e., altering the isotopic values of the sample) mainly comes through two ways: adding foreign water vapor, or exposing the sample to evaporation. To prevent contamination through foreign water, make sure your hands and gloves are completely dry, and do not blow on any of the analysis materials because water vapor from your breath could condense onto the materials. For example, if you see a piece of lint on the vials, caps, or sample holders, use tweezers to remove the lint instead of blowing it off. To prevent evaporation, cap each sample vial after withdrawing the water sample or standard. In addition, we want to prepare the sample in the sample holder, insert the sample holder into the 4 ml IM vial, and immediately insert the vial into the IM to begin analysis.

## **2. Analyzing Samples**

### **2.1 Cleaning the syringe between liquid samples**

Cleaning the syringe at the beginning of the day and between water samples ensures that any residual water inside the syringe is rinsed out with your current water sample or standard. The IM syringe is stored in a beaker of distilled water to keep the syringe plunger lubricated and to prevent any salts or minerals that may have been in your samples from hardening inside the syringe.

1. Wipe off syringe needle and body with a dry kimwipe.
2. Withdraw >6 µl of sample with the syringe and discard the sample onto a kimwipe.
3. Repeat Steps 1 and 2 to rinse the syringe a total of two times.

## **2.2 Preparing the vial, cap, and flat sample holder**

Before loading a water sample or standard, prepare your consumables:

1. Flush a 4 ml IM vial with dry air for at least 6 minutes.
2. Fit a plastic cap with a septum, with the shiny side of the septum facing outwards away from the vial.
3. Using pliers and tweezers, insert 2 “paper dots” (glass filter paper cut into circular pieces using a hole punch) between the flaps of a flat sample holder (tri-fold metal strip) and line up the “paper dots” with the round outline on the sample holder so that they are centered over the small hole in the center. Close the sample holder, fold up the small triangles on the side, and crimp the middle and sides of the sample holder to ensure good contact of the “paper dots” with the metal sample holder.
4. Fold one end of the strip ( $\frac{1}{8}$ ”) up 90 degrees to help the metal strip rest flatly against the bottom of the vials. Place the strip down on the lab bench to make sure it lays flat and that the small hole in the center is facing up.

## **2.3 Loading a water sample**

After the vial, cap, and sample holder are prepared, you can inject your water sample onto the sample holder.

1. From your 20 ml sample glass vial, use the syringe to withdraw exactly 3  $\mu$ l of sample. Check that there are no bubbles in your syringe. Place the syringe gently down and close the 20 ml sample vial.
2. With pliers, pick up the prepared tri-fold metal strip, with the small hole facing up.
3. Place the syringe needle tip in the hole and slowly (over 5-8 seconds) inject the sample onto the paper dot and hold the syringe needle in place against the hole for several more seconds. Injecting the sample slowly ensures that the filter paper has time to absorb the sample and that the sample will not leak onto the metal strip.
4. Remove a 4 ml glass IM vial from the vial flush apparatus. Using tweezers, gently place the loaded metal strip into the 4 ml glass vial with the folded end toward the bottom of the vial and with the small hole facing up.
5. Securely tighten the cap, and immediately, but gently, insert the 4 ml glass vial into the IM. Check that the metal strip remains seated at the bottom of the vial.
6. Immediately select “Ok” on the Coordinator window to begin analysis.

For all samples, to reduce sample evaporation, we want to inject the sample immediately before we insert the vial into the IM and start the analysis. The Coordinator window gives you a 60-second delay between samples. It usually takes about 30 seconds to load a sample, so you may find yourself with a prepared sample, but the Coordinator window is not yet ready to start analysis. Therefore, during the 60-second delay, wait about 30 seconds, and then prep the water sample so that you can inject the sample onto the metal strip, place the metal strip into the vial, and immediately insert the vial into the IM to begin analysis.

## 2.4 Consumables

For every sample (either standard or unknown), use a new sample holder with new “paper dots.” For every 2 samples, use 2 vials: this way, one vial is being flushed with zero air while the other vial is used for analysis. So, every other sample, change to 2 new vials to rotate between flushing and analysis. The cap and septum can be used 4-6 times until you reach septum capacity. Since each sample may require a different number of runs until you reach stable isotopic values, when you change the cap and septum will not be dependent on whether it is a new sample or not.

## 2.5 Loading sample description .csv files

Whenever the Coordinator is open, you can load a sample description .csv file and update the sample descriptions, even for past runs (as long as they are in your current Coordinator session.) After you close out of the Coordinator window, you can also manually change the description directly in the final .csv file.

1. To load the sample description .csv file in the Coordinator window:
  - a. In the Coordinator window, click “Load Sample Descriptions” button near top:
  - b. Select file:  
*C:/Picarro/G2000/AppConfig/Config/Coordinator/SAMPLETYPE\_PERIPHERAL\_ANALYSISDATE.csv.*
    - i. SAMPLETYPE: e.g., “Precip”, “Soil”, or “Stem”
    - ii. PERIPHERAL: e.g., “IM”, or “Vap”
    - iii. ANALYSISDATE (yyyymmdd), e.g., 20150203 for Feb 3, 2015.

2. To update the .csv file:
  - a. Open the file in Notepad++. The headers are “Vial, Description.”
  - b. “Vial” is the overall run number for that specific Coordinator session.
  - c. “Description” is the sample name, followed by the sample-specific run number, e.g., “Shantz DI 01,” “MB1\_E3\_20141003 01.”

## **2.6 Logging**

At the beginning of each day, write the date, operator, and the starting gas level in the gas tank (e.g., 500 psi). Note which recipe you are using, e.g., “High T – gas @ 2.5 psi” or “Woody Stem 180 – gas @ 3 psi.” For each run, record the overall run number for that Coordinator session, the sample name and sample-specific run number, estimated H<sub>2</sub>O volume (from Coordinator), H<sub>2</sub>O peak max (from Coordinator), and any other notes.

Recording and checking the H<sub>2</sub>O volume and H<sub>2</sub>O peak max helps check your sample loading is consistent. A consistent sample loading technique will help produce consistent peak shapes. For example, when running water samples, H<sub>2</sub>O volume should be consistent (within 0.2 µl) from run to run. If the H<sub>2</sub>O volume is more variable, you may have bubbles in your syringe that are producing inconsistent sample volumes. If H<sub>2</sub>O peak max differs by more than 3,000 ppm or 4,000 ppm between runs, your sample holder may not be lying flat in the vial.

## **2.7 Shutdown procedure at the end of the day**

1. After uploading the newest Sample Descriptions .csv file, close out of the Coordinator window.

2. Physically turn off IM (using switch at back of IM) and turn off the gas. We generally leave the analyzer itself running overnight.
3. Record ending gas level in logbook.
4. Place IM syringe back in storage beaker.

## 2.8 Examples of stabilized isotopic values

To determine the isotopic values of samples, we run each sample multiple times until the values stabilize. Because of the memory effect, the difference in  $\delta^{18}\text{O}$  or  $\delta^2\text{H}$  values should decrease with each run of any specific sample, until the values appear to converge on a stable value. To determine when the values of a water sample are stabilized, we look for both an oscillation in the values and for the last 3 runs to have a standard deviation less than the instrument (analyzer and Induction Module) long-term precision. Generally, with each run of a water sample, the isotopic values will monotonically increase toward a stabilized value, and then will begin oscillating around some value. This monotonic increase is caused by memory from the “paper dot”, which has atmospheric water vapor adsorbed onto the surface during storage. We look for both  $\delta^{18}\text{O}$  and  $\delta^2\text{H}$  values to oscillate at least once (Figure 1). It usually takes about 3-4 runs for  $\delta^{18}\text{O}$  values to oscillate, and then another 1-3 runs for  $\delta^2\text{H}$  values to oscillate. In addition to seeing this oscillation, we look for the last 3 runs to have  $\delta^{18}\text{O}$  values with a standard deviation less than 0.8 ‰ and  $\delta^2\text{H}$  values with a standard deviation less than 3 ‰ (Figure 1). For samples that don’t use a “paper dot”, e.g., stem and soil samples, we only need to use the standard deviation cut-offs to determine isotopic values stabilization because there is no “paper dot” memory effect (Figure 2).

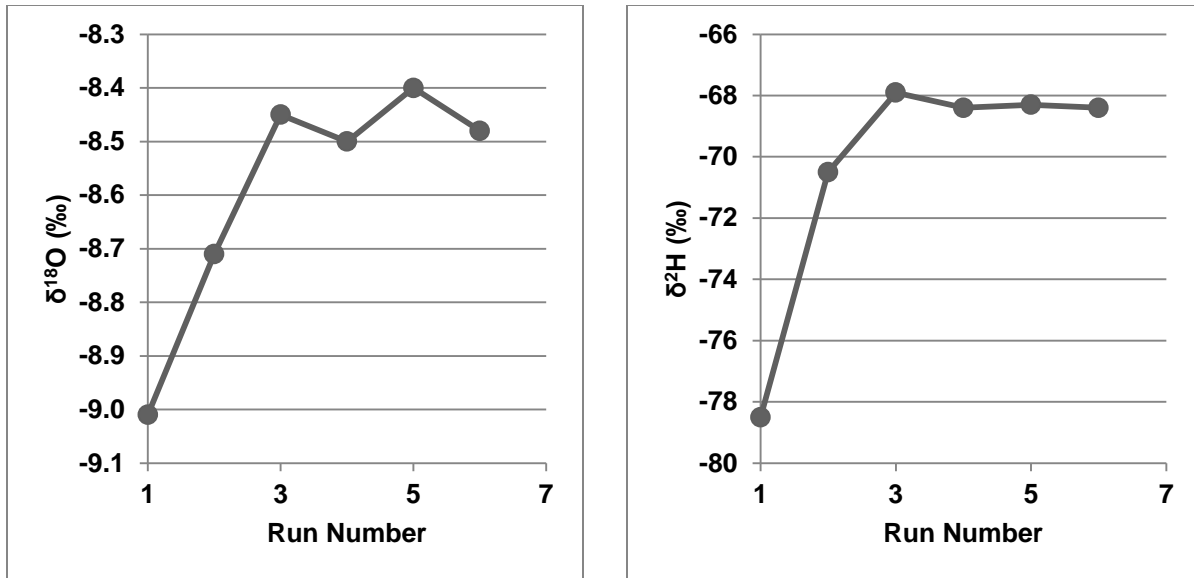


**Figure 1.**  $\delta^{18}\text{O}$  values (left) and  $\delta^2\text{H}$  values (right) from a water sample that was run 6 times. Note how the first oscillation of  $\delta^{18}\text{O}$  and  $\delta^2\text{H}$  values appears on run number 4, but we analyze the sample an additional 2 times to so that the last 3 runs (in this case, run numbers 4, 5, 6) have values with standard deviations less than the long-term precision of the instrument.

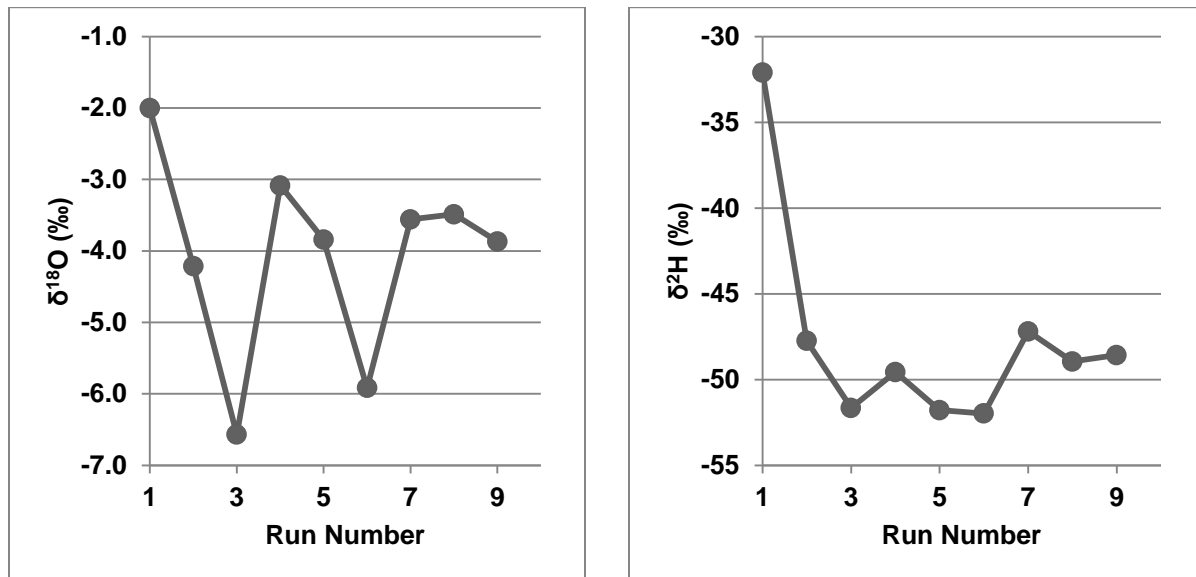


**Figure 2.**  $\delta^{18}\text{O}$  values (left) and  $\delta^2\text{H}$  values (right) from a stem sample that was run 9 times. Note how the values oscillate beginning on run number 4, but we analyze additional runs of the sample until the last 3 runs (in this case, run numbers 7, 8, 9) have values with standard deviations less than the long-term precision of the instrument.

## **2.9 Tips**

1. Check gas flow every 3-4 runs for the first 12 runs of the day. The gas flow tends to slip a bit at the beginning of the day but then stabilizes.
2. The minimum number of runs needed for one sample is 4 runs. The first run is always excluded because of the memory effect (from the previous sample, and from the “paper dots” if applicable), and we need at least 3 values to average together to calculate the sample isotopic values.
3. When re-using the same septum between different runs, rotate the vial so that the IM needle pierces a fresh portion of the septa for each analysis run. If the needle re-pierces a hole in the septa, this could cause a leak in the IM gas flow and produce inconsistent isotopic values.
4. The inductive heating process of the Induction Module is affected by the relative position of the “paper dots” in the tri-fold metal strip and by the relative position of the sample holder in the IM vial. The more consistent your sample and vial loading techniques are, the more consistent your peak shape and data will be.

## **3. Troubleshooting**

### **3.1 Safe Mode**

If the analyzer status log window says, “The instrument has been placed into Safe Mode,” try to restart the analyzer.

1. From the Desktop, select the folder “Diagnostic.” Select “Stop Instrument”, and then select “Stop Software and drive.” The Picarro GUI will close.

2. Take this opportunity to install any Microsoft or software updates that need computer restarts since this is a rare moment when the analyzer is restarted.
3. Use the green power button in the front of the analyzer to shut down the analyzer.
4. Wait 10 minutes, and then use the green power button to re-start the analyzer.
5. If there is still an error after the analyzer restarts and warms up, call Picarro technical support.

### **3.2 Clogs or leaks in the IM**

If flow through the flowmeter is not normal, there could be a clog or leak in the IM plumbing. This could occur after you replace a needle assembly, carbon filter, or oxidation cartridge. To identify the location of the clog or leak:

1. First check if all IM valves are working by using Arduino to turn on valves one at a time. If the valves are working, you will hear an audible click sound when the valve turns on.
2. To determine if there is a clog or leak, disconnect the IM from the analyzer by sliding the IM output tube from the analyzer input tube so that you can access the IM outflow tube. Make sure the gas is set at 2.5 psi and that there is a vial with cap and fresh septum inserted into the IM.
3. Open Arduino and check valve configuration 1011, both with the IM gas outflow unobstructed, and while blocking the IM gas outflow with your finger.
4. If there is low flow while the IM gas outflow is unobstructed, there may be a clog. Common sources of clogs are the bulkhead or the carbon filter.

- a. One main source of clogs is the bulkhead. This is the first piece of plumbing the incoming gas travels through when entering the IM (half of bulkhead is inside IM and half of bulkhead is outside IM). With valves set at 1100 and gas at 2.5 psi:
  - i. Check flow before bulkhead: Disconnect flowmeter from bulkhead, and flow through flowmeter should be ~650 sccm. Cover flowmeter outflow with finger, and flow should drop to 0 sccm.
  - ii. Check flow after bulkhead: Reconnect flowmeter to bulkhead. Open up the IM case and inside the IM, disconnect bulkhead outflow from 1/8" stainless steel tubing. Flow should be normal, ~140 sccm. If the flow is low, then the bulkhead is the source of clogs. Cover bulkhead outflow with finger. Flow should drop to 0 sccm.
  - iii. If the problem was the bulkhead, remove the bulkhead and check that the orifice inside has not rotated. This rotation was the source of our IM clog from July 2014. When you hold the bulkhead up to the light, you should see a clear pinprick of light coming through the orifice. Otherwise, you may need a new bulkhead from Picarro.
- b. Another source of clogs in the carbon tube.
  - i. Check flow before carbon tube by removing the carbon tube. Flow should be normal, ~140 sccm. If flow through bulkhead was normal, but is low at this step, the clog should be between bulkhead and carbon tube.
  - ii. Check flow after carbon tube by reinstalling the carbon tube firmly but do not cover with the transfer tubing or spring. Flow should be normal, ~140

scm. Cover outflow with an old septum (Caution: carbon tube will be very hot if the IM was on). Flow should drop to 0 scm. If the flow before the carbon tube was normal but flow after carbon tube is low, then clog is likely in carbon tube, and the clog problem will hopefully be solved by replacing the carbon tube.

5. If there is positive flow through the flowmeter while you are blocking the IM gas outflow, then there may be a leak. Common sources of leaks are around the oxidation cartridge or at the needle assembly. The IM manual describes how to check the needle for leaks or clogs. If you recently changed the plumbing between the gas tank and the IM (e.g., if you disassembled the system and moved the instrument to a different room), the leak may also be in the Swagelok connections between the gas tank and the IM.

### **3.3 Error: “First error at line 102”**

If you see the message, “Error Parsing failed with several errors. / First error at line 102. in state StateSetup / Exiting coordinator...” in the Coordinator window when starting up, the file RecipeMBW.ini may have a formatting error, which can happen after you adjust the recipes. Open RecipeMBW.ini and check that all recipes have all parameters defined, and that any recipes that are commented out are completely commented out.

APPENDIX D: ADDITIONAL PROTOCOL FOR ANALYZING STEM SAMPLES ON THE  
PICARRO INDUCTION MODULE

Daphne J. Szutu<sup>1,2</sup>

<sup>1</sup>School of Natural Resources and the Environment, University of Arizona, Tucson, AZ 85721

USA

<sup>2</sup>[daphne@email.arizona.edu](mailto:daphne@email.arizona.edu)

## 1. Stem analysis steps

1. Remove sample vial from fridge.
2. Shake out one stem sample onto the cutting surface, then close and parafilm the vial before returning the vial to the fridge.
3. Handle the stem sample with gloves. Make sure the box cutter is clean. From the stem, cut off a cross-section about 3-5 mm thick and discard. This reduces evaporation effects from the exposed stem surface during storage.
4. From the freshly exposed surface, cut another cross-section about 1-2 mm thick. Insert this stem “dot” into the flat sample holder (tri-fold metal strip), crimp the stem “dot” securely into the metal strip, and immediately place metal strip into an IM vial, cap vial, and insert vial into the IM.
5. Run stem samples using recipe "Woody Stem 180" at 3 psi. (Important: your blanks and standards should also be run using this same recipe at the same gas flow!)
6. The H<sub>2</sub>O volume extracted from each stem dot should be between 4 and 8 µl; keeping a consistent H<sub>2</sub>O concentration between samples will reduce concentration-dependence effects. You can control this extracted volume through your cross-section thickness (a thicker stem sample cross-section will have more water than a thinner stem sample cross-section).
7. For each new stem sample run, cut off a cross-section about 2-3 mm thick and discard, before cutting a fresh cross-section about 1-2 mm thick. This will reduce evaporative effect from the exposed stem surface between runs.
8. For each stem sample, use two new metal strips and alternate, so that one metal strip is being used for analysis while the other metal strip is cooling down to room

temperature. This way, you are always loading the stem “dot” into a cooled metal strip. Use a new metal strip when the triangles on the side of the metal strip fall off, or when the strip no longer lays flat.

## **2. Stem recipe used for creosotebush stem samples (“Woody Stem 180”)**

polyA = 0.00003

polyB = 0.03

polyC = 15

h2oLowThreshold = 250

preheatTime = 0

heatTime = 180

h2oEndHeatThreshold = 200

## **3. Experiments to more quickly reach a stable isotopic value**

After working with Kate Dennis at Picarro to establish a preliminary stem recipe (one that extracts all water present in the sample matrix), we observed that the stem isotopic values were taking a longer time to reach a stable value. The water samples generally reached a stable isotopic value within 6 runs, but the stem samples in some cases needed more than 10 runs to reach a stable value, and in some cases we could not determine a stable value even after 20 runs. To determine whether we could analyze stem samples as efficiently as water samples, we pursued several experiments to test different sample processing protocols.

### **3.1 Bark on vs. bark off experiment**

In March 2015, J. Garland ran an experiment testing whether taking the bark off the stem would make a difference on how quickly the isotopic values stabilized or on the final stabilized isotopic value. The hypothesis was that taking the bark off before analysis may lead to the stem isotopic values stabilizing more quickly because the bark may contain water that had undergone evaporative enrichment during stem storage. J. Garland ran the experiment using mixed-conifer stem samples collected at the Mount Bigelow phenocams site in the Santa Catalina Mountains Critical Zone Observatory. He analyzed 2 replicates each of 3 stem samples. For each stem sample, one replicate had the bark on during analysis and one replicate had the bark removed immediately before analysis. In addition, for each stem sample, he analyzed 20 runs of the sample.

He did not find a difference in bark-on and bark-off samples in how quickly the isotopic values stabilized, and in fact many of the samples did not have stable isotopic values even after 20 runs (Figure 1). The result of this experiment is that we kept the bark on the stem sample when analyzing stem samples for our final stem sample analysis protocol because this allowed the stem cross-section to stay together more easily after cutting.

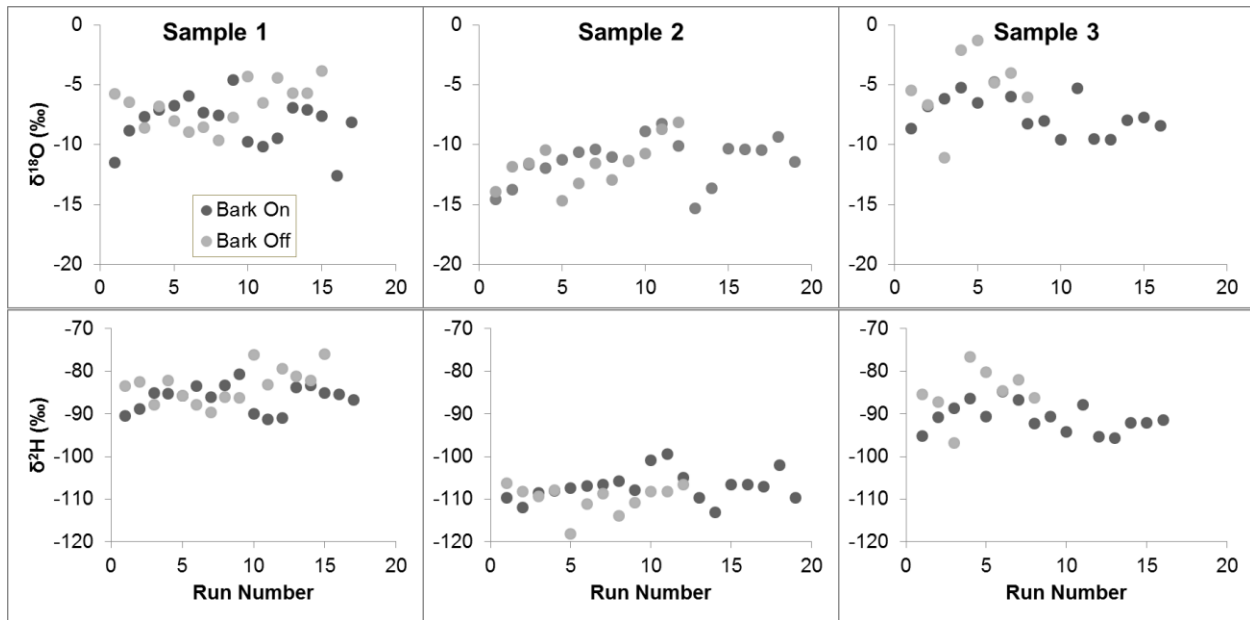


**Figure 1.**  $\delta^{18}\text{O}$  and  $\delta^2\text{H}$  values of 3 stem samples analyzed; each sample was analyzed both with bark on during analysis (“Bark On”) and with bark removed before analysis (“Bark Off”).

### 3.2 Dry ice experiment

The objective of this experiment was to see if we can improve how quickly the stem sample isotopic values stabilize. The hypothesis is that evaporation during stem sample prep reduced precision of the apparent isotopic values, so that reducing evaporation would cause the isotopic values to stabilize more quickly.

To prevent evaporation, we tried preparing the stem sample over dry ice (solid carbon dioxide at  $-79\text{ }^\circ\text{C}$ ), with the idea that the air directly above the dry ice surface would remain cold enough that any liquid water in the stem sample would not evaporate. However, putting a sample or metal sample holder directly on the dry ice caused the sample and holder to become so cold that atmospheric air condensed onto the sample and holder and introduced foreign water into our sample.

We then tried to prevent atmospheric air condensation by separating the stem sample from the dry ice with 2-4 layers of plastic in addition to keeping a flowing air current running above the sample (by directing a table fan to blow air above the dry air). However, we still observed condensation on the sample within 5 minutes.

Finally, we tried keeping the stem sample on dry ice, and keeping the dry ice and sample in a closed (but not sealed) styrofoam cooler. We again separated the stem sample and dry ice with 2 layers of plastic, and did not see condensation on the sample within 15 minutes. Possibly, the off gassing of carbon dioxide inside the styrofoam cooler kept the air cold and dry enough that atmospheric water could not condense quickly onto the sample or sample holder. Using this method, L. Hamman did 12 runs of a single stem sample, but did not see a significant difference in how quickly the stem isotopic values stabilized (Figure 2).

The result of these experiments with dry ice was that it did not significantly help increased stem sample analysis efficiency, so we did not include it as part of our final stem sample analysis protocol.

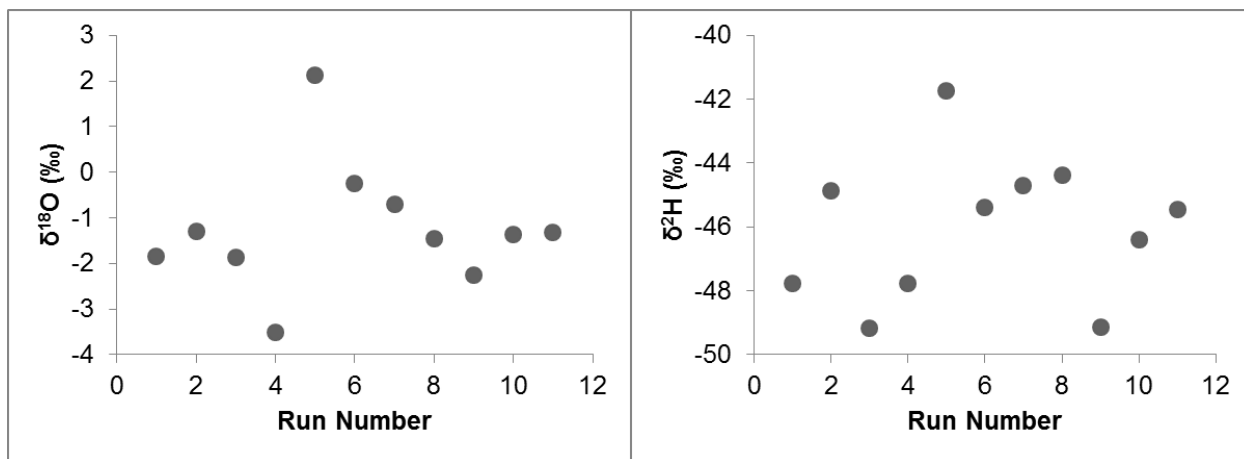


**Figure 2.**  $\delta^{18}\text{O}$  and  $\delta^2\text{H}$  values of one stem sample analyzed. The stem sample was stored over dry ice while not being actively prepared for analysis and the operator waited 15 minutes between each analysis run.

### 3.3 Concentration dependence experiment

In analyzing water samples, we could precisely control the volume of water inserted into the IM because we used a syringe to withdraw water from the sample vial. However, because we used a box cutter to slice stem samples for analysis, and because it is difficult to precisely control the thickness of stem slices produced, the volume of water extracted varied between different stem samples, usually between 3 and 10  $\mu\text{l}$  of water extracted. To test whether or not this difference in water extracted was impacting how quickly the isotopic values stabilized, we tested the concentration dependence of the analyzer. L. Hamman analyzed different concentrations of Shantz DI water: 3, 3.5, 4, 4.5, 5, 5.5, 6, 6.5, 7, 7.5, 8, 8.5, 9, 9.5, and 10  $\mu\text{l}$ . Although there were variations in the isotopic values across the range of water volumes, these variations were smaller than the long-term precision of the analyzer: 0.77 ‰ for  $\delta^{18}\text{O}$  and 2.4 ‰ for  $\delta^2\text{H}$  (Figure 3). The result of this experiment is that the magnitude of the concentration-dependence effect was within the magnitude of our analyzer precision, so we did not incorporate a concentration-dependence correction to our isotopic values.

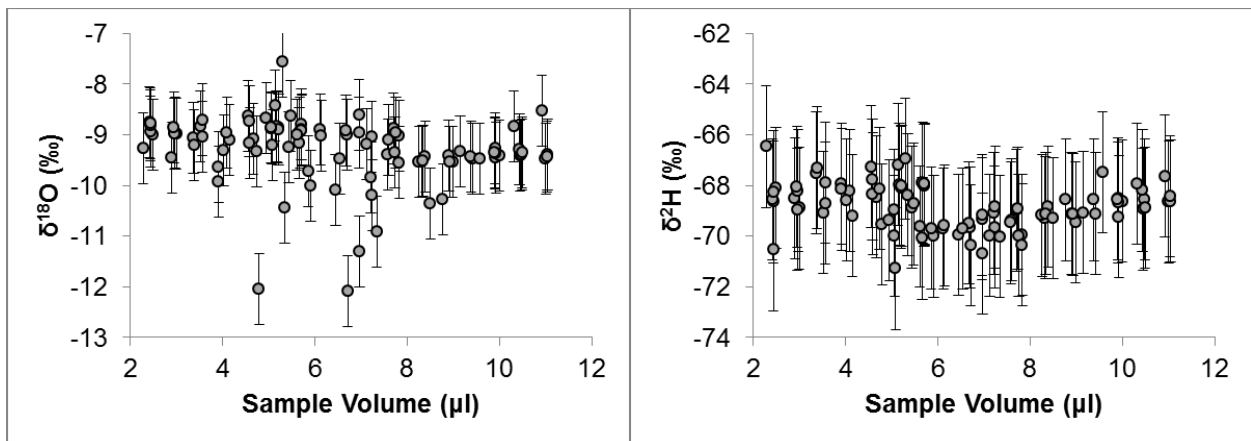


**Figure 3.**  $\delta^{18}\text{O}$  and  $\delta^2\text{H}$  values of our secondary standard water (Shantz DI water) analyzed at volumes 2-12  $\mu\text{l}$ . The error bars represent the long-term precision of the analyzer. This figure shows that any concentration-dependence variation present is smaller than the magnitude of the analyzer long-term precision.

### 3.4 Cutting a fresh surface

Our final experiment to reduce the effects of evaporation was to cut and discard a stem cross-section slice each time before cutting and analyzing a stem cross-section slice with a freshly exposed surface. After we removed the stem segment from the sample vial, we cut off a 3-5 mm thick cross-section slice from one end and discarded that cross-section slice. This reveals a surface that had not been exposed to evaporation during storage. From that fresh surface, we then cut a 1-2 mm thick cross-section slice for analysis. For subsequent samples, we cut a 1-2 mm thick cross-section slice, discarded that slice, and cut a second 1-2 mm thick cross-section slice for analysis. The result of this experiment was that stem samples isotopic values tended to stabilize within 10 analysis runs (Figure 4).

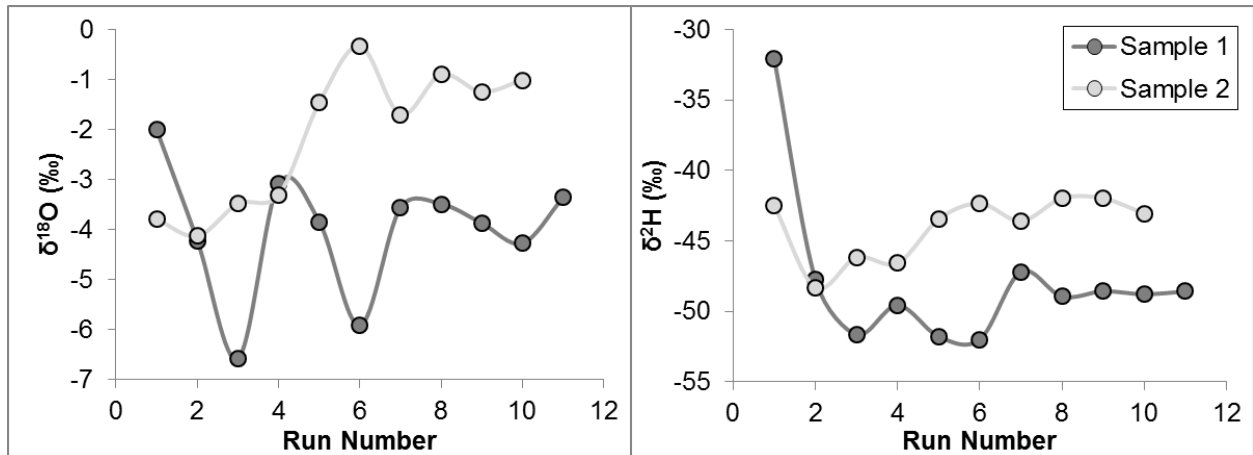


**Figure 4.**  $\delta^{18}\text{O}$  and  $\delta^2\text{H}$  values of two stem samples following the stem analysis protocol of cutting a 2 mm thick cross-section, discarding that cross-section, then cutting a 1 mm thick cross-section to analyze. Using this protocol, the stem sample isotopic values tended to stabilize within 10 analysis runs.

APPENDIX E: ADDITIONAL PROTOCOL FOR ANALYZING SOIL SAMPLES ON THE  
PICARRO INDUCTION MODULE

Daphne J. Szutu<sup>1,2</sup>

<sup>1</sup>School of Natural Resources and the Environment, University of Arizona, Tucson, AZ 85721

USA

<sup>2</sup>[daphne@email.arizona.edu](mailto:daphne@email.arizona.edu)

## 1. Soil analysis steps

1. Prepare 2 sets of powder sample holders. One set is a 5 mm-diameter cylinder with 2 steel wool stoppers. Hold the cylinders up to the light, look through the cylinder, and check that the cylinders are clean of dust.
2. The steel wool stoppers prevent your soil sample from falling out of the cylinder, but still allow gas flow through the cylinder. Using tweezers, insert one of the steel wool stoppers at one end of the metal cylinder. Hold the cylinder up to the light and check that you can see some light passing through the steel wool stopper to check that gas can flow through.
3. Remove sample vial from fridge. Use a small metal scoop to transfer some soil sample into the metal cylinder. The amount of sample will vary from sample to sample (i.e., less sample is needed if the sample is wetter, and more sample is needed if the soil is drier). We want the estimated volume of water extracted to be the similar to that extracted from the water standard (i.e., 4-10  $\mu\text{L}$  of water extracted from each soil sample), which usually means enough soil to fill the cylinder 1/4 to 1/3 full.
4. Once you are finished transferring sample into the metal cylinder, immediately cap the 20 ml sample vial. Make sure to close it securely to prevent evaporation.
5. Place the second steel wool stopper into the other end of the metal cylinder and visually check that there are spaces for airflow pathways.
5. Gently shake the metal cylinder a few times to level out the soil sample inside.
6. Immediately place metal holder into the 4 ml IM vial, cap vial, and insert vial into the IM. Most soil samples can be analyzed using recipe “Sandy 25.4 480”, but drier soils may need a recipe with a longer heating time to extract all water. In that case, try

recipe “Sandy 25.4 600” or “Sandy 25.4 900.” (Important: your blanks and standards should also be run using this same recipe at same gas flow!)

7. After the sample run is complete, remove steel wool stoppers from metal cylinder and discard the soil inside. Roll up a section of steel wool to thread through the metal cylinder to remove dust in the cylinder, and dust off the steel wool stoppers.
8. Similar to the stem samples, alternate sample holders between sample runs so that you are always loading soil into a cooled sample holder. You can reuse the metal cylinders for different samples.
9. When finished with the sample, parafilm the sample vial and return to fridge.

## **2. Soil recipe used for creosotebush stem samples (“Sandy Test 25.4 480”)**

polyA = 0.00003

polyB = 0.4

polyC = 25

h2oLowThreshold = 250

preheatTime = 0

heatTime = 480

h2oEndHeatThreshold = 200

## **3. Developing a satisfactory recipe to analyze soil samples**

I used the default recipes, but results (and Kate’s e-mails) showed that the recipe heating intensity and length needed to be increased in order to extract all water from the soil. To test different soil samples, I experimented with injecting a standard water (Shantz DI) into oven-

dried soils and testing different recipes. I expected to find a recipe by comparing my apparent isotopic values with the true values of Shantz DI water analyzed that same day. However, this experiment did not work because during the sample processing time, atmospheric air would condense in the dry soil pores and add foreign water sample to the injected Shantz DI water signal. This foreign water sample would be as much as 1  $\mu\text{l}$ , about 25% of the total extracted sample volume. In the end, I went with a recipe that vaporized all of the water out of the soil matrix. I determined this point by ensuring that the final water volume “flatlined” at the end of the sample analysis period, indicating that no more water vapor was being flushed from the sample vial into the analyzer.

APPENDIX F: PICARRO ANALYZER CALIBRATION TEST

Daphne J. Szutu<sup>1,2</sup>

<sup>1</sup>School of Natural Resources and the Environment, University of Arizona, Tucson, AZ 85721

USA

<sup>2</sup>[daphne@email.arizona.edu](mailto:daphne@email.arizona.edu)

To test the Picarro L2130-i analyzer and Induction Module calibration, I analyzed a water sample from Jen Johnson. Jen gave me a sample of water with a  $\delta^{18}\text{O}$  value of  $-14.18 \pm 0.09 \text{ ‰}$  and a  $\delta^2\text{H}$  value of  $-102.7 \pm 0.9 \text{ ‰}$  (analyzed by Chris Eastoe at the UA Geosciences Environmental Isotope Laboratory). I analyzed her sample and got an apparent  $\delta^{18}\text{O}$  value of  $13.74 \text{ ‰}$  and an apparent  $\delta^2\text{H}$  value of  $-101.6 \text{ ‰}$ . I then corrected my apparent results with a linear offset calibration using my secondary standard, Shantz DI water (true  $\delta^{18}\text{O} = -9.00 \text{ ‰}$ , true  $\delta^2\text{H} = -67.8 \text{ ‰}$ ), which that day had an apparent  $\delta^{18}\text{O}$  value of  $-8.56 \text{ ‰}$  and a  $\delta^2\text{H}$  value of  $-67.4 \text{ ‰}$ . I calculated the true isotopic values of Jen's sample to be  $\delta^{18}\text{O} = -14.2 \text{ ‰}$ ,  $\delta^2\text{H} = -102 \text{ ‰}$ . Since my calculated values are within the precision of the true values (Figure 1), it seems that the analyzer calibration and linear offset technique are satisfactory.

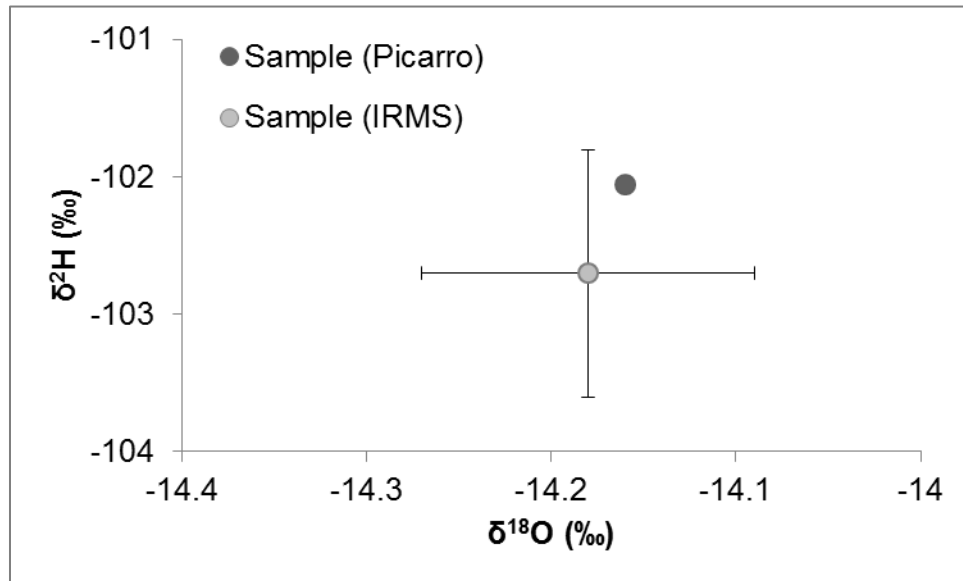


**Figure 1.** The same sample analyzed on our Picarro L2130-i analyzer and at the UA Geosciences Environmental Isotope Laboratory using isotope ratio mass spectroscopy (IRMS). The plotted error bars are the long-term precision of the IRMS analyzers ( $\pm 0.09 \text{ ‰}$  for  $\delta^{18}\text{O}$  and  $\pm 0.9 \text{ ‰}$  for  $\delta^2\text{H}$ ). The sample  $\delta^{18}\text{O}$  and  $\delta^2\text{H}$  values, analyzed on the Picarro, fall within the IRMS analytical precision.

APPENDIX G: PRECIPITATION ISOTOPE COLLECTION: TESTING FOR  
EVAPORATION FROM BOTTLE COLLECTORS

Daphne J. Szutu<sup>1,2</sup>

<sup>1</sup>School of Natural Resources and the Environment, University of Arizona, Tucson, AZ 85721

USA

<sup>2</sup>[daphne@email.arizona.edu](mailto:daphne@email.arizona.edu)

## 1. Precipitation bottle construction

I constructed a precipitation sampling bottle using a 250 ml or 500 ml HDPE bottle and an 8 ml plastic funnel (from Ace Hardware). In the middle of each bottle cap, I drilled a 5 cm diameter hole (this diameter is a little larger than the narrowest point of the funnel neck). I inserted the funnel neck through the hole and secured the funnel in place with silicone caulk. To prevent evaporative enrichment of my precipitation sample while the bottle is in the field, I prepared each 250 ml HDPE bottle with 25 ml of mineral oil and each 500 ml HDPE bottle with 35 ml of mineral oil, which produced a mineral oil layer about 5 cm thick. Every 2 weeks, if there has been precipitation, I collected the bottles of mineral oil and precipitation and replaced them with bottles of only mineral oil.

## 2. Testing bottles for evaporative enrichment

To test whether the precipitation samples underwent evaporation during the 2-week collection period, I set out four 250 ml HDPE bottles with 25 ml of mineral oil and varying volumes of water of a known isotopic composition (a secondary standard, Shantz DI water). The four bottles had 0 ml, 10 ml, 25 ml, and 50 ml of Shantz DI water in addition to the 25 ml of mineral oil. I set these four bottles out on April 15, 2015, and collected the bottles almost two weeks later on April 27, 2015.

During this period, there was about 15 mm of rain at the site, on April 26, 2015. To determine whether evaporation had affected the isotopic composition of the initial Shantz DI water, I used the isotope-mass balance and mass balance equations:

$$M_{Final} = M_{Shantz} + M_{Precip} \quad (1)$$

$$M_{Final} * R_{Final} = M_{Shantz} * R_{Shantz} + M_{Precip} * R_{Precip} \quad (2)$$

where M is the mass of water and R is the ratio  $\delta^{18}\text{O}$  or  $\delta^2\text{H}$ .

My first step was to characterize the precipitation isotopic values: Bottle 4 (Table 1) initially had no Shantz DI water combined with the mineral oil, so I was able to measure  $R_{Precip}$ :  $\delta^{18}\text{O} = -6.3 \pm 0.8 \text{ ‰}$  and  $\delta^2\text{H} = -35 \pm 3 \text{ ‰}$ . For Bottles 1-3 (Table 1), I measured  $M_{Final}$  and  $R_{Final-measured}$ , and I was able to calculate  $M_{Precip}$  for each bottle using Equation 1. I then used Equation 2 to solve for  $R_{Final-calculated}$  for Bottles 1-3 and compared  $R_{Final-measured}$  with  $R_{Final-calculated}$ . The differences between  $R_{Final-measured}$  and  $R_{Final-calculated}$  were within analyzer precision ( $\pm 0.8 \text{ ‰}$  for  $\delta^{18}\text{O}$ , and  $\pm 3 \text{ ‰}$  for  $\delta^2\text{H}$ ), so I concluded that evaporation did not have a significant effect on the precipitation collected in the sampling bottles.

**Table 1.** Mass and  $\delta^{18}\text{O}$ ,  $\delta^2\text{H}$  values used to test for evaporative enrichment of collected precipitation.

Bottle #	$M_{Shantz}$ [g]	$M_{Final}$ [g]	$M_{Precip}$ [g]	$R_{Final-measured}$ [‰]		$R_{Final-calculated}$ [‰]		Difference [‰]	
				$\delta^{18}\text{O}$	$\delta^2\text{H}$	$\delta^{18}\text{O}$	$\delta^2\text{H}$	$\delta^{18}\text{O}$	$\delta^2\text{H}$
1	10	25	15	-7.0	-47	-7.4	-49	-0.4	-2
2	25	40	15	-8.0	-55	-8.0	-57	0.0	-2
3	50	64	14	-8.5	-60	-8.4	-62	0.1	-2
4	0	14	14	-6.3	-35	--	--	--	--